PI: Friedrich B. Prinz
Institution: Carnegie Mellon University
Phone: (412)268-2499
E-mail: fbp@andrew.cmu.edu
Contract Title: Shaping By Deposition
Contract Number: N00014-88-K-0642

Project Summary

A system was developed for rapidly manufacturing custom tooling based on stereolithography (SLA) and robotic thermal spraying. The system automates and integrates these technologies within into a unified CAD/CAM environement. A novel process for making sprayed steel dies was developed and demonstrated by producing several complex die patterns. A robotic spray testbed facility was implemented. An automated pattern design system was developed which generates the parting line/parting surface models from design models for creating injection mold tooling. An industrial "Rapid Tool Manufacturing" consortium was formed to further guide sprayed steel tooliing research and to facilitate technology transfer. The consortium members include: Goodyear, Alcoa, General Motors, Ford, and EMTEC (The Edison Materials Technology Center).

Detailed Summary of Technical Results

The rapid tool manufacturing system is based on the integration of stereolithography and thermal spraying. Stereolithography (SLA) is a process which quickly creates complex shaped plastic prototype models directly from a vat of liquid photocurable polymer by selectively solidifying it with a scanning laser beam. Thermal arc spraying is then used to deposit metal onto the SLA model patterns. By incrementally depositing multiple fused layers, a freestanding metal structure is formed by separating the metal shell from the plastic substrate. This shell is used in the fabrication of custom tooling by filling it's cavity with appropriate backing materials (FIGURE 1). Previuos state-of-the-art in sprayed metal tooling was limited to zinc alloy deposition. Zinc-based tools are relatively soft and are used primarily in prototyping and low-batch production applications. Their use in some low-stress applications, such as reaction injection molding, are possible on a higher-batch production basis. Thick coatings of zinc can be deposited because this metal has low residual stress upon cooling. In contrast, the higher melting point and Young's modulus of steel compositions, which could be used to make superiors prototype tools and production-quality dies, has limited their use for making sprayed tooling.

One goal of this project was to extend this technology to steel-based deposition for fabricating superior prototype and production-quality tooling. To achieve this we have developed a new process for making sprayed steel dies. The new process uses low melt metal alloy patterns as self-anchoring mechanisms

for holding sprayed metal shells in place while making sprayed metal dies. In this process, molten metal (i.e., composing the die material) is deposited by spray deposition (e.g., arc, plasma, or combustion) onto a pattern made of low melting point metal alloys. The sprayed metal will bond locally to the pattern by superficially melting and abrading a very thin layer of the low melt alloy. This creates an "anchor pattern" to facilitate coating adhesion. The pattern geometry is negative image of the desired tool shape. The sprayed metal must have a melting point greater than that of the pattern material. For example, a pattern made of tin-bismuth Cerro alloys (melt temp. approx. 280 degrees F.) would satisfy the requirement for spraying with steel. The sprayed metal anchors to the surface of the Cerrometal pattern. The Cerro pattern thus shapes the sprayed metal and clamps it to the pattern surface. The clamping action is critical since sprayed metal, in particular steel, has a tendency to warp and peel away from the pattern surface. This "clamping" action counters this tendency. A thick sprayed metal shell is deposited and is then backed up with a mass castable material (e.g., tooling epoxy). The Cerrometal pattern is then melted away by placing the pattern/shell/backing system into a furnace or by using a torch. The result is a sprayed metal die. The low melting point of Cerrometal also permits these Cerro patterns to be quickly created by casting or spraying Cerrometal onto patterns made rapidly from stereolithography. To demonstrate the process we fabricated several complex shaped 420 stainless-steel shapes including a fan blade die pattern, a frisbee tool (FIGURE 2), and a sculpture of a human face.

Another limitation of the sprayed tool process had been that it has relied on manual spraying by a skilled technician to adjust process parameters such as arc voltage, wire feed rate, and air pressure, as well as to control the gun motion relative to the substrate. Errors in the technician's judgment, operator fatigue, and poor spray technique yield poor quality tooling. In particular, precise control of the deposition of steel onto Cerro-metal is crucial to minimzie the temperature rise in Cerro-metal due to the mismatch in C.T.E.s between Cerro-metal and steel. In addition, systematic studies of spray parameters in relation to the structural quality of sprayed metal shells for tooling applications had not been reported in the literature. Therefore methods and strategies to achieve consistent and predictable process performance have been be developed.

In particular, we have implemented a robotic spray testbed facility. The system includes a 6-DOF GMF S700 robot with a 7th DOF servo-controlled turntable, a computer controlled arc gun, temperature and depth sensors, and an inert gas atomization system. Robot trajectories are planned off-line based on CAD design models. This planning stage is currently in development. Trajectory optimizations (e.g., mapping 5-DOF spray pathes into 7-DOF robot space) are also carried out in this off-line planning stage. Trajectories are transmitted via ether-net to a host PC which coordinates the robot controller and the arc gun, and communicates with the depth and temperature sensors. The development of complete spray programs is faciliated by the use of a high-level command interpreter which has been developed. The robot programmer synthesizes spray programs by specifying for example alternative spray strategies, number of spray passes, wait times or acceptable temperature ranges before proceeding with spraying, and depth measurement actions. Robot/workpiece calibration has also been automated. The testbed also includes inert gas atomization apparatus. We have begun to investiagte the sprayed shell microstructure as a function of alternative inert-gas atomization environments as well as the spray parameters. Microstructure is assessed with metalographic apparatus.

In addition, a CAD package has been developed for automated ejectability analysis and parting surface generation for injection mold tool design. Computer design models are first evaluated for part ejectability given the desired draw direction and constrained to be manufactured in a two part mold. This information helps the designer to create manufacturable designs. Non-ejectable regions are high-lighted on a CAD display to give feedback to the designer. The parting line and parting surface models are then created subject to geometric and process constraints. The union of part design and parting surface models forms impressions of the mold cavities. Cavity patterns are then quickly built with stereolithography.

Patents:

- 1990 - *Patent pending*, "Rapid Tool Manufacturing," Weiss, L. E. and Prinz, F. B.
- 1991 - U.S. Patent No. 5,079,974, "Sprayed Metal Dies," Weiss, L. E. and Schultz, L.

Publications:

1. (*accepted*) Kutay, A. and Weiss, L. E., "Economic Analysis of Robotic Operations: A Case Study of a Thermal Spraying Robot," Robotics and Computer Integrated Manufacturing
2. Weiss, L. E., et. al., "A Rapid Tool Manufacturing System Based On Stereolithography and Thermal Spraying", ASME's Manufacturing Review, March, 1990.
3. Kutay, A. and Weiss, L., "Assessment of the Strategic Benefits of Robotic Operations: A case study of a Thermal Spraying Robot," IEEE International Conf. on Managment of Enginerring and Technology, IEEE Engineering and Management Society, Portland Ore., Oct., 1991
4. Fussell, P.S., Hartmann, K.W., Kirchner, H.O.K., Patrick, E.P., Prinz, F.B., Schultz, L., Thuel, L. and Weiss, L.E., "A Sprayed Steel Tool for Permenent Mold Casting of Aluminum," SAE Aerospace Atlantic Conf., Dayton, Ohio, Apr. 1991
5. Fussell, P. S., Kirchner, H. O. K., Prinz, F. B., and Weiss, L. E., "Controlling The Microstructure of Arc Sprayed Shells," Solid Freeform Fabrication Symposium, The University of Texas At Austin, August, 1991
6. Choi, Y., Gursoz, E. Levent, Weiss, L. E., and Prinz, F. B., "Rapid Prototyping from 3D Scanned Data Through Automatic Surface and Solid Generation," 1990 ASME Winter Annual Meeting, Nov., Dallas, Texas.
7. Fussell, P. S. and Weiss, L. E., "Steel-Based Sprayed Metal Tooling," Solid Freeform Fabrication Symposium, The University of Texas at Austin, August, 1990.
8. Gursoz, E. L., Weiss, L. E., and Prinz, F.B., "Geometric Modeling for Rapid Prototyping and Tool Fabrication," Solid Freeform Fabrication Symposium, The University of Texas at Austin, August, 1990.
9. Weiss, L. E. and Fussell, P. S., "Steel Shape Fabrication by Spray Deposition," National Conference on Rapid Prototyping, Univ. of Dayton, June, 1990.
10. Gursoz, E. L., Weiss, L. E., and Prinz, F.B., "Geometric Modeling for Rapid Prototyping, "National Conference on Rapid Prototyping, Univ. of Dayton, June, 1990.

11. Fussell, P. S., Kirchner, H. O. K., Prinz, F. B., and Weiss, L. E., "Controlled Microstructure of Arc Sprayed Metal Shells," The Engineering Design Research Center, Carnegie Mellon University, EDRC 24-57-91, May 1991

12. Bhargava, R., Weiss, L. E., and Prinz, F. B., " Automated Ejectability Analysis and Parting Surface Generation for Mold Tool Design," EDRC 24-58-91, The Engineering Design Research Center, Carnegie Mellon University, Pgh., PA., May, 1991

13. Kutay, A. and Weiss, L. E., "The Economic Evaluation of Thermal Spraying Robots in Rapid Tool Manufacturing", The Robotics Institute, CMU-RI-TR-90-07, Feb. 1990

14. Weiss, L. E., et. al., "Rapid Prototyping of Tools", The Robotics Institute, CMU-RI-TR-89-25, 1989

15. Weiss, L. E., et. al., "A Rapid Tool Manufacturing System Based On Stereolithography and Thermal Spraying", 1989 Annual Research Review, The Robotics Institute, Carnegie Mellon University

SELECTED PUBLICATIONS ATTACHED

FIGURE 1

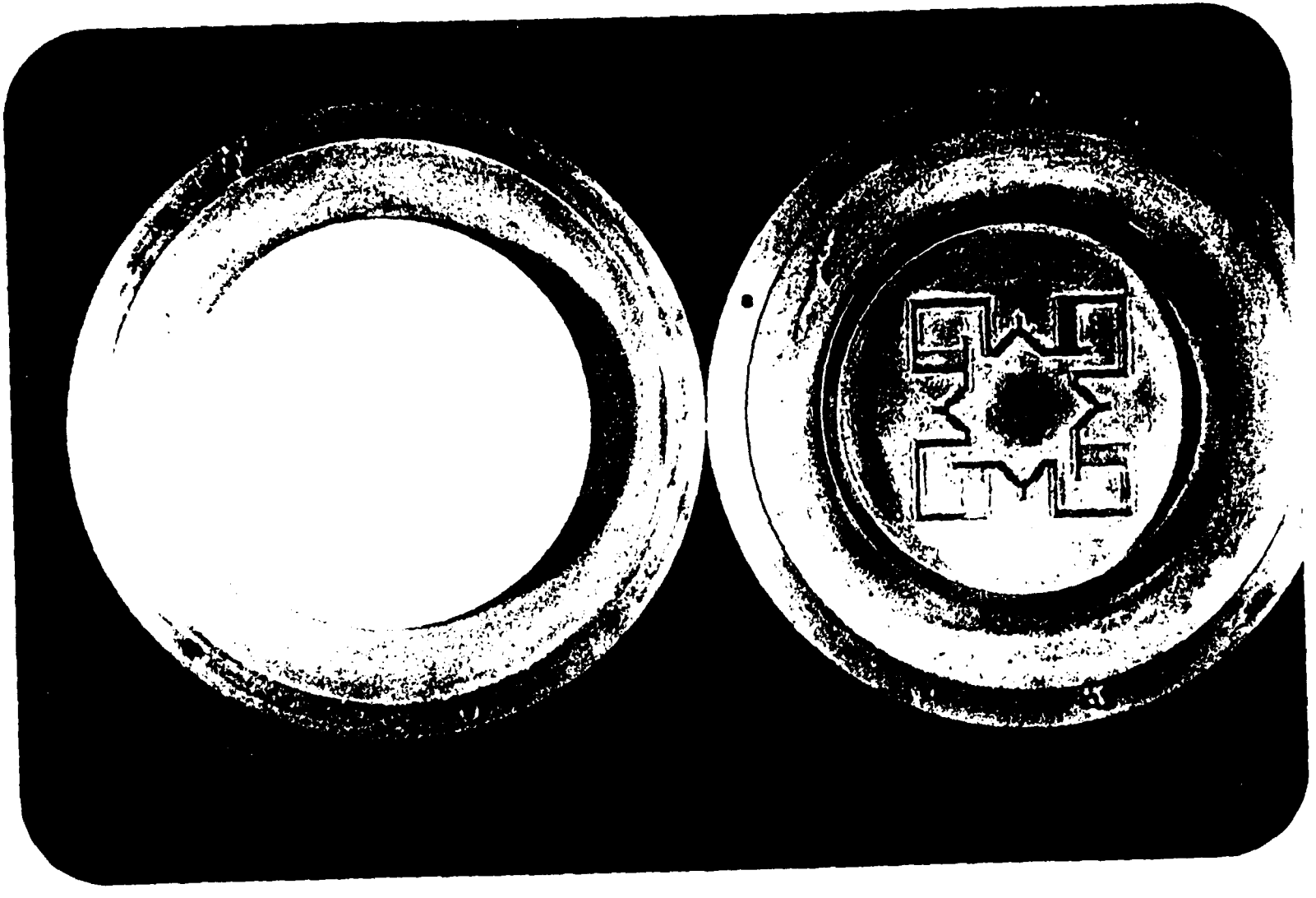

FIGURE 2

RESEARCH

A Rapid Tool Manufacturing System Based on Stereolithography and Thermal Spraying*

LEE E. WEISS, E. LEVENT GURSOZ, F. B. PRINZ, PAUL S. FUSSELL,† SWAMI MAHALINGAM, and E. P. PATRICK†
The Robotics Institute and The Engineering Design Research Center of Carnegie Mellon University, Pittsburgh, PA

This paper describes a system for rapid tool manufacturing based on the integration of stereolithography and thermal spraying. With stereolithography apparatus (SLA), plastic prototype models are built directly from liquid photopolymers by laser scanning. Thermal spraying is then used to incrementally deposit metal onto the SLA models to build the tool. A broad range of tooling can be fabricated including injection molds, forming dies, and EDM electrodes. The system integrates SLA and thermal spraying into a CAD/CAM environment which includes robotic spray capability, and computer-aided process planning. Information flows efficiently from design through fabrication by incorporating a common geometric modeling system for part and process representations. Our goal is to demonstrate that automating and integrating these processes, within a unified modeling environment, can significantly improve productivity through rapid fabrication and also reduce costs. We are building a system testbed for an injection mold tooling paradigm.

INTRODUCTION

The capability to manufacture a wide variety of quality products in a timely and cost-effective response to market requirements is a key to global competitiveness. The opportunities for improving manufacturing technology range across the entire spectrum of industries, materials, and manufacturing techniques. There is no single technological innovation which, by itself, will significantly improve productivity; rather it is a systems issue which involves rethinking many manufacturing activities. One such activity is the manufacture of tooling (i.e., design, prototype, and fabrication) such as dies and molds required for the high-volume production methods that generate most of our manufactured products. Tooling manufacture is typically an expensive and time-consuming process. The reasons lie not only in the fabrication costs and time constraints imposed by conventional machining methods, but also in the organizational framework. In most organizations, different groups employ different processes to design and manufacture tools and products, and the expertise in tool design and product design reside in different groups, impeding communications between them. The representational and physical models used in design, prototyping, and manufacturing are often incompatible with one another, so that transitions between the stages are time-consuming and error-prone. Products often make several complete cycles through design, prototyping, and fabrication before reaching production. Thus, new product development or product modification implies a series of iterative changes for both product manufacturers and toolmakers. For all these reasons, a rapid and smooth transition from product concept to production remains a challenge.

This paper describes the development of a unified CAD/CAM tool manufacturing system to address this challenge for an injection molding paradigm. In this system, both prototyping and tooling fabrication are based upon compatible shaping deposition processes, while the underlying geometric and process models share a common representational scheme. Our goal is to demonstrate that automating and integrating these processes can significantly improve productivity through greater design flexibility, rapid fabrication, and reduce cost.

Shaping deposition processes build three-dimensional shapes by incremental material buildup of thin layers, and can make geometrically complex parts with little difficulty. These processes include selective laser sintering [1], laminated object manufacturing [2], ballistic powder metallurgy [3], three-dimensional printing [4], stereolithography, and near-net thermal spraying. Our system incorporates the commercially available technologies: stereolithography apparatus (SLA) and arc spray equipment. Stereolithography[1] is a new process which creates plastic prototype models directly from a vat of liquid photocurable polymer by selectively solidifying it with a scanning laser beam. In arc spraying, metal wire is melted in an electric arc, atomized, and sprayed onto a substrate surface. On contact, the sprayed material solidifies and forms a surface coating. Spray coatings can be built up by depositing multiple fused layers which, when separated from the substrate, form a free-standing shell with the shape of the substrate surface. By mounting the shell in a frame and backing it up with appropriate materials, a broad range of tooling can

*This research has been supported in part by the Defense Advanced Research Agency under the Office of Naval Research Contract N00014-88-K-0642, and in part by the National Science Foundation Engineering Design Research Center at Carnegie Mellon University.

†Alcoa Laboratories, Alcoa Center, PA.

[1]Stereolithography has been commercialized by 3D Systems, Inc. (Valencia, CA).

be fabricated including injection molds, forming dies, and EDM electrodes. For example, the cavities of injection molds can be fabricated by direct deposition of metal onto plastic SLA models of the desired part and backing the framed shell with epoxy resins. Relative to conventional machining methods, the sprayed metal tooling approach has the potential to more quickly and less expensively produce tools, particularly for those parts with complex shapes or large dimensions. Thus, with stereolithography, an initial part shape or prototype is quickly created. Thermal spraying is then used to make tools based on the part shapes produced by stereolithography.

The potential effect of combining thermal spraying with stereolithography to build tooling is enhanced by integrating and automating these processes within a unified CAD/CAM environment. The goal of integration is to reduce the number of iterative cycles through design, prototyping, and fabrication. CAD-based evaluation and modification tools can operate on design models to help the designer create manufacturable designs on the basis of requirements and limitations of the downstream processes. For example, there are certain shape features in thermally sprayed parts which are difficult to spray. The system should identify these features so that the designer may modify them before reaching the fabrication stage. Another example is to automatically critique ejectability by analyzing whether there is sufficient draft for part ejection from an injection mold. If drafts are not sufficient, the system should identify this geometric problem and bring it to the designer's attention.

Another step in the CAD/CAM approach is to automate the thermal spray process with robotics. Tooling manufacture by thermal spraying is currently a labor-intensive artform. Shifting emphasis to robotic spraying, driven by an off-line trajectory and process planner, will improve tooling quality by achieving consistent and predictable performance of the sprayed metal shell.

Finally, the level of integration and the number of different models in this CAD/CAM system requires geometric representations that can be abstracted at several levels and that can be manipulated over several dimensions. Rather than use several different modeling environments customized for the demands of each subsystem, the models in our framework for design, analysis, and fabrication share a single common *unifying* geometric representation implemented in the software modeling system NOODLES. With this approach, model manipulation capability is robust and models need not be transformed between subsystems.

The system which we are developing represents a significant departure in tool manufacturing compared with conventional methodologies. The majority of ongoing research [5, 6] focuses on automating numerical control (NC) fabrication by removing material from metal blanks. Manufacturing a broad class of complex geometries is difficult without extensive programmer and operator intervention, so that NC fabrication remains expensive and relatively time-consuming. In addition, the fabrication of prototype parts has remained disjoint from the processes to fabricate the production part. In contrast, geometric complexity is not an issue with SLA, so that complex metal shapes can be fabricated by direct metal deposition onto the SLA models. Also, tooling fabrication builds directly upon the prototyping process. Such process compatibility and system integration will facilitate a continuous transition from design to prototyping to mass production within a single manufacturing enterprise.

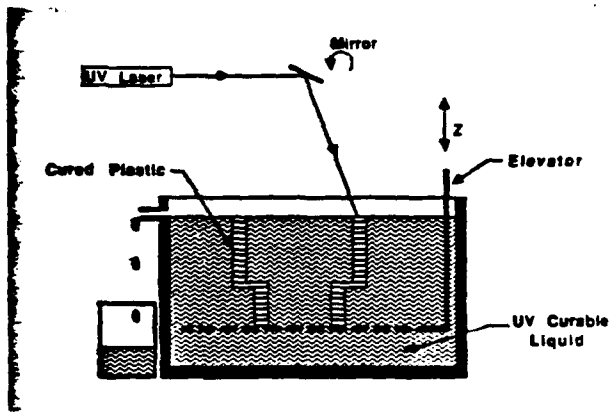

FIG. 1. Stereolithography apparatus

This paper describes the system framework and the components which have currently been developed, and is organized as follows: First, the stereolithography and sprayed tooling processes are reviewed. The procedures for spraying SLA model patterns to build injection mold tooling are then described. A case study for manufacturing a geometrically complex plastic turbine-blade design using these processes is presented. The limitations of the sprayed tooling method are identified, and some potential solutions are suggested. A framework for planning robotic spraying is then presented. The robotic spray testbed facility is currently being built, including a robot with a coordinated positioning worktable, and a computer controlled arc spray system. Next, the geometric representation NOODLES and its applications to CAD/CAM modeling and process planning are described.

STEREOLITHOGRAPHY

Stereolithography is a process which quickly makes plastic prototypes of arbitrary geometric complexity directly from the computer models of the parts. The stereolithography apparatus (SLA) does not require experienced model makers, and the machine runs unattended once the building operation is started. It is relatively straightforward for the designer to program and run the SLA.

SLA is the product of 3D Systems, Inc. of Valencia, CA. Their system (Fig. 1) is composed of a vat of photosensitive liquid polymer, an x–y scanning ultraviolet laser beam with a 0.25 mm (0.01 in.) beam diameter, a z-axis elevator in the vat. The laser light is focused on the liquid's surface and cures the polymer, making solid forms wherever the light has scanned. The depth of cure is dosage-dependent. The physical object to be created, as described by a boundary representation model,[2] is first "sliced" into thin cross-sectional layers along the z-axis. For each slice, the laser's trajectory is dictated by the cross sections boundary and by the bounded region.

The elevator platform is initially positioned at the surface of the liquid. As the laser draws a cross section in the x–y plane, a solid layer is formed on the elevator platform. The

[2]In the 3D Systems device, this is a triangulated, planar surface PHIGS B-Rep

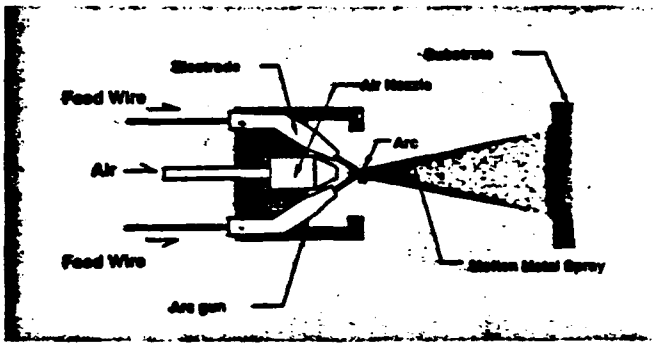

FIG. 2. Electric arc spraying

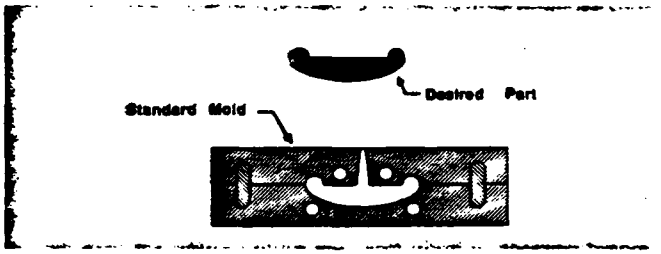

FIG. 3. Conventional mold

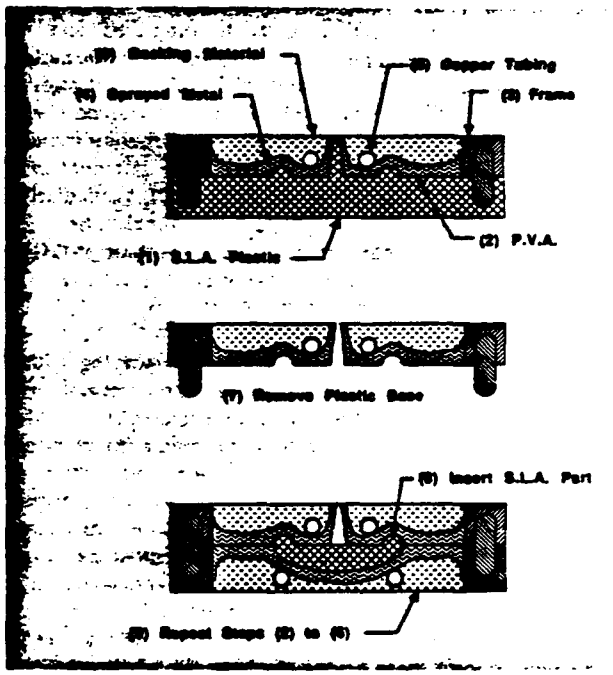

FIG. 4. Sprayed tool process

platform is lowered and then the next layer is drawn in the same way and adheres to the previous layer. The layers are typically between 0.13 and 0.5 mm (0.005 and 0.020 in.) thick. A three-dimensional plastic object thus grows in the vat, starting at the object's bottom and building to the top.

To save time, the SLA laser does not fully cure each cross section. Rather, the laser cures the boundary of a section, and then cures an internal structure, or honeycomb, that traps the uncured fluid. Top and bottom surfaces, on the other hand, are fully cured. These surfaces are cured by commanding the laser to draw the whole surface with overlapping lines; the result of this operation is called skin-fill. Final curing under separate ultraviolet lights solidifies the complete part. One of our goals is to enhance the SLA process by creating efficient slicing and vector generation algorithms which operate directly within the unifying geometric modeller NOODLES. An algorithm for this operation is described later. The current accuracy of SLA parts is of the order of 0.25 mm (0.010 in.), while surface texture is dependent on the building orientation. Additional postprocessing, such as carefully sanding and grinding the part, is therefore required for making accurate and smooth models. Since stereolithography is so new, we expect rapid improvements as the equipment and resins evolve with broadening commercial competition.

There is an engineering cost to preparing a part design for SLA construction. Support structures are added to the part to hold it together while it is being built, the part must be oriented in the vat for best surface quality and fastest build time, and SLA process parameters must be planned. One example of the latter is the choice of layer thicknesses in the part; they do not have to be constant throughout the part, and their choice has a first-order effect on the accuracy, the surface quality, and the build time of the part.

SPRAYED TOOLING

Tooling can be fabricated with arc spraying upon appropriate substrate patterns. Examples which demonstrate this process for fabricating injection molds using SLA patterns are described below and compared with conventional pattern-making techniques. The combination of stereolithography with thermal spraying provides a tooling fabrication process which builds directly upon prototype models. These models are rapidly produced and the ability to modify them for spraying applications is straightforward.

The concept of sprayed metal tooling has been in existence for decades [7]. Current commercial technology uses electric arc spraying. The arc spray process (Fig. 2) uses two spools of metal wire which are fed to a spray gun where the wire tips form consumable electrodes. A high current is passed through the electrodes creating an arc which melts the wire tips. The molten particles are atomized by a high pressure air jet directed at the arc and are accelerated in the air stream. These particles strike the surface where they flatten out and quickly solidify.

A conventional machined injection mold is shown in cross section in Fig. 3. The holes represent cooling/heating channels, and the injection geometry is that of a simple sprue gate. Alternatively, the fabrication steps for building a sprayed mold using SLA patterns are depicted in Fig. 4.

The steps are:

- **STEP 1:** Build SLA pattern used to make one mold half. This pattern is the complement of the interior of this mold half. In this example, the mold pattern includes the partial part shape, a parting plane, and sprue gate.
- **STEP 2:** Apply a water-soluble release agent onto the plastic pattern, such as polyvinyl alcohol (PVA), to facilitate separation of metal from plastic.
- **STEP 3:** Place a metal frame onto the pattern.
- **STEP 4:** Spray metal onto the pattern and around inside edge of frame. Alloyed zinc compositions are used for this particular process because of their relatively low re-

FIG. 5. Sprayed turbine blade mold

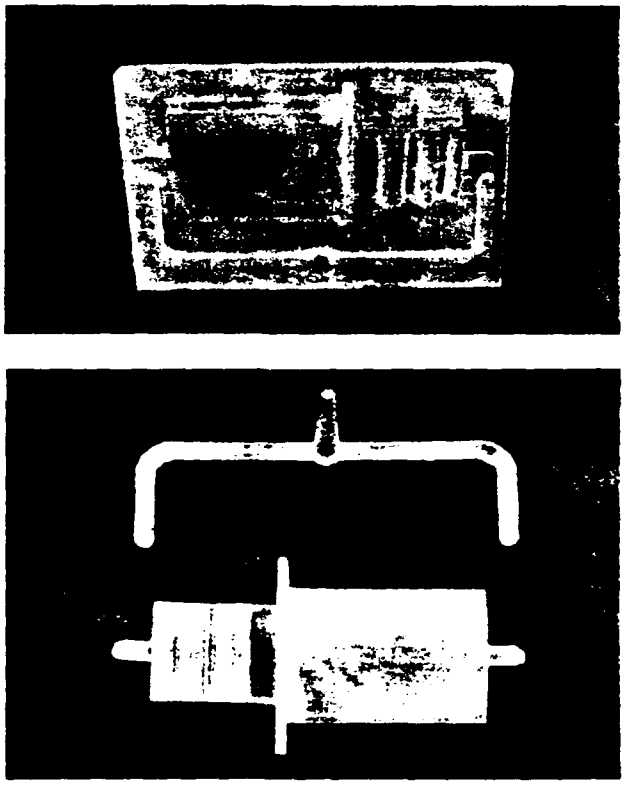

FIG. 6. SLA mold patterns: (A) pattern for first mold half; (B) inserts for second mold half.

sidual stress. Sprayed shell thicknesses are typically on the order of 2–7 mm. Fine pattern details are accurately replicated by this spray process.

- **STEP 5:** Lay in place copper tubing for heating and cooling channels for the injection mold process. Additional injection mold components, such as prefabricated ejector pin assemblies (not shown), can be added in STEP 1 and sprayed in place in STEP 4.
- **STEP 6:** Pour in a backing material to support the metal shell. Typical backing materials include epoxy mixed with aluminum shot.
- **STEP 7:** Separate the substrate pattern from the mold half. This is aided by dissolving the PVA in water. This completes the fabrication of the first mold half.

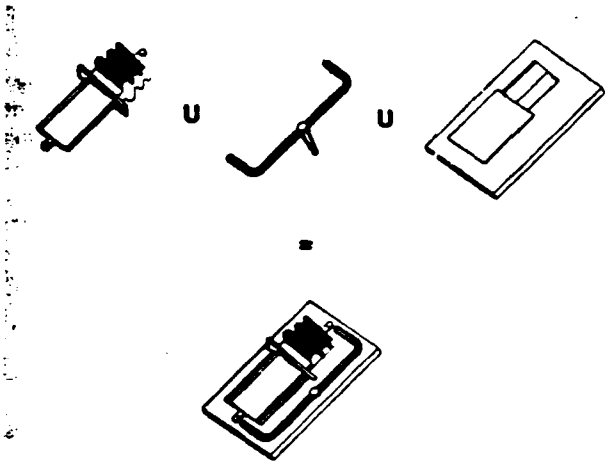

FIG. 7. Model of SLA pattern

- **STEP 8:** With SLA, build a model of the whole part to be molded, including runners and gates, and insert the model into the first mold half. This forms the pattern for spraying the second mold half.
- **STEP 9:** The second mold half is completed by repeating STEPS 2–7.

The mold fabrication is completed by removing the SLA insert.

Using these steps, we have fabricated the injection mold in Fig. 5 for making a polyethylene turbine blade. This example is interesting because of this shape's complexity and useful since molded plastic blades can be used for making castings for metal blades. This tool also includes a nonplanar parting surface and a complex runner system. The fabrication of this tool requires three SLA mold patterns, shown in Fig. 6 which can be built simultaneously in the vat. The first pattern in Fig. 6 is sprayed to make the first half of the mold. In contrast to the planar parting surface in the first example, the blade mold requires a nonplanar parting surface to permit ejection of the molded blade from the tool. To create this pattern, the computer models of the blade and runner are embedded into the parting plane model in Fig. 7 using simple union operators. Another major advantage of using SLA to create spray patterns is demonstrated by this nonplanar parting plane example. Conventionally, the first mold half can be prepared by partially embedding a complete prototype model of the part into, say, melted paraffin. The paraffin then cools to form a planar parting surface around the remaining partial part shape. With this approach it is difficult to sculpt nonplanar surfaces. Other approaches which build up parting planes with sheet-wax, clay, or plaster are tedious and difficult. Machining complex patterns is time-consuming and expensive. With SLA it is straightforward and relatively quick to build complex patterns, with nonplanar parting surfaces, and include the runner system in these models.

Once the first half of the mold is completed, the initial pattern is removed and SLA models of the blade with tab gates and the runner with the injection sprue gate are inserted into the mold cavities. The process is then repeated to build the second mold half.

Limitations

It has been estimated [7–9] that there can be an order of magnitude reduction in both the cost and time for producing injection mold tooling by thermal spraying in comparison with conventional machining methods. Similar savings could also be realized for manufacturing other types of tooling such as forming dies or EDM electrodes. The question arises: Why hasn't the use of sprayed metal tooling proliferated considering these potential savings? There are several reasons:

- **Zinc for Prototypes and Small Batch Applications:** Alloyed zinc is the only metal, as reported in the literature, to be commercially successful in the fabrication of sprayed tooling using the aforementioned steps. More involved spray processes for steel deposition have been described [10], and there are reports that a handful of shops have built sprayed steel tools.

  During the spraying process, molten metal is sprayed onto previously solidified layers of the shell. Residual stress is created in the shell by the shrinkage of the metal as it solidifies. This stress is intensified by the temperature gradient between cooler layers and the freshly deposited hot layer. The net effect of the residual stress is to limit the maximum thickness of the shell. The effect manifests itself when the shell peels away from the substrate as new layers are applied. Steel, stainless steel, and many other alloys demonstrate this problem; zinc, on the other hand, can be sprayed to significant thicknesses. There is no clear prediction of this behavior for layered spraying processes in the literature.

  Zinc-based tools are relatively soft and are used primarily in prototyping and low-batch production applications. Prototype tooling is used to make parts for marketing and customer evaluation and for preliminary part testing. Prototype tools are also used to evaluate a tool design (e.g., to assess gate locations in the runner system) before committing that design to a machined steel tool. Beyond prototype tools, the sprayed tool process should be extended to fabricating steel tools for production quality tooling.
- **Difficulty in Making Patterns:** The time and cost of making complex patterns with conventional machining is roughly the same as directly machining a tool. Thus, the benefits of sprayed tooling, including its speed and relatively low cost, are lost with conventional patternmaking techniques. Improved pattern-making abilities, such as provided for by SLA, should be pursued.
- **Poor Process Control:** The sprayed tool process is currently limited to manual spraying by a skilled technician who must adjust process parameters such as arc voltage, wire feed rate, and air pressure, as well as control the gun motion relative to the substrate. Errors in the technician's judgment, operator fatigue, and poor spray technique yield poor quality tooling. The difficulties in quality control are accentuated when spraying large shapes which may take days to spray. Further, a systematic study of spray parameters in relation to the structural quality of sprayed metal shells for tooling applications has not been reported in the literature. Therefore, methods and strategies to achieve consistent and predictable process performance must be developed.
- **Shapes That Are Hard To Spray:** The spray gun should ideally be aimed so that the trajectories of the atomized metal particles are close to the substrate's surface normals. This assures maximal splattering of the molten particles. Some part designs have geometric features which make it difficult to satisfy this condition. Particles which strike the surface tangentially (e.g., greater than about 45° from the normal) do not sufficiently splatter, resulting in either poor adhesion, increased porosity, or overspray. For example spraying concave surfaces with small aspect ratios (e.g., holes with small diameter-to-depth ratios) is difficult, if not impossible, since particles tend to strike the steep sidewalls at acute angles and bounce off into the hole. Therefore, alternative strategies and technologies should be investigated to extend the scope of geometries which can be effectively sprayed.

Several areas of research should be investigated to address these issues. We have identified and demonstrated the use of SLA for rapidly fabricating the complex mold patterns. Another element is to incorporate robotic spraying, driven by an off-line path planner which uses knowledge of metal spraying. The use of robotic automation has several ramifications. It will facilitate process control by its consistent and tireless performance and it can be easily integrated with sensory feedback (e.g., temperature measurement) for additional on-line control. We believe that the ability to reliably spray steel will require such tight process control. Complex shapes need tightly controlled spray trajectories. Robotic spraying will facilitate these trajectories. Off-line trajectory planning based on design models will not require tedious "teach by showing" operations, while the incorporation of process models to formulate spray strategies will improve spray performance compared to manual operation. This paper presents a framework for the robotic spray planning system.

For "hard-to-spray shapes" there are a number of possible directions to pursue. While the accurate aiming capability of robotic spraying will be helpful, the ability to spray concave shapes with small aspect ratios (e.g., small deep holes) is still limited by the divergence of particles from the spray gun and the limitation of spraying along the line of sight. The use of continuous detonation spray guns which have highly focused spray beams should be investigated for this application.

Ultimately the design system should account for "hard to spray shapes" by having up-to-date knowledge of the spray capabilities. Such a system should give feedback to the part designer about the manufacturing process ramifications of part geometry prior to the fabrication stage. Our system will build upon ongoing research at Carnegie Mellon on design for manufacturing [11] to provide such feedback.

ROBOTIC SPRAYING

The need to execute accurately spray paths based on process knowledge and to repeat consistently operations makes a robotic system essential in the rapid tool manufacturing domain. Arc spraying robots currently provide repeatability in surface coating applications [12, 13]. However, the spray paths are manually generated with a teach pendant for all but the simplest of part geometries. Automated and intelligent decision-making capabilities, using design models and process knowledge for off-line path generation, are absent from these systems.

Automated thermal spraying requires the scheduling of the arc spray parameters and the selection of the robot path. These parameters include: arc voltage, wire feed rate, atomiz-

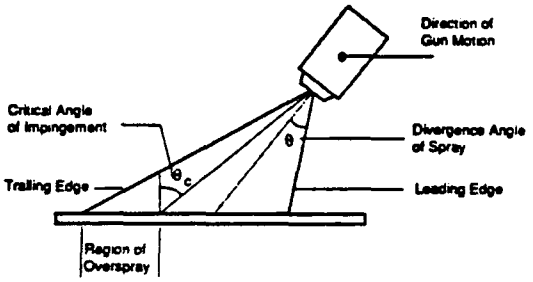

FIG. 8. Overspray

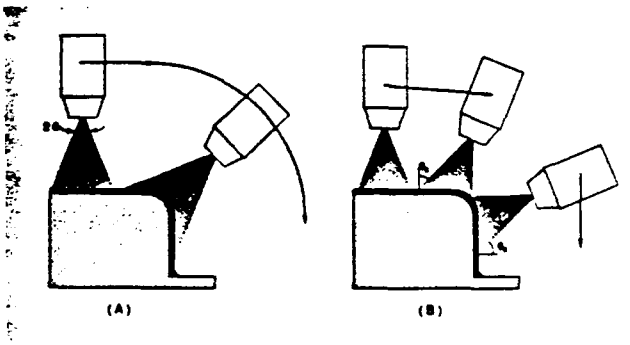

FIG. 9. Spray paths

ing gas pressure, atomizing gas type, wire diameter, and nozzle geometry. Many of these parameters are directly affected by the type of material being sprayed. Because the number of parameters is high, an experimental testbed is crucial to study systematically how these parameters affect shell quality. Some insight into this problem may be gained from published statistical methods for tuning the thermal spray process parameters to produce optimal thin surface coatings [14].

Although arc parameters directly affect the sprayed shell quality [15], the path of the gun is of equal importance. Robot paths must be found that traverse the substrate to deposit a uniform layer even when the substrate presents geometric features that make spraying difficult.

For example, consider overspray as shown in Fig. 8. Particle trajectories should align with the surface normals to assure maximal splattering of the molten particles. As the angle of impingement increases, that is, as the angle between the particle trajectory and the surface normal increase, the shell quality degrades. After some critical impingement angle θ_c, the particles bounce off the surface as wasted overspray or become entrapped in the shell reducing its strength. Although θ_c is a function of the spray parameters, $\theta_c = 45°$ has been used as a rule-of-thumb [16]. The amount of overspray generated is therefore dependent upon the gun orientation relative to the part surface. The following examples illustrate how this information can be accounted for in planning.

For a simple planning algorithm, the spray path is defined by a grid on the surface of the substrate. In this algorithm, the spray gun is oriented normal to the surface and follows each line of the grid with a constant standoff distance. This strategy is referred to as the surface-normal tracking strategy. To analyze the overspray performance of this strategy, consider the convex corner of the cross section shown in Fig. 9 (A). θ is defined as the spray divergence angle. There is no overspray so long as all of the spray hits a flat surface, the gun axis is perpendicular to the flat surface, and $\theta \leq \theta_c$. However, this strategy produces overspray on both the vertical and horizontal surfaces as the gun negotiates the corner.

An alternative two-step strategy (Fig. 9B) eliminates overspray for this example. As the gun approaches the corner, it is oriented so that the trailing edge of the spray cone makes an incident angle of θ_c. As the leading edge starts traversing the curved surface, its incident angle increases and spraying is stopped when it becomes θ_c. At this time both the leading and the trailing edges make incident angles of θ_c so that there is no overspray on any surface. The gun is then reoriented so that the leading edge makes an incident angle of θ_c with the vertical surface, and repositioned so that the trailing edge makes an incident angle of θ_c with the curved surface. Spraying is restarted from this position and proceeds down the vertical surface.

These two strategies demonstrate spray planning for a simplified two-dimensional case. In practice, strategies will have to be synthesized which account for the interaction of the spray cone with three-dimensional and more complex shapes, and which address a range of spray performance requirements. However, these examples demonstrate one important result. The first strategy only considers geometry, while the second strategy also considers process limitations; the framework of considering both geometry and process resulted in a superior strategy.

Robot paths must be found to traverse the workpiece given these process limitations. The basis of one approach to this problem is a planner based on geometry features, such as the corner feature of the example. A feature-based strategy uses extracted features to recognize spray problem areas, and then uses successful strategies, predetermined for each feature, to generate a robot path plan. The capability to define and extract three-dimensional features is being developed within the NOODLES environment [17]. One goal of our research is to identify a useful set of features for spray planning and to develop effective spray strategies for them.

The discovery of a good path for the spray torch is critical to successful robotic spraying. Equally critical is the translation of the torch's path into a complete, reachable, and smooth robot trajectory. It is simple to create trajectories that are unreachable by the robot. A second difficulty coming from off-line generated paths is the problem of creating paths that result in smooth robot motion. The tool manufacturing system will build upon robot path optimization research at Carnegie Mellon [18]. This work addresses both the reachability and path smoothness challenges.

NOODLES MODELING

The representational requirements for modeling systems, including the levels of abstraction, the nature of the analyses, and the geometric manipulations, vary with the context of the model's use. In CAD/CAM applications, the models for design, analysis, and evaluation, and fabrication are quite different for each subsystem. In typical systems numerous modeling environments are incorporated to satisfy the requirements of each subsystem. An approach which incorporates several different modeling environments has several drawbacks. First, it is error-prone and inefficient since models must be transformed between each separate environment. Second, nonuniform data structures make the software difficult to manage.

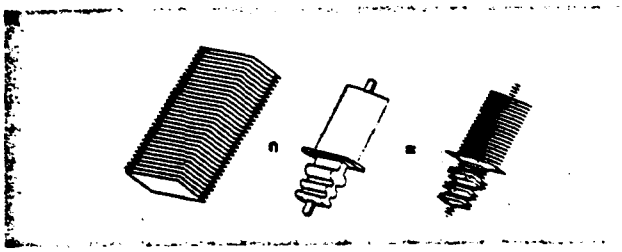

FIG. 10. Slicing with NOODLES.

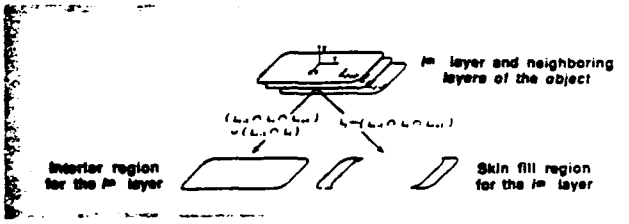

FIG. 11. Locating skin-fills and interiors with NOODLES

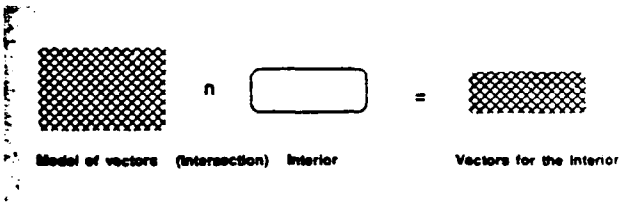

FIG. 12. Vector generation with NOODLES

Finally, it is not easily extendible to new system applications which may require a mixture of the attributes of different environments. We feel the key to successful integration is to provide a modeling environment in which design models, description of prototype models, and manufacturing methods are uniformly treated. To address this issue, our manufacturing system is built upon a geometric modeling environment, NOODLES [19], where subsystem models share a common representational and manipulation scheme.

The following examples demonstrate some of the diverse modeling requirements for this CAD-based manufacturing system:

- The user designing a part should be allowed to select the appropriate modeling description paradigm depending upon the immediate need. For example, designs, at times, can best be synthesized using constructive solid geometry, or building solids up from sets of surfaces, while, at others, sweeping lower-dimensional elements, such as curves and surfaces, into solid representations produce more satisfactory results.
- The SLA process planner must convert solid models into an ordered set of $2\frac{1}{2}$ D cross sections (i.e., cross sections with an associated depth or thickness) and span these cross sections with appropriate drawing vectors. This operation inherently involves working simultaneously in several dimensions since one generates planes from solid models, and then vectors, or line segments, from the planes.
- The robotic spray planner operates with yet other abstractions. Grids are projected onto the object's shell to produce surface patches which are analyzed for spraying action. In turn, the spraying actions are modeled as curvilinear paths which sweep the relevant portions of the tool geometry into volumes for interference testing. At this level, assessing the interference is not constrained to be intersections between solids, but also intersections between surfaces and surfaces, or surfaces and solids.
- Features are the most complex level of abstraction for this system. The spray planning system, for example, needs to extract convex corner features from the geometric descriptions in order to aim properly the spray to avoid overspray.

Geometric modeling can be performed at various levels, such as wire-frame, surface, or solid modeling. The previous examples suggest that all levels are required in the system. Although solid modeling approaches have the richest information, the representation of lower level elements such as lines and surfaces is not explicit. Furthermore, operations provided within solid modeling approaches do not apply when nonsolid elements are used. The ideal geometric modeling system should uniformly represent and operate on nonhomogeneous (i.e., mixed dimensions) elements such as vertices, lines, surfaces, and solids. NOODLES offers an environment where nonhomogeneous elements are uniformly represented and permits Boolean operations between elements of any dimensionality.

One example which uses nonhomogeneous representations is the planning of the layered shape deposition processes. The first step is to obtain the cross sections of the object. These sections are obtained from the Boolean intersection between the object and a stack of planar faces that are appropriately spaced. Figure 10 shows that the result of this nonregular operation is a collection of cross sections. Identification of the interior and skin-fill areas for SLA applications can also be achieved with set operations. The intersection between the projections of contiguous cross sections identifies the interior area; the differences between these cross sections produce the skin-fill areas (Fig. 11). Finally, the vectors to be scanned by the laser are obtained by intersecting appropriate grids with the portions of the cross section. For example, as shown in Fig. 12, the interior area of a cross section is intersected with a cross hatch grid. The object boundaries for the laser are quickly found from the perimeters of the cross sections. Similarly, the grids for robotic path planning are defined by the perimeters of the intersection of the surface boundary of the object with two perpendicular sets of stacks of planar faces.

A feature extraction algorithm is also being developed which automatically recognizes form features of objects represented in NOODLES [17]. This algorithm uses a graph grammar to describe and recognize shape features, based on an augmented topology of the modeled objects which contain these features. The NOODLES representation provides the information for construction of the augmented topology graphs. These graphs constitute the search space for the recognition of the subgraphs which correspond to the features. In injection molding, features like ribs and bosses are recognized in this manner [20]. Once a feature is recognized by mapping the descriptive subgraph into the object graph, various regimes in the subgraph are also identified with their counterparts in the surface model. The relevant attributes for a feature can thus be evaluated by referring to the actual representation. For instance, the draft angle attributes of the rib features in an injection molded part is very relevant for assessing ejectability.

When a rib is recognized by identifying certain surfaces on the object with the opposing sides of the rib, the draft angle can be computed using the geometric information in the model.

FUTURE WORK

The extension of this system to superior prototype tools and production-quality tooling will require further research and development into steel-based sprayed tools. High-volume production-quality manufacturing and prototype tools used for high impact loading applications, such as stamping, require steel tooling. This requires not only the capability to spray steel shells, but also to develop complementary backing materials. These materials must have matching coefficients of thermal expansion with steel, and have sufficient ruggedness and strength. This backing requirement may be extremely difficult to achieve for mass production tools requiring tens of thousands of loading cycles and high impact resistance. An incremental approach would be to first develop backing materials for *low-batch* production steel tools. Such tools would have several advantages:

1. Die designs first prototyped in zinc-based alloys, including those conventionally machined from Kirksite, often do not adequately predict the performance of their machined steel counterparts. Surface frictional and thermal characteristics differ for these materials. The machined steel dies must then be further iterated to achieve acceptable performance. This process is costly and time-consuming. Sprayed steel prototype tools would more accurately predict the performance of machined steel tools and would reduce the number of redesign/refabrication iterations.
2. If sprayed steel tools could be made *on-demand* and inexpensively and also be able to withstand thousands of cycles, then multiple tools could be produced as needed for use in production. This gives the advantage of quicker response to market demands.

Our initial experimentation shows that 420 stainless steel, for example, can be deposited onto SLA parts without distorting the plastic. However, the process for steel is less forgiving than for zinc. Therefore, robotic spraying seems to be critical to *reliably* and *consistently* spray steel. One significant challenge for steel spraying will be to find a release agent which meets the needs of withstanding the heat of the molten metal, of being strong enough to hold the sprayed metal in the presence of considerable stress, and of releasing after spraying. Release agents, currently proprietary, exist which begin to satisfy these requirements.

Another approach to fabricating production quality tooling is to use electric discharge machining (EDM) to form high-quality steel dies. The EDM process can be enhanced for forming complex shapes by first manufacturing the EDM electrodes using the SLA/thermal spray system concept; this reduces the costs and time to produce the electrodes. Multiple electrodes are typically required for roughing and then for fine detail and each can quickly be made with spraying. The roughing die can be an SLA made part, thinly coated with copper. The process for the final electrode would include: Build an SLA die pattern of the complement of the desired EDM shape, add a frame, spray the die pattern with copper, insert electrode conductor wire, and finally back up the copper shell.

CONCLUSION

This paper presents a framework for a rapid tool manufacturing system based upon the integration of stereolithography and thermal spraying. These processes are particularly well suited for building complex shapes. The basic fabrication processes have been demonstrated experimentally, the system issues have been identified, and our current research directions have been outlined including automated spraying and geometric modeling. A testbed is being built within this framework. We feel that a testbed based on stereolithography and thermal spraying integrated in a unifying CAD/CAM environment will help prove the promise of timely and cost-effective tool manufacture.

The ultimate goal of our research will be to develop a system capable of quickly manufacturing sprayed steel tooling in a cost-effective fashion.

REFERENCES

1. Deckard, C R (1987). Recent Advance in selective laser sintering, in *Fourteenth conference on production research and technology*, NSF, Ann Arbor, MI, October.
2. Colley, D P (1988). Instant Prototypes, *Mechanical Engineering*, July.
3. Hauber, D (1987). Automated fabrication of net shape microcrystalline and composite metal structures without molds, in *Manufacturing processes, systems and machines: 14th conference on production research and technology*, S K Samanta, Ed., NSF, Ann Arbor, MI, October
4. Sachs, E (1989). Three dimensional printing: rapid tooling and prototypes directly from a CAD model, in *Advances in manufacturing systems engineering*, ASME, Winter Annual Meeting, 1989.
5. Hayes, C, and Wright, P (1989) Automating process planning: using feature interactions to guide search, *Journal of Manufacturing Systems*, 8(1).
6. Cutkosky, M R, and Tenenbaum, J M (1987) CAD/CAM integration through concurrent product and process design, in *Proceedings of the symposium on intelligent and integrated manufacturing*, ASME, December
7. Garner, P J (1971). New mold making technique, *SPE Journal*, 27(5), May
8. Menges, G (1986). *How to make injection molds*, Hanser Publishers, Munich, Vienna, New York.
9. Thorpe, M L (1980) Progress report: sprayed metal faced plastic tooling, Tech. Report 5, Tafa Inc., November
10. Walkey, G J, and Adgate, F N. Metal dies, U.S. Pat 3,533,21, 1970
11. Finger, S, Fox, M, Navinchandra, D, Prinz, F B, and Rinderle, J (1988) Design fusion: a product life cycle view for engineering designs, *IFIP workshop on intelligent CAD*, IFIP, September
12. Metco Inc. (1985). Six axis robot developed for thermal spray coating, *Robotics World*, February.
13. Tafa Inc. (1985). Arc spray robot can coat at twice manual speed, *Robotics World*, March.
14. Van Doren, S L (1984) A statistical method of plasma spray parameter testing in *Proceedings of the second national conference on thermal spray*, ASM, Long Beach, CA, October
15. Thorpe, M L (1988) How recent advances in arc spray technology have broadened the ranges of applications, in *Thermal spray technology new ideas and processes*, ASM International, October.
16. Franklin, J (1986). Designing for thermal spraying, *Engineering*, July/August.
17. Pinilla, J M, Finger, S, and Prinz, F B (1989). Shape feature description and recognition using an augmented topology graph grammer, in *Engineering design research conference*, NSF, Amherst, MA, June
18. Hemmerle, J S (1989). *Optimal path placement for kinematically redundant manipulators*, PhD dissertation, Carnegie Mellon University
19. Gursoz, E L, Choi, Y, and Prinz, F B (1988). Vertex-based representation of non-manifold boundaries, in *Second workshop on geometric modelling*, M J Wozny, J Turner, and K Preiss, Ed., IFIP, New York, September.
20. Gadh, R, Hall, M A, Gursoz, E L, and Prinz, F B, (1989) Knowledge driven manufacturability analysis from feature-based representations, in *Symposium on concurrent product and process design*, ASME, San Francisco, December

Lee E. Weiss is a Research Scientist in the Robotics Institute and in the Engineering Design Research Center of Carnegie Mellon University. He is also the Staff Scientist for The Department of Radiology of Shadyside Hospital in Pittsburgh. His current research interests include rapid tool manufacturing and biomedical applications of micromechanisms.

E. Levent Gursoz is a Research Scientist in the Engineering Design Research Center at Carnegie Mellon University. He is the principal developer of the NOODLES geometric modeling system. His current research interests include nonmanifold geometric modeling and intelligent manufacturing systems.

Friedrich B. Prinz is a Professor in the Department of Mechanical Engineering and Director of the Engineering Design Research Center at Carnegie Mellon University. His current research interests focus on geometric modeling, intelligent design, rapid prototyping, and manufacturing. Professor Prinz is also a member of the Robotics Institute, where he works on model-based robot programming and robot calibration.

Paul S. Fussell is currently working on a Ph.D. in Mechanical Engineering at Carnegie Mellon University, and he is located at the Alcoa Technical Center in Pittsburgh. He has worked on robot controller designs, implementations, and more recently on robot process integration. His current research interests include rapid manufacture of sprayed steel tooling.

Swami Mahalingam is a Ph.D. student in Mechanical Engineering at Carnegie Mellon University. His research interests are in robot path planning. His previous work includes gait planning for autonomous walking robots. His current focus is on planning paths for robotic spraying applications.

Edward P. Patrick is a Senior Technical Specialist in the Product Manufacturing Technology Division of Alcoa Laboratories. He has been a principal in developing manufacturing processes for aluminum heat exchangers, lightweight automotive wheels, and autobody structure. He is currently involved with the development of processes for manufacturing advanced sprayed tooling.

US005079974A

United States Patent [19]

Weiss et al.

[11] Patent Number: 5,079,974

[45] Date of Patent: Jan. 14, 1992

[54] **SPRAYED METAL DIES**

[75] Inventors: **Lee E. Weiss**, Pittsburgh; **Lawrence L. Schultz**, Gibsonia, both of Pa.

[73] Assignee: **Carnegie-Mellon University**, Pittsburgh, Pa.

[21] Appl. No.: **705,321**

[22] Filed: **May 24, 1991**

[51] **Int. Cl.**[5] **B21K 5/20**; B21D 37/20; B22C 7/00

[52] **U.S. Cl.** **76/107.1**

[58] **Field of Search** ..... 76/107.1, 101.1, DIG. 6

[56] **References Cited**

U.S. PATENT DOCUMENTS

2,944,338	7/1960	Craig	76/107.1
3,533,271	10/1970	Walkey et al.	76/107.1
4,231,982	11/1980	Jansson	76/107.1

FOREIGN PATENT DOCUMENTS

0110139	6/1983	Japan	76/107.1
0034230	2/1990	Japan	76/107.1

Primary Examiner—Roscoe V. Parker
Attorney, Agent, or Firm—Ansel M. Schwartz

[57] **ABSTRACT**

A method for forming a sprayed metal die comprising the steps of first building a positive pattern of the die. Then, there is the step of spraying a first metal, having a first melting temperature, onto the pattern to form a first metal substrate. Next, there is the step of separating the pattern from the first metal substrate. Next, there is the step of spraying a second metal, having a second melting temperature higher than the first melting temperature, onto the first metal substrate to form a second metal substrate which bonds to the first metal substrate to resist shrinkage due to residual stress within the second metal substrate. Next, there is the step of heating the first and second substrates to a temperature higher than the first melting temperature, yet lower than the second melting temperature, to melt away the first metal substrate from the second metal substrate.

17 Claims, 1 Drawing Sheet

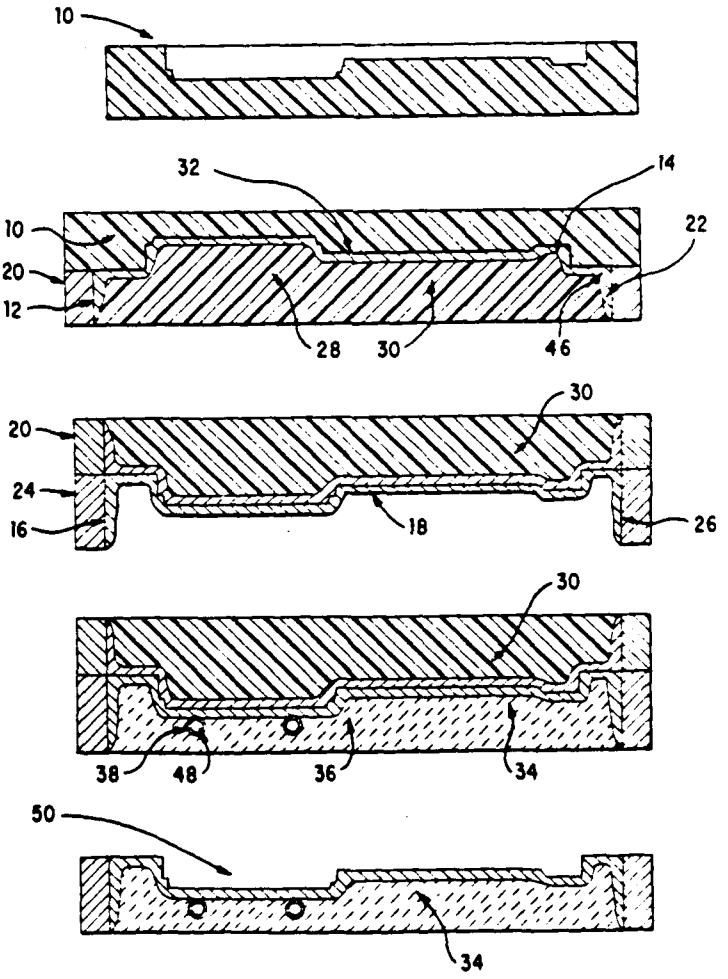

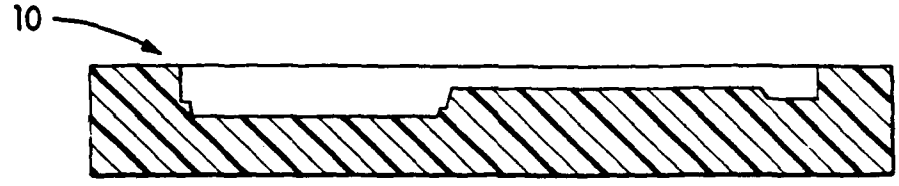

FIG. 1A

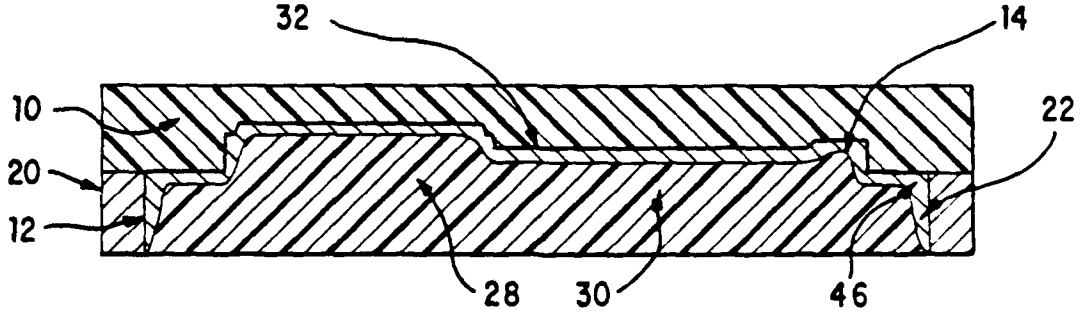

FIG. 1B

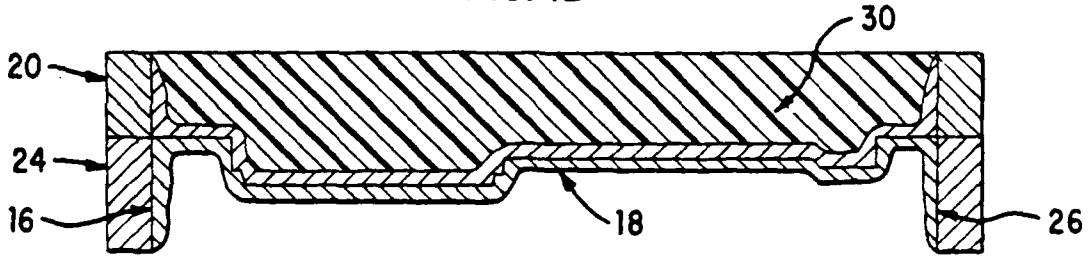

FIG. 1C

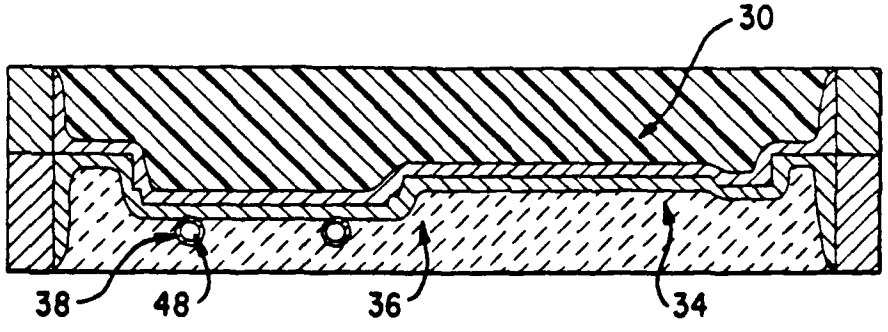

FIG. 1D

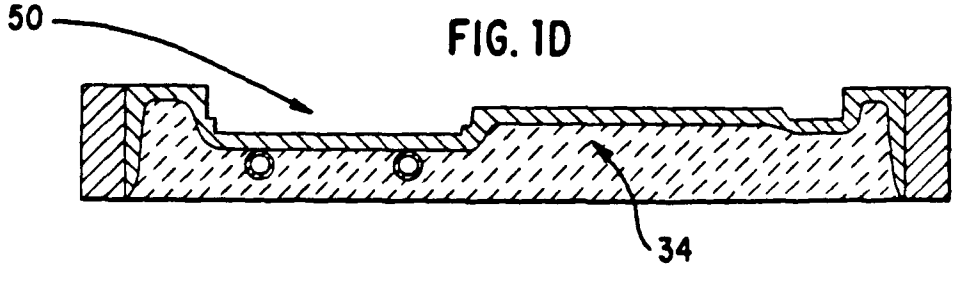

FIG. 1E

SPRAYED METAL DIES

FIELD OF THE INVENTION

The present invention is related to sprayed metal tooling. More specifically, the present invention is related to a method for resisting shrinkage of sprayed metal dies.

BACKGROUND OF THE INVENTION

As part of the complete design cycle, CAD representations must ultimately be converted into physical forms including prototype parts and tooling to manufacture the parts. The ability to quickly fabricate physical shapes, to minimize the time and cost required to reiterate designs, is one key to manufacturing competitiveness. A sprayed metal tooling system provides a method to rapidly build custom tooling directly from prototype patterns quickly produced, for instance, with stereolithography apparatus (SLA). The sprayed metal tooling process uses thermal spraying, for instance, electric arc spraying whereby metal wire is fed to a torch, melted in an electric arc, gas atomized, and sprayed onto a substrate surface. On contact, the sprayed material solidifies and forms a surface coating. Spray coatings can be built up by depositing multiple bonded layers which, when separated from the substrate, form a free-standing shell with the shape of the substrate surface. By mounting the shell in a frame, and backing it with appropriate materials, a die can be fabricated. For example, the cavities of prototype injection models can be fabricated by direct deposition of zinc metal onto plastic SLA models of the desired part and backing the frame shell with epoxy resins. Sprayed metal tooling is described more fully in U.S. Pat. No. 3,533,271 to Burbank et al.

Steel, however, cannot be effectively deposited by the sprayed metal tooling process. In practice, during the spraying of the molten steel, residual stress is created in the steel shell as it solidifies. This residual stress causes the steel to peel away from the substrate as new layers are applied. Not only steel but many other alloys with high melting temperatures exhibit this problem.

Zinc and zinc alloys, in contrast, can be sprayed to significant thicknesses with nominal shrinkage to form an accurate shell. Previous processes for making sprayed steel tooling required that release agents, such as PVA, first be applied to the patterns. The release agent helps to hold the sprayed metal in place. The patterns could be machined or made with solid-freeform-fabrication techniques. However, PVA is not effective in holding sprayed steel in place because of the extremely high residual stress associated with sprayed steel. Thus, sprayed steel tends to peel off the pattern after a thin layer has been built-up. In addition, PVA tends to burn-off when high melting point metals, such as steel, are sprayed onto it.

In the present invention, a low melting point metal is first sprayed onto the pattern. The low melting point metal can withstand the heat of the rapidly solidifying sprayed metal and, in fact, it helps conduct the heat away. More importantly, the low melting point metal clamps the steel down, by local anchoring, until a backing material can be poured to mechanically stabilize the sprayed shell. The present invention provides a method for accurately forming steel shells on a pattern, such as those produced with a stereolithography apparatus, by resisting shrinkage due to high residual stresses within the shell during a spray tooling process.

SUMMARY OF THE INVENTION

The present invention pertains to a method for forming a sprayed metal die comprising the steps of first building a positive pattern of the die. Then, there is the step of spraying a first metal, having a first melting temperature, onto the pattern to form a first metal substrate. Next, there is the step of separating the pattern from the first metal substrate. Then, there is the step of spraying a second metal, having a second melting temperature higher than the first melting temperature, onto the first metal substrate to form a second metal substrate which bonds to the first metal substrate to resist shrinkage due to residual stress within the second metal substrate. Next, there is the step of heating the first and second substrates to a temperature higher than the first melting temperature, yet lower than the second melting temperature, to melt away the first metal substrate from the second metal substrate.

In a preferred embodiment, the building step incudes the step of building the positive pattern by solid freeform fabrication, such as stereolithography. Preferably, after the building step, there is the step of mounting a first frame on the pattern and the step of spraying a first metal includes the step of spraying the first metal around an inside edge of the first frame. Preferably, after the separating step, there is the step of mounting a second frame onto the first metal substrate and the step of spraying a second metal includes the step of spraying the second metal around an inside edge of the second frame.

In a more preferred embodiment, before the separating step, there is the step of pouring a first backing material onto the first metal substrate to support it. Preferably, the first backing material is comprised of epoxy. Alternatively, the backing material can be the first metal and is formed by continual spraying until it is built up to the proper thickness. Furthermore, before the spraying a first metal step, there is the step of applying a releasing agent to the pattern. Preferably, the releasing agent is polyvinyl alcohol. It is also preferable after the step of spraying a second metal, the step of pouring second backing material onto the second metal substrate to support it.

In an even more preferred embodiment, before the second pouring step, there is the step of orienting cooling channels about the second metal substrate. Further, the second backing material is comprised of an opposite backing material, such as a castable material, for instance, epoxy or ceramic.

BRIEF DESCRIPTION OF THE DRAWINGS

In the accompanying drawings, the preferred embodiments of the invention and preferred methods of practicing the invention are illustrated in which:

FIGS. 1*a*-1*e* are schematic representations showing a first embodiment of the sprayed metal die process of the present invention.

DESCRIPTION OF THE PREFERRED EMBODIMENT

Referring now to the drawings wherein like reference numerals refer to similar or identical parts throughout the several views, and more specifically to FIG. 1 thereof, there is shown a method for forming a sprayed metal die. The method comprises the steps of

first building a positive pattern **10** of the die. Then, there is the step of spraying a first metal **12**, having a first melting temperature, onto the pattern **10** to form a first metal substrate **14**. Next, there is the step of separating the pattern from the first metal substrate **14**. Then, there is the step of spraying a second metal **16**, having a second melting temperature higher than the first melting temperature, onto the first metal substrate **14** to form a second metal substrate **18** which bonds to the first metal substrate **14** to resist shrinkage due to residual stress within the second metal substrate **18**. Next, there is the step of heating the first and second substrates, **14** and **18**, to a temperature higher than the first melting temperature, yet lower than the second melting temperature, to melt away the first metal substrate **14** from the second metal substrate **18**. The heating step can be accomplished with the use of a torch or placing the first and second substrates **14**, **18** into a furnace.

In a preferred embodiment, the pattern **10** is built by solid freeform fabrication, such as stereolithography. After the building step, there is preferably the step of mounting a first frame **20** on the pattern **10**. Preferably, the step of spraying a first metal **12** includes the step of spraying the first metal **12** around the inside edge **22** of the first frame **20**. Preferably, after the separating step, there is the step of mounting a second frame **24** onto the first metal substrate **14**. Preferably, the step of spraying a second metal **16** includes the step of spraying the second metal **16** around the inside edge **26** of the second frame **24**. Next, before the separating step, there is the step of pouring a first backing material **28** onto the first metal **12** to support it. Preferably, the backing material **28** is comprised of epoxy **30**. Further, there is a step of applying a releasing agent **32** to the pattern **10**, before the step of spraying a first metal **12**. Preferably, the releasing agent **32** is PVA (polyvinyl alcohol), although, for instance, teflon can also be used.

In a further preferred embodiment, after the step of spraying the second metal, there is the step of pouring a second backing material **34** onto the second metal substrate **18**. The second backing material **34** can be any appropriate material that will serve as backing. Preferably, the second backing material **34** is comprised of an epoxy or chemically bonded ceramic **36**. Furthermore, before the pouring of a second backing material **34**, there is preferably the step of orienting cooling channels **38** about the second metal substrate **18**.

If a die requires two halves, then the above described process can be used to form a first die half and the complete die is made by forming a mating die half with the first die half. Preferably, this is accomplished by repeating the above steps used to form the first die half to form the mating die half.

In the operation of the preferred embodiment, a positive pattern **10** of the die is constructed using the process of stereolithography. Stereolithography, is well known in the art, and is a process which quickly constructs plastic prototypes of arbitrary geometric complexity directly from the computer models of the parts or dies. In this manner, stereolithography is used to build a positive pattern **10** of the desired die part in plastic. Further information on using stereolithography to produce patterns **10** is disclosed in *Advances in Manufacturing Systems Engineering*, ASME, Winter Annual Meeting, 1989.

A first frame **20** of aluminum or carbon steel is then constructed and mounted onto the pattern **10**. A release agent of polyvinyl alcohol (PVA) is then applied to the pattern **10** and frame **20**. Next, a first metal **12** is sprayed onto the pattern **10** to form a first metal substrate **14**. The first metal **12** has a first melting temperature which is greater than that of the plastic pattern **10**.

Cerro metal alloys, manufactured by Cerro Metal Products Co., P.O. Box 388, Bellefonte, Pa. 16823, were found as suitable materials for the first metal **12**. Cerro metal has a melting temperature between 150° F. and 340° F. and is sprayed onto the pattern using a thermal spray gun whereby Cerro metal is melted, atomized and sprayed onto the pattern **10**. On contact, the sprayed Cerro metal solidifies and forms a substrate **14** which is comprised of Cerro metal. As shown in FIG. **1***b*, the Cerro metal is sprayed around the inside edge **26** of the aluminum frame **20** to form a lip **46** which serves to support the frame **20**. Electric arc spraying is well known in the art, and is fully explained in *New Die Making Technique*, SPE Journal, 27(5), May 1989. Spraying Cerro metal to a thickness of at least 1 mm was found to be sufficient.

Next, epoxy **30** is poured onto the substrate **14** of Cerro metal and within the frame **20** to form a backing material. After the epoxy **30** sets, the substrate **14** is separated from the pattern **10**. The PVA allows for easy separation. The epoxy **30** supports the substrate **14** of Cerro metal as it is separated from the pattern **10**. Next, a prefabricated second frame **24** is mounted onto the substrate **14**. The frame **24** is preferably comprised of steel and rests on frame **20** as shown in FIG. **1***b*. A clamp (not shown) is used to hold the frame **20** to frame **24**. Next, steel is sprayed onto the first substrate **14** of Cerro metal and within frame **24** to form a second metal substrate **18** comprised of steel. The steel must be applied in thin layers and allowed to sufficiently cool between layers so as not to overheat the substrate **14** of Cerro metal. The steel is applied to a thickness of approximately 0.75 mm.

The sprayed steel anchors to the surface **52** of the Cerro metal by superficially melting and abrading the surface **52**. This anchoring prevents the second substrate **18** from shrinking due to the residual stress created as the steel cools. The first substrate **14** of Cerro metal, therefore, serves to shape the sprayed steel and anchor it to the pattern **10**.

Next, copper tubing **48** is oriented about the substrate **18** of steel, to form cooling channels **38**. The cooling channels **38** improve the heat transfer properties of the finished die **50** which is necessary during the casting of aluminum or injection molding. Next, a backing of a chemically bonded ceramic **36** or epoxy is poured onto the second substrate **18** of steel to encase the copper tubing **48** and to substantially fill the frame **24**. The ceramic **36** serves to support the second substrate **18** during the operation of the die **50**. Finally, the first substrate **14** of Cerro metal and the second substrate **18** of steel are heated to at least the melting temperature of the Cerro metal (150°-340°) to melt away the Cerro metal from the steel. The frame **20** of aluminum can then be removed, leaving behind the desired die **50** comprised of the second steel substrate **18**, backed by ceramic **36** and surrounded by the steel frame **24**.

Although the invention has been described in detail in the foregoing embodiments for the purpose of illustration, it is to be understood that such detail is solely for that purpose and that variations can be made therein by those skilled in the art without departing from the spirit and scope of the invention except as it may be described by the following claims.

What is claimed is:

1. A method for forming a sprayed metal die comprising the steps of:

building a positive pattern of the die;

spraying a first metal, having a first melting temperature, onto the pattern to form a first metal substrate;

separating the pattern from the first metal substrate;

spraying a second metal, having a second melting temperature higher than the first melting temperature, onto the first metal substrate to form a second metal substrate which bonds to the first metal substrate to resist shrinkage due to residual stress within the second metal substrate; and

heating the first and second substrates to a temperature higher than the first melting temperature, yet lower than the second melting temperature, to melt away the first metal substrate from the second metal substrate to form the die.

2. A method as described in claim 1 wherein the building step includes the step of building the positive pattern by solid freeform fabrication.

3. A method as described in claim 2 wherein the building step includes the step of building the positive pattern by stereolithography.

4. A method as described in claim 3 including after the building step, the step of mounting a first frame on the pattern; and wherein the step of spraying a first metal includes the step of spraying the first metal around an inside edge of the first frame.

5. A method as described in claim 4 including after the separating step, the step of mounting a second frame onto the first metal substrate; and wherein the step of spraying a second metal includes the step of spraying the second metal around an inside edge of the second frame.

6. A method as described in claim 5 including before the separating step, the step of pouring a first backing material onto the first metal substrate to support it.

7. A method as described in claim 6 wherein the first backing material is epoxy.

8. A method as described in claim 7 which includes before the spraying a first metal step, the step of applying a releasing agent to the pattern.

9. A method as described in claim 8 wherein the releasing agent is comprised of polyvinyl alcohol.

10. A method as described in claim 9 which includes after the spraying a second metal step, the step of pouring a second backing material onto the second metal substrate to support it.

11. A method as described in claim 10 which includes before the second pouring step, the step of orienting cooling channels about the second metal substrate.

12. A method as described in claim 11 wherein the second backing material is comprised of a chemically bonded ceramic or epoxy.

13. A method as described in claim 1 wherein the die is a first die half; and including after the heating step, the step of forming a mating die half with the first die half.

14. A method as described in claim 13 wherein the step of forming the mating die half includes the steps of:

building a positive pattern of the mating die half;

spraying the first metal onto the pattern to form a third metal substrate;

separating the pattern from the third metal substrate;

spraying the second metal onto the third metal substrate to form a fourth metal substrate which bonds to the third metal substrate to resist shrinkage due to residual stress; and

heating the second and third substrates to a temperature higher than the first melting temperature, yet lower than the second melting temperature to melt away the third metal substrate from the fourth metal substrate to form the mating die half.

15. A method as described in claim 5 including before the separating step, the step of spraying continually the first metal to form a backing to support the first metal substrate.

16. A method as described in claim 15 which includes before the spraying a first metal step, the step of applying a releasing agent to the pattern.

17. A method as described in claim 16 which includes after the spraying a second metal step, the step of pouring a second backing material onto the second metal substrate to support it.

* * * * *

CONTROLLED MICROSTRUCTURE OF ARC SPRAYED METAL SHELLS

P. S. Fussell, H. O. K. Kirchner,
F. B. Prinz, L. E. Weiss

EDRC 24 - 57 - 91

May 1991

CONTROLLED MICROSTRUCTURE OF ARC SPRAYED METAL SHELLS

P. S. FUSSELL
Alcoa Laboratories
Alcoa Center, Pennsylvania 15069 USA

H. O. K. KIRCHNER
Institut de Sciences des Matériaux
Université Paris-Sud F 91405 Orsay, Cedex, FRANCE

F. B. PRINZ
Engineering Design Research Center
Carnegie Mellon University
Pittsburgh, Pennsylvania 15213 USA

L. E. WEISS
Robotics Institute
Carnegie Mellon University
Pittsburgh, Pennsylvania 15213 USA

13 May 1991

Abstract—Shells made of sprayed ferrous materials are becoming newly feasible for prototype and limited production tooling. A systematic study of the microstructure of arc-sprayed ferrous structures is presented demonstrating why these structures display a degree of mechanical anisotropic behavior. To address this effect, the results of controlling oxide with inert atomization gases are presented, and methods for tailoring the composition and orientation of the lamellæ through robotically controlled deposition are shown.

Zusammenfassung—Aus gesprühtem Stahl hergestellte Gussformen können für Prototypen und für Kurzserien bestimmte Werkzeuge verwendet werden. In einer systematischen Studie der Mikrostruktur von lichtbogengesprühten Stahlschichten wird dargelegt, warum diese Strukturen grosse mechanische Anisotropie zeigen. Durch Zerstäubung mit inertem Gas wird der Oxidgehalt gesenkt. Die Aufbringung der Schichten wird durch Roboter gesteuert, dies erlaubt, die Zusammensetzung und Orientierung der aufgebrachten Schichten zu kontrollieren.

CONTENTS

FIGURES AND TABLES

1. Rapid Tooling

Rapid manufacturing of tooling for injection molding, stamping, composite layup or similar processes where the shape of the tool is critical is a challenging problem with considerable commercial potential [1]. The creation of such tooling by arc–spraying zinc and zinc alloys has been in the commercial literature for at least 25 years [2], and thick sprayed zinc structures have been in the literature for 65 years [3]. These alloy systems, however, are relatively soft and prone to wear and loading failure; their usefulness is largely limited to prototype tooling applications and low pressure applications such as reaction injection molding tooling. Tools made from ferrous systems[4, 5], as shown in Figure 1, are of far greater applicability, both for superior prototyping and limited production. They present much greater wear resistance compared to zinc systems, they are stronger, and they withstand the demands of elevated temperature service. Further, the demands of the injection molding application are well matched to the ferrous shell structures produced by arc spray, particularly the support of hoop stresses in the tool structure, the tolerance of compressive in the the ferrous shell, and the tool face wear resistance to abrasive plastics such as glass filled nylon.

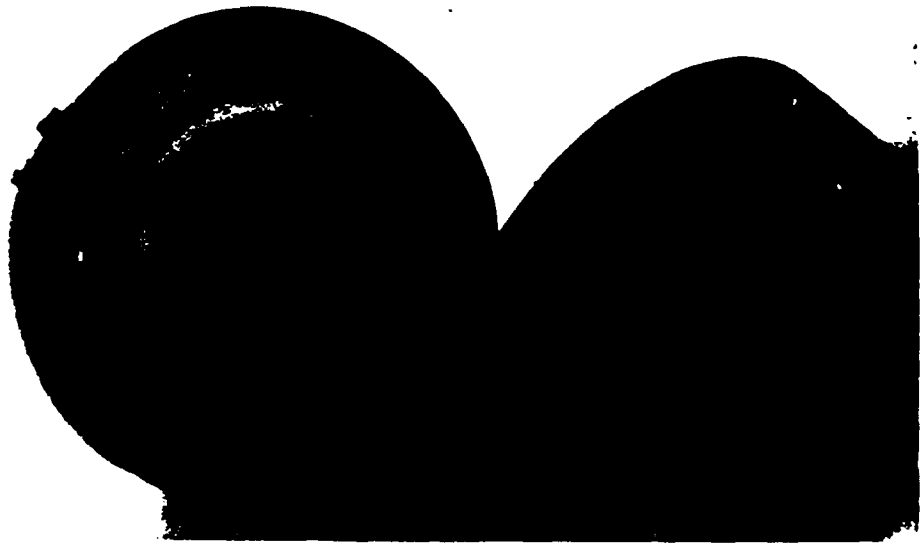

Fig. 1. A 420 stainless steel sprayed injection mold for a flying disk.

Our system uses a computer based geometric modeling system (NOODLES [6]) to describe the parts and patterns needed to make the part's mold or die. A solid freeform fabrication process, a

stereolithography apparatus† in this case, autonomously creates the pattern in a matter of one or two days. The shells are fabricated by robotically spraying metal using an arc–spray device to create the tooling face and structure. The back side of the tooling cavity is then filled with a support material to sustain the compressive service loads. Figure 2 shows a cross section of such a tool. The material choice aspects of this problem are made complex by the elevated service temperatures (as high as 450 °C); it is desirable to match the coefficients of thermal expansion of the sprayed tooling material and the backing material.

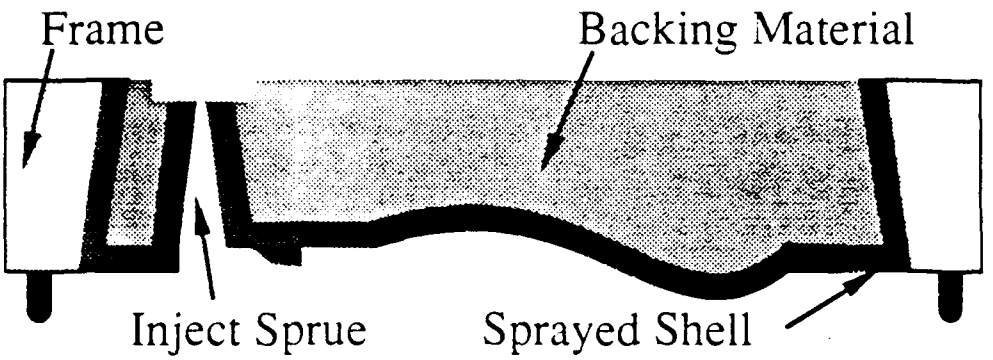

Fig. 2. Schematic cross section of a sprayed tool.
The frame interior is angled to help support compressive loads on the tool face.

The synergy of a coherent, computer based three-dimensional modeling system, a rapid prototyping fabrication device, and robotically based spraying system has made this approach for manufacturing low volume tooling economically appealing, particularly for geometrically complex shapes: the time needed to manufacture such a tool is of the order of one week; and the cost of the manufactured tool is substantially less than a conventionally made one-of-a-kind mold or die.

The direct linkage of the part's computer model and the part's tooling results in paperless manufacture; changes in the part's geometry are directly communicated to the next iteration of tooling, and unacceptable aspects of the design, from a manufacturing perspective, are communicated back to the part's computer model. Using the robot to manipulate the arc–spray gun has three striking advantages: any particular schedule for spraying a mold or die half is repeatable; moreover the robot is precise, meaning, for example, an intended standoff of 10 cm is precisely executed; and the robot is reprogrammable for new tooling designs. This combination yields immediate benefits in the quality of sprayed ferrous alloy shells. The robotic repeatability is required for consistency in

† Stereolithography has been commercialized by 3D Systems, Inc. of Valencia, California under US Patents 4 330 B1, and 4 929 402.

the sprayed shell, as well as consistency in this experimental work. The robot, being a programmable mechanism with considerable freedom of motion, is also capable of spraying complex surface geometries.

The basic fabrication of these sprayed ferrous tools had been problematical. In making sprayed tooling, metal is first sprayed onto a substrate, and then removed from that substrate; thus the interface layer between substrate and coating is by design weak in order to permit that separation.

After the arc-spraying is completed, the shell and the substrate still contain considerable internal stress, albeit in equilibrium. These thermally induced stresses can be very large [7]. When the shell is separated from the substrate, the shell deforms as it comes to a new equilibrium. Our current process art limits this to roughly 1 mm deflection in 500 mm length of shell for a 2 mm thick shell. Secondly, the sprayed shells are backed with a mass castable ceramic or filled epoxy to principally provide tool compressive strength. If the shell and the backing material have different coefficients of thermal expansion, then the normal thermal cycling of a tool will create shear at the shell, backing interface. The presence of internal stress in the shell, as well as a mis-match of coefficients of thermal expansion, also raise questions of the shell's geometric stability at elevated temperatures, and over long times. Finally, the spray process is poorly suited for spraying into narrow channels and small aspect ratio holes.

As much of the tool's function is determined by its geometry, much of the tool's strength and wear characteristics are determined by the microstructure of the sprayed shell. The focus of this work is the microstructure of the sprayed shell, with emphasis on designing aspects of the microstructure to meet the demands placed on the tool's inner shell. This is one important component of the research needed to make successful ferrous tools; this work will help guide the future efforts in the larger research program.

2. Metal Spraying Techniques

2.1 Osprey, plasma, and flame techniques..A variety of techniques are available for depositing metal by a spray process. The Osprey process [8, 9] provides large deposition rates (1000 kg hr^{-1}) by atomizing a molten stream of liquid drawn from a pool of liquid metal. This is generally done in a chamber under inert conditions. It is possible to superheat the liquid pool. The deposition rates are such that a contiguous liquid surface is present on the substrate.

Plasma systems [10-14], at the other end of the spectrum, deposit material at a rate from 0.1 kg hr^{-1} to 5 kg hr^{-1}. These systems function by propelling powdered material in a stream of gas heated by an electrical arc: gas temperatures are reported to be as high as 20 000 K [14].

Deposition rates of a few kg hr^{-1} are problematical, for typically the powder particles are not entirely melted. Plasma systems permit a wide latitude in choice of materials, as well as good of control of the resulting microstructure; they are mostly used for coating.

Flame systems, similar in concept to oxy–acetylene cutting and heating torches, melt a powder, wire, or stick of material in the flame and then use the combustion gases to blow the molten particles to the substrate. The deposition rates vary between 4 kg hr^{-1} and 20 kg hr^{-1}. As this process essentially uses a heating torch, the substrate is heated, while the particles are conveyed in a gas stream of combustion products.

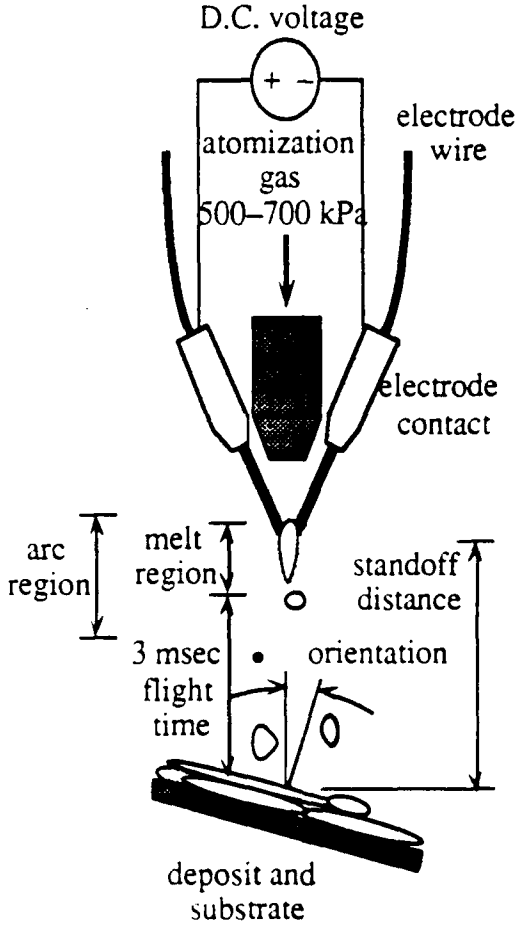

Fig. 3. Schematic of an arc–spray gun and deposited particle flight times.

High velocity variants of flame and plasma systems greatly increase the kinetic energy of the particles in order to reduce the porosity of the sprayed material. The high speed flow of molten material also serves as an abrasive to the substrate.

2.2 Arc–spray. The effort reported here uses an arc–spray system [15, 16]. It is comparable in cost to the low cost flame system while avoiding the inherent products of combustion, it is

extremely easy to use, and it uses widely available materials (any conductive material that can be drawn into a wire can be used as feedstock, and welding electrode wire is particularly easily obtained).

The arc–spray gun is arranged as in Figure 3. Two consumable electrode wires are fed through contact tips to the area of the arc. A D.C. power supply establishes an arc between the wires, melting them in the arc. A column of atomizing gas, ranging from 480 kPa to 690 kPa (70 psi to 100 psi) ablates the molten material from the wires, atomizes the molten droplets and carries them, in a spray, to the substrate. For steel systems, the arc voltage typically ranges from 26 volts to 31 volts; the arc current ranges from 50 amps to 300 amps giving a temperature of 10^4 K in the arc [14]. Deposition rates for an arc–spray system range from 1 kg hr^{-1} to 20 kg hr^{-1}.

The structures resulting from the arc–spray process are suitable for the tooling applications at hand[16, 17], and the arc–spray process permits a deposition rate that allows a timely build-up of the tool shell thickness. At the same time, the pattern substrate, and already deposited material, are not subjected to excessive heat load. Finally, the process is not particularly abrasive, meaning that relatively delicate pattern substrates can be used to provide the shape of the tool. In exchange for lower particle speeds, arc–sprayed materials display a higher porosity. This will affect the fatigue life of the tool, as well as the strength of the material.

2.2.1 Parameters. Within the arc–spray process, there are a number of parameters that can be controlled to affect the quality of the deposited shell [18, 19]. These principally include:

standoff distance — the distance the particles must travel from arc to substrate;

gun orientation — the orientation of the spray gun with respect to the substrate's surface normal, and thus the direction of impact of the sprayed particles upon the substrate;

traverse speed — the traverse speed of the spray gun over the substrate; this directly affects the flux of particles arriving at the substrate;

gas pressure — the atomization and accelerating gas pressure in the spray gun.

arc energy — the energy being consumed in the arc; the resistance of the arc is essentially constant at a constant material consumption rate, so the arc power (and hence the arc specific energy) is set by the power supply voltage;

material consumption rate — the amount of material being presented to the arc per unit time; it is specified as a feed rate of the consumable electrode. Not all of this material is deposited — a fair proportion is lost to overspray.

Table 1 shows an overview of the relationship between these parameters and some effects in the spray and shell's microstructure.

2.2.2 Solidification and Microstructure. Our aim is to influence the shell's microstructure indirectly by directly influencing the spray's characteristics. The porosity and oxide levels should be kept at a minimum (ideally zero), the particle sizes should be uniform, each with a uniform temperature, while imparting no heat load onto the substrate or previously sprayed shell. A measure of compromise is needed in setting the spray parameters.

	Porosity	Oxide	Size of Particles	Temp. of Particles	Heat Load on Shell	Orientation of Laminae
Standoff Distance	o	o		•	•	
Orientation	•					•
Travel Speed					•	
Gas Pressure	•	o	•	o	o	
Energy of Arc	o	o	o	•	•	
Material Deposition Rate	o		o	o	•	

Table 1. Qualitative affect of parameters on spray characteristics.
'•' implies 1st order contribution, 'o' implies a lesser influence.

The porosity in Table 1 can be most directly influenced by either increasing the particle's kinetic energy or increasing the time for coalescence on the substrate; gas pressure, standoff distance (and therefore their speed) and adding more superheat to the particles are the means to this end. Orientation has a first order affect on porosity for shadowing reasons - previously deposited

particles will act as obstructions to incoming particles; worse, the hole formed in the shadow of a previously deposited particle is large, and is clustered with other such holes. Figure 4 schematically shows this effect, and Figure 16 shows the effect in the microstructure. We have found that orientation angles greater than 30° lead to unacceptable porosity. Oxide formation is a kinetic reaction, so, beyond eliminating or reducing oxygen in the vicinity of the molten metal or lowering the temperature of the reacting products, reducing the time for the formation of oxides is of significance; this matches the increase of kinetic energy for porosity reasons. Particle size is principally determined by atomization in the arc; coalescence in the arc and on the substrate are minor secondary factors in arc–spray. Beyond the first layers deposited, the orientation of the built-up laminar structure is controlled exclusively by the orientation of the torch. Individual lamella morphology is a function of both the particle size, as well as the orientation of the torch with respect to the substrate's surface. The impact of the molten particles on the substrate is greatly influenced by the angle between the particle's trajectory and the local surface normal; orientations increasingly distant from the surface normal produce a more fragmented lamella. This effect, combined with the shadow effect, produces undesirable microstructural features.

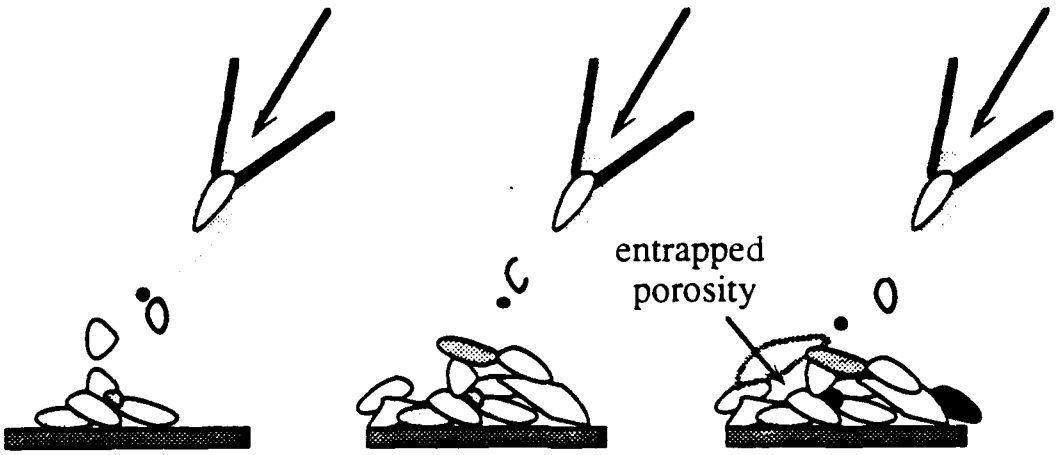

Fig. 4. A schematic of the shadow effect of porosity formation.

There is room for considerable improvement in the arc–spray process [15]; nozzles are only beginning to be designed to optimize any particular aspect of spraying, and the control of the arc is an open–loop affair. Nozzle designs should be directed to create a cone of narrow and sharp spatial definition, while maintaining a uniformly hot, homogeneous beam of sprayed material. Synergic power supply technology routinely available in the arc–welding domain could be applied to better control the formation of metal droplets in the region of the arc. These efforts, for relatively little cost, could well yield large returns in the quality of arc–sprayed metal tooling.

Naïve methods of depositing metal shells results in poor quality shells; spraying with the intention of creating sound microstructures has lead us to investigate methods of making shells with lower oxide levels, lower porosity, oriented lamella, and shells built of sprayed composites.

3. EXPERIMENTAL ARRANGEMENT

The experimental arrangement used in this work is organized around a robotically moved arc–spray gun. Both the robot and the arc–spray system are coordinated by a IBM-AT computer; all of the experiments reported here were controlled from the IBM-AT. The design and modeling work is done on 12-MIP class workstation computers of various makes. The arc–spray gun and power supply are commercial products (the gun is a Miller BP–400 and the power supply is a Miller Mogularc 400R); the arc–spray controller is a Miller custom built process controller that is interfaced to and controlled by the external computer which sets the wire feed rate and arc voltage, as well as starts and stops the arc process. The robot is a GMF S-700 6 axis robot, with additional degrees of freedom in a rotating table. Programs are uploaded and downloaded through the IBM-AT computer, and the IBM-AT computer initiates robotic motion. The robotic manipulator provides a high degree of motion repeatability in making the sprayed structures; the computer controlled power supply and arc–spray system gives a similar repeatability to the process variables in the sprayed structures.

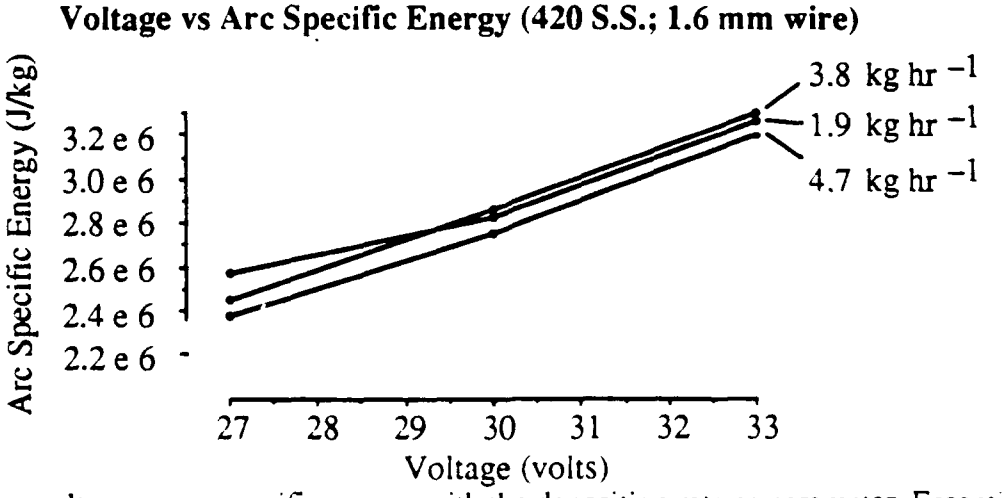

Fig. 5. Arc voltage *vs* arc specific energy with the deposition rate as parameter. Essentially the energy per unit mass melted is proportional to the control voltage, but independent of the deposition rate.

For a given deposition rate, the arc current and arc resistance are relatively constant as the arc voltage is varied; thus the power consumed in the arc is largely controlled by the voltage setting. Figure 5 shows the affect of increasing arc voltage on specific energy, all other variables held

constant. With this type of equipment, this is the simplest way to increase the energy available to heat the metal particles.

The experiments were conducted at the lower end of the arc–spray parameter ranges, with a deposition rate of about 2.0 kg hr^{-1} and specific energy expenditure of 2.6 MJoules kg^{-1} (0.74 kWH kg^{-1}) of metal consumed. With the programmed torch travel speed of 500 mm s^{-1} a deposit of 0.1 mm is applied during each cycle of 24 passes. In all cases, the standoff distance was the same 16.5 cm (6.5 inches) from the arc to the substrate. Similarly, the orientation was, except as noted below, normal to the substrate (*i. e.*, the particles traveled along a course parallel to the surface normal).

The atomizing gas, in our facility, comes either from an air compressor (capable of supplying 1.2 MPa (175 psi) pressure) or from a cluster of compressed gas bottles. The process produces a broad spectrum of particle sizes, ranging from +100 micron diameter particles to sub-micron particles.

Due to the large surface/volume ratio of the sprayed droplets, oxidation in flight and after impingement is a problem. The obvious way to circumvent the detrimental effect of oxidation and avoid the ensuing brittleness of the deposit is to minimize the partial pressure of oxygen in the gaseous atmosphere [20] and keep turbulence as low as possible. The influence of these factors was studied by choosing three experimental setups, as shown in Figure 6. Either the robotically manipulated jet was directed towards the substrate without any protective cover (Figure 6a), or it was protected by a shroud (Figure 6b) that minimized turbulence of the surrounding atmosphere. In this arrangement the hot jet and the yet hot deposit is mainly flushed by the gas of the jet. Additionally an arrangement was tried (Figure 6c) where the spray gas was flushed through the shroud to provide inert gas for the turbulent mixing of the jet. The shroud is attached to the nozzle and moves with it. Although the distance between nozzle and substrate is kept as constant as possible in the robotic operation, there always remains a gap between shroud and substrate. Thus it is practically not possible to prevent contact between the surrounding atmosphere and the jet or the hot deposit, but obviously the shroud protects the jet rather well when and after it leaves the nozzle (and is still slow, hot and reactive). Near the substrate turbulence might draw in some of the surrounding atmosphere, but there the temperature of the droplets and thus the rate of oxidation is already lower. More importantly, the atomization and shroud gas flow rates are large enough to force a net outflow of gas from the shroud/substrate gap. Further, observation shows that particles emerging from the shroud,substrate gap are essentially all overspray — none adhere to the substrate or are otherwise incorporated in the shell.

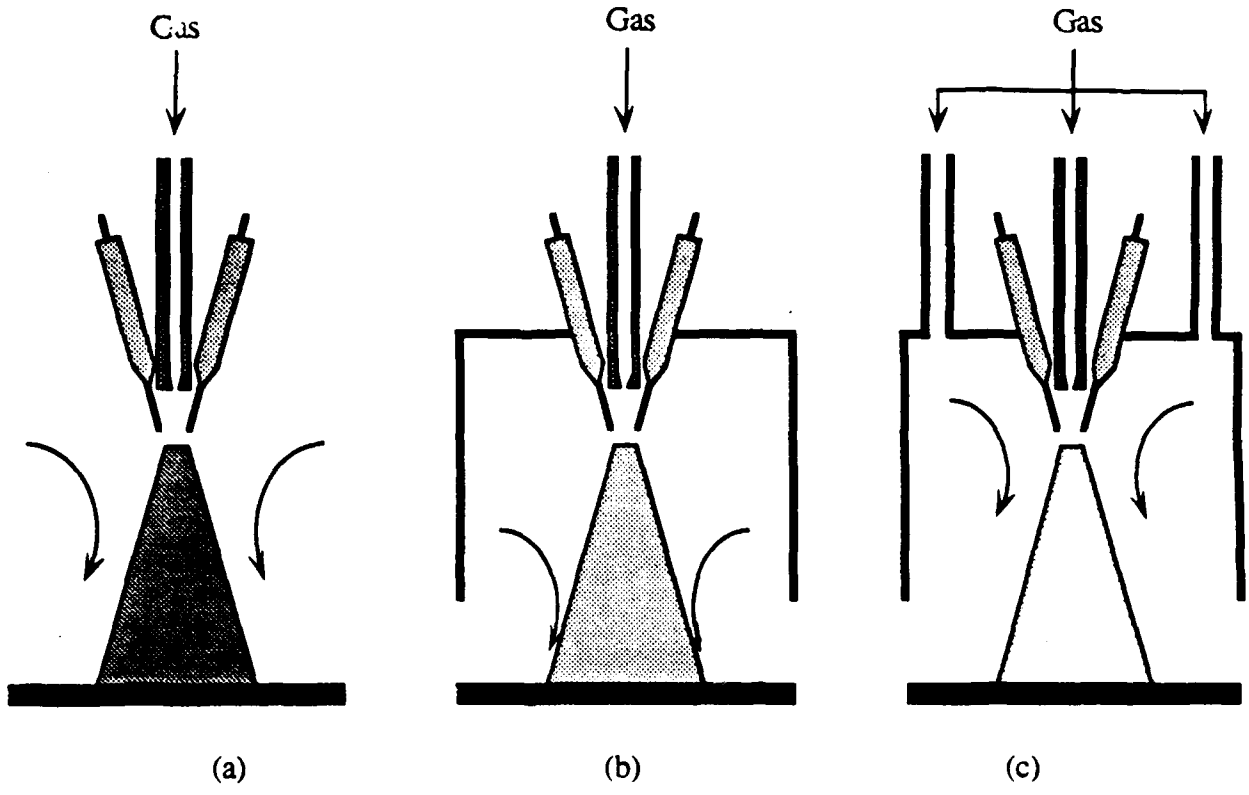

Fig. 6. Shroud arrangement for inert atomization and cover gas. (a) no protective cover, (b) protective shroud, (c) protective shroud with protective gas flow.

In these three arrangements three different gases were used: air, nitrogen and argon. The change from the first to the second cuts down the oxygen partial pressure by a factor of five at reasonable cost, while the change from nitrogen to the heavier argon increases cost dramatically but further reduces the oxygen exposure. Further, the use of argon prevents any potential problems with nitride formation in the ferrous systems [21], and the arc is much more stable in an argon atmosphere than in a nitrogen atmosphere [22].

The metal deposition schedule for these experiments was:

Step 1. arc–spray a path consisting of 12 cycles of back-and-forth motion across a substrate (7 mm low carbon steel plate in most cases)

Step 2. wait for the temperature of the sprayed shell to return from its heated state (typically 60°C) to some nominal level (typically 40°C)

Step 3. repeat until adequate shell thickness for sectioning was reached. Generally this procedure was repeated eight to ten times, giving a typical shell thickness of 1.3 mm.

Various materials were sprayed (compositions are in weight %):

(a) Plain carbon steel 1080. The composition is 0.8 % C, remainder Fe.

(b) Stainless steel 420 (a martensitic stainless steel) with a composition 0.15% C minimum, 1% Mn, 1% Si, 12-14% Cr, 0.04% P, and 0.03% S

(c) Bronze of 2% Si, remainder Cu.

(d) Invar of 36% Ni, remainder Fe.

These materials were sprayed onto mild steel that had been glass bead peened.

The samples sprayed in a completely inert atmosphere were made in a closed vacuum chamber. The chamber was evacuated to 0.7 kPa (5 torr), then backfilled to 57 kPa (430 torr) with argon. The arc–spray gun was inserted into the chamber and during spraying a vane vacuum pump was used to hold the pressure at 57 kPa. The atomization gas for these experiments was argon, and the wire guide tubes were pressurized by argon as well. The substrate for these experiments was a 46 cm diameter mandrel.

4. CHARACTERIZATION OF SPRAY

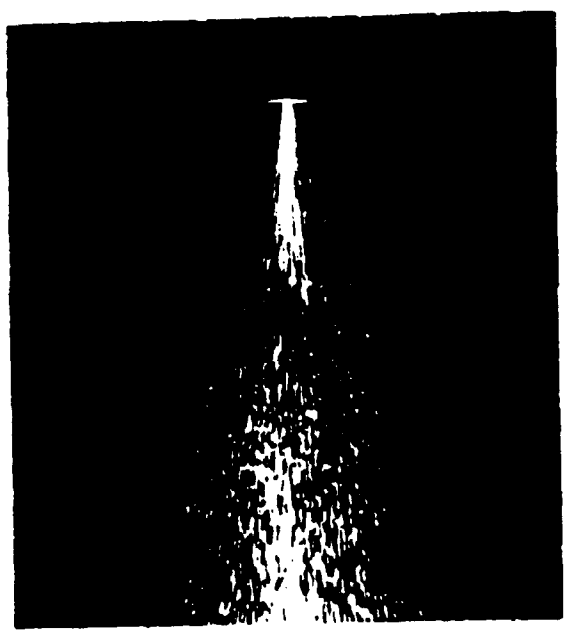

Fig. 7. Spray of 420 stainless steel in air with air atomization.

4.1 Particle velocity. Spray from the arc–spray gun is shown in Figure 7. This photo was taken with the focal plane shutter moving perpendicularly to the direction of travel of the sprayed particles; the exposure time was 250 μseconds. The photo shows the irregular nature of the arc–spray; the process sputters along rather than continuously depositing a fine shower of metal – a gap in the stream of spray is noticeable 25 cm from the arc. It is also apparent that particles along the periphery of the spray's cone are moving more slowly than those along its axis.

From the photographic evidence, particle velocity is measured to vary between 40 and 70 m s^{-1}. This speed, of course, varies as the particles leave the arc at zero velocity, accelerate in the gas stream moving at subsonic velocity, and then, as the gas stream disperses and slows, decelerate from the resistance of the gas stream. The speed of the particles should also be strongly influenced by their particular size, which, in turn, is influenced by the atomization gas pressure. Mathur [9] discusses atomized particles in a gas stream in some detail in reference to the Osprey process. As far as aerodynamics are concerned, there is little difference between the arc–spray process and the Osprey process; the velocity measurements from Figure 7 and the micrographs of section 5 show that we are in the same regime as the Osprey process: droplets of 10-20 μm diameter move at a speed of 40 to 70 m s^{-1}. Our particle flux, however, is lower and particle temperature higher.

4.2 Material build-up. The arc–spray system builds up shells by depositing particles onto the substrate. They individually splat–quench; there is never a complete liquid layer on the surface of the deposit in this process at the material deposition rates under consideration. The deposit is created by the build-up of these individually solidified particles. Arata [23] reports that particles in the arc–spray system cool within 125 μseconds of impact on a substrate. This suggests that these particles are cooling at least at a rate of 10^4 K s^{-1}. The resulting solidification rates are 25 cm s^{-1}. Moreau [24] has shown cooling rates in individual lamellæ of molybdenum and partially stabilized zirconia at 10^8 K s^{-1}, measuring the temperature evolution and showing that solidification is complete in 20 μseconds. This suggests solidification rates of about 150 cm s^{-1}. The substrate receiving the arc–sprayed droplets is as cold as a substrate in splat-quench ribbon producing systems, but the droplets in the arc–spray configuration are much smaller. Therefore we achieve cooling rates of at least 10^4 to 10^6 K s^{-1}.

These high cooling rates allow, in principle, depositing of metastable or quasicrystaline alloys which might have interesting properties [25, 26].

5. MICROSTRUCTURE

5.1 Optical Metallography. In order to discuss the essential features observed, the micrograph of the Invar alloy is shown in high magnification as Figure 8 (b). This figure shows that the total

deposit is built up of lamella which range from 4 to 10 μm thickness and range from 50 to 100 μm length. Each of these lamella is a solidified droplet, indicating that the average droplet–diameter

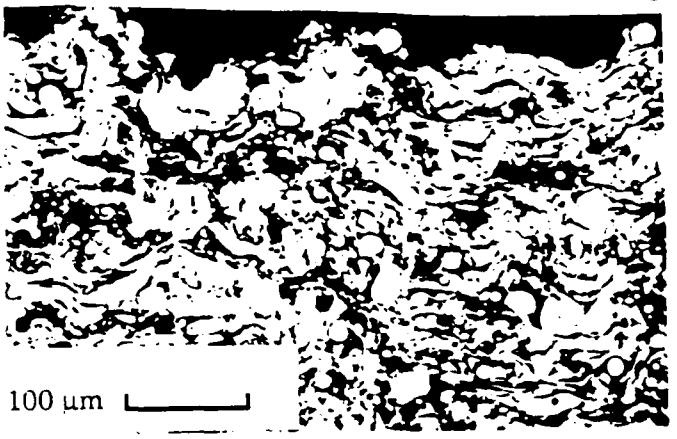

(a) Last deposited material near shell surface.

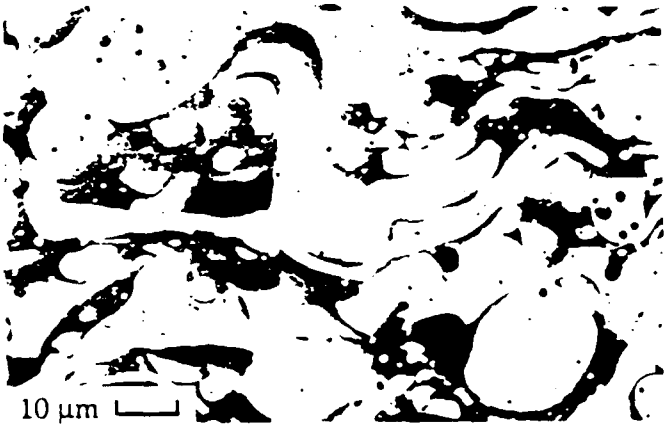

(b) Center of deposited material.

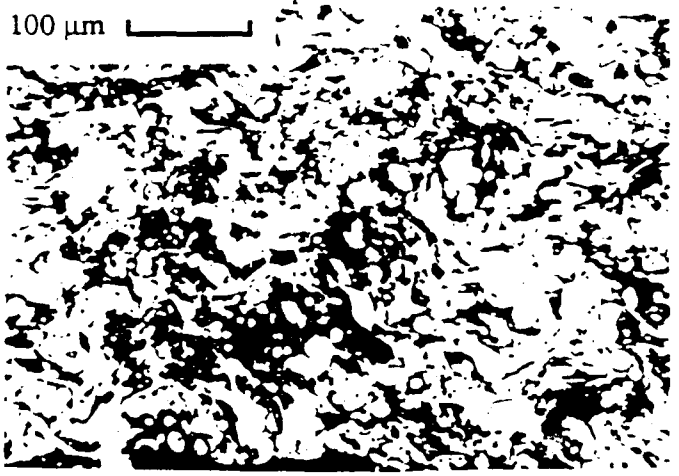

(c) First deposited material near substrate interface.

Fig. 8. Optical micrographs of cross section of 6 mm of deposited Invar.

ranges from 10 to 20 μm in diameter to 100 μm. The largest lamella in these micrographs suggests an original particle of perhaps 140 μm in diameter.

The micrograph indicates several things: droplets solidify in isolation – there has never been a liquid pool on the surface. The uniformity of the size distribution implies that splashing is not important: upon impinging on the surface, droplets hardly break up but flatten out to lamella before they solidify. The arc-gun was oriented so that the particles arrived normal to the surface for the material sprayed in this sample. Three different shades of gray are visible in Figure 8, particularly Figure 8(b), white, gray and black. By X-ray energy dispersive analysis, Figure 9, we verified the white area as being metal, the grey areas being oxide and the black areas being pores. The original composition of Invar is Fe–36 w% Ni; the composition has been changed in this sample by the heavy oxidation (roughly 30% of this sample is oxide). The bright regions are about Fe–40 w% Ni, and the dark regions are roughly Fe–18% Ni. Nickel oxidizes more slowly than iron, so it is unsurprising that the oxide regions are predominantly iron. If, however, the goal of spraying Invar was to

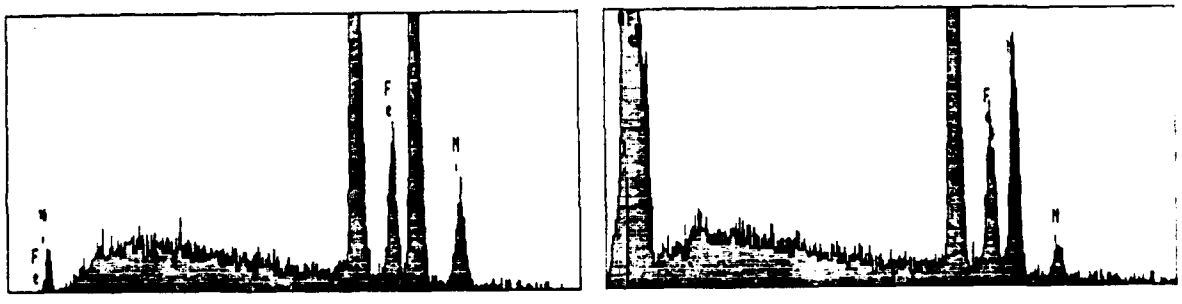

(a) Spectrum for bright (metal) regions (b) Spectrum for dark (oxide) regions

Fig. 9. X–Ray dispersive analysis of atmosphere sprayed Invar.

have a shell made of low coefficient of thermal expansion material, then this goal cannot be met by spraying in air – the composition change has moved the alloy away from the Invar effect. The morphology of the oxide particles raises the interesting question how the formation of lamella (and not spheres) of oxide was possible. If liquid metal droplets had hit the surface, and had splat out into lamella before becoming oxidized, one would expect the lamella to be surrounded by oxide, giving a microstructure with intergranular oxide and, presumably, undesirable mechanical properties. The presence of oxide lamella indicates another mechanism: metal droplets have oxidized in the arc and in flight between the nozzle and the substrate, forming droplets of liquid oxide that hit the surface and squash out to lamella. The discussion of section 4.1 indicates that the droplets spend about 3 msec in flight, they have been heated to less than the arc temperature 10^4 K [14], but more than the oxide liquidus (1670 K for Fe_3O_4, 1830 K for FeO). Apparently these liquid

iron droplets can oxidize to liquid Fe_3O_4, Fe_2O_3, and FeO while being kept well superheated for 3 msec.

5.2 Oxide. The oxide and porosity levels in the deposited shells are shown in Figure 10 with micrographs of these shells. The oxide and porosity measurements shown here have been performed using an image analysis program analyzing scanned images from photomicrographs. The level of uncertainty in these measurements is high. Fowler [27].has shown that with eight repetitions on a single sample, it is possible to operate within a 95% confidence band for porosity measurements, but oxide measurements require more measurements. This can be seen in this data in the 0.8%C – Fe column; the oxide and porosity values vary in unexpected ways compared to the other materials. Further, spray-gun designs greatly influence the porosity and oxide levels in the sprayed shell. The measurements here, therefore, should only be used to represent what trends are possible with inert gases.

With the open unprotected arrangement of Figure 6a one obtains an oxide content of approximately 30% for both steels and the Invar alloy if air is used for atomization. This drops to 10% to 15% oxide for a nitrogen atomization gas in an air environment. If oxidation had occurred only in the nozzle, no oxidation should have occurred at all, but the turbulence of the air-atmosphere still causes oxidation. This is largely prevented by using the arrangements of either Figure 6b, or better even, Figure 6c. These decrease the oxidation content to about 8%. If argon is used in the nozzle with the protection of Figure 6b or 6c, the oxide content falls to less than 8%. If the experiment is conducted in a vacuum chamber backfilled with argon, the oxide content drops to less than 2%, but this arrangement is experimentally expensive. In the Argon backfilled chamber, the measurement of oxide reflects wire contamination more than in-spray formed oxide.

5.3 SEM Metallography. Figure 11 shows a backscatter image of the sprayed eutectoid steel (0.8% C). Depending upon the quench rate of the material, and the temperature history of the material, several phases and mixtures of phases are possible: pearlite, a mixture of ferrite (α) and cementite (Fe_3C), upper bainite, lower bainite, martensite, and retained austenite (γ) [28]. For this composition of steel, pearlite and the bainite transformations can be avoided if the cooling rate from 996 K to 473 K is at least 200 K s^{-1} [29]. If the cooling rate is much faster, martensite particle formation will be suppressed as well [30, 31]. The 25 μm particle in the center of Figure 11 shows an already solidified particle when it arrived at the substrate. This particle is entirely composed of

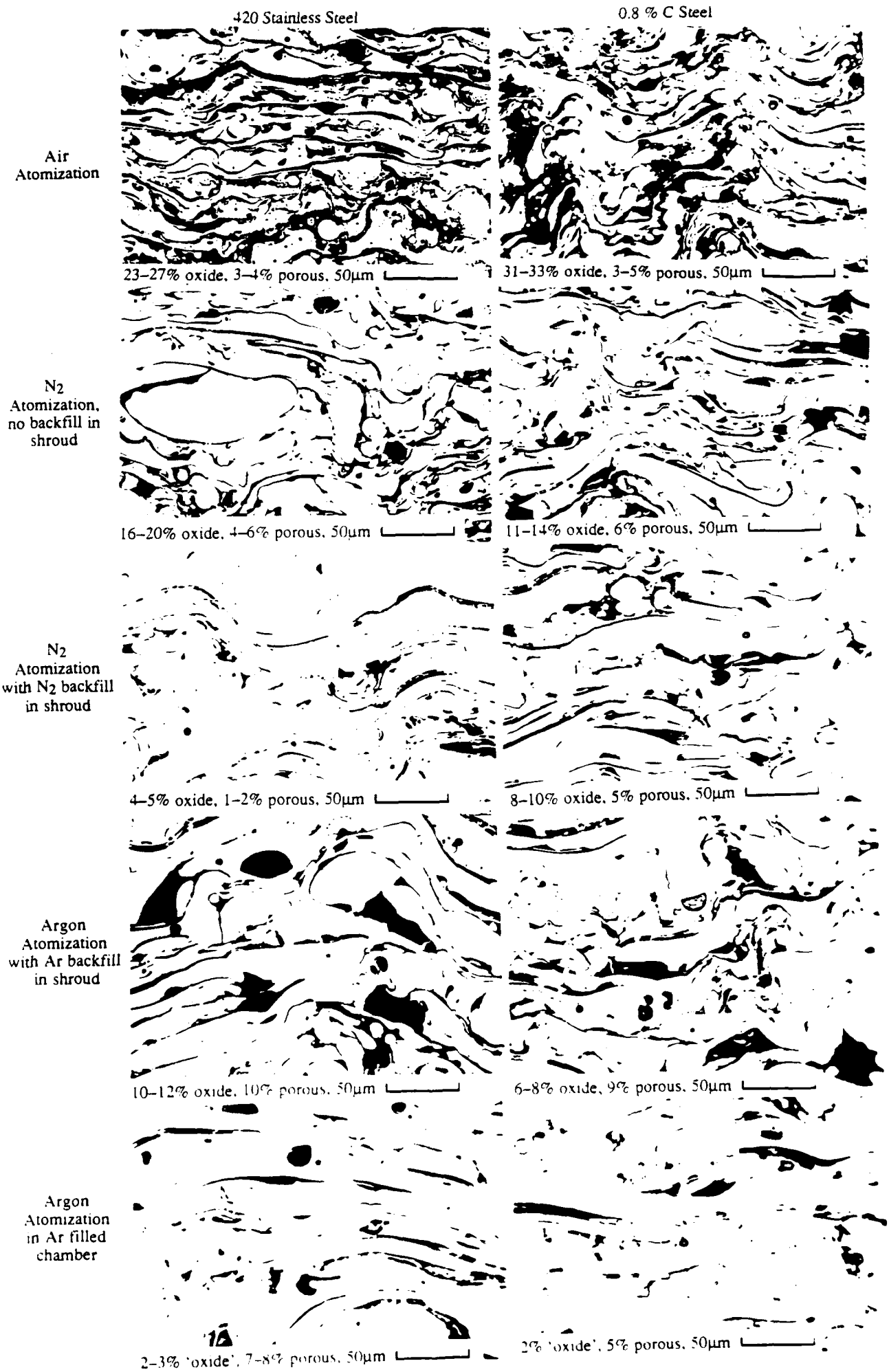

Fig. 10 (a) metallographic section... the 0.8% C steel and 420 stainless steel deposits.

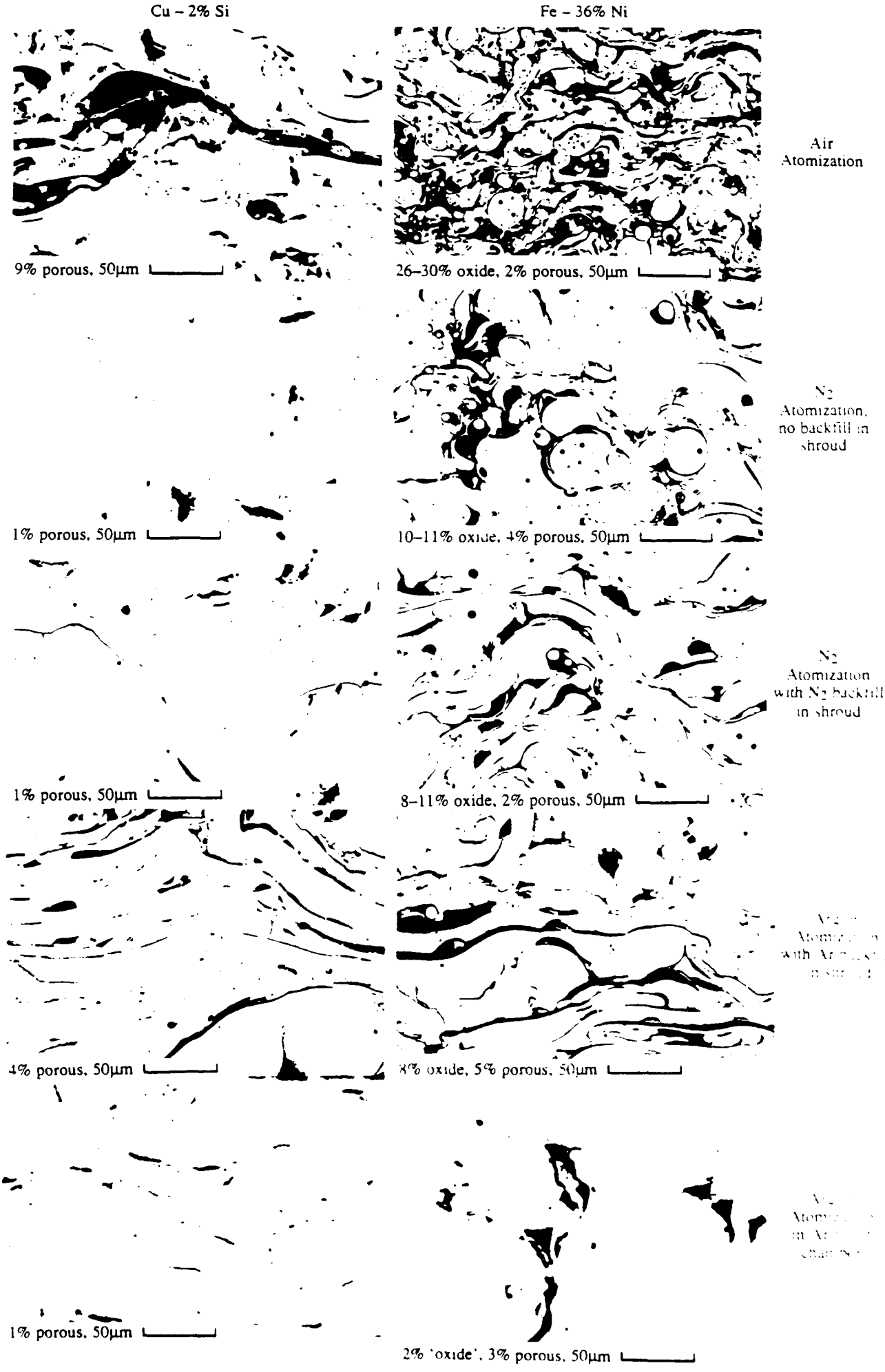

Fig. 10 (b) metallographic sections of [illegible]pper and Invar deposits.

retained austenite. The lamella below and surrounding the particle arrived at the substrate in a molten state, and subsequently solidified. The cooling of this lamella was such that martensite particles formed in the last deposited, or upper, portion of the lamella, while the lower region of the lamella is only

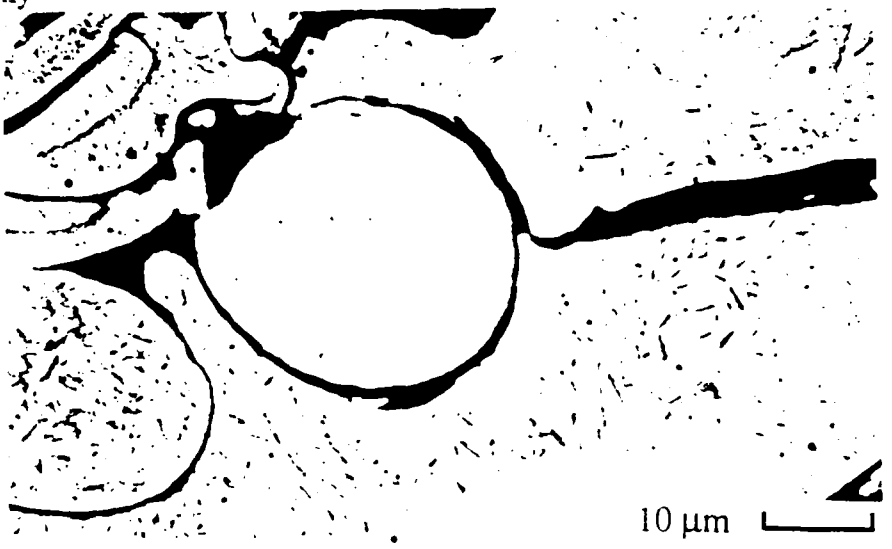

Fig. 11. SEM microphotograph of the sprayed 0.8% C steel: Showing martensite formation surrounded by retained austenite. The martensite particles are acicular in appearance in this section (probably being lenticular in three dimensions) and vary in size: they are of the order of 0.5 µm by 4 µm.

retained austenite. This shows the cooling rate was highest near the lamella-substrate interface, and that the region of the splat away from the interface stayed longest at high temperature. The lamellae and particles in this figure probably arrived at the substrate nearly simultaneously; the solidified particle forced itself onto the previously arrived lamella, forcing the liquid surface up and around. In the larger lamella of Figure 11, small pores, of the order of 0.1 µm to 0.5 µm in diameter, are also visible. These appear in all of the sprayed materials from this process, and are an artifact of the violence of the ablation and atomizing processes.

The microstructure in the lamella of arc-sprayed material is the same as the structure of splat ribbon materials, while the interfaces between the lamellae are much worse. This is the problem with the process. The production of splat-ribbons is a continuous casting process. The arc-spray process deposits liquid droplets individually on the solid surface, each of these droplets undergo thermal stresses during cooling and this can lead to decohesion or microcracking along the lamella-lamella interface. The usual consolidation methods, like HIP or forging (cold or hot working) are in conflict with our intentions for this sprayed material, and therefore more subtle methods like ... glazing or shot peening of each layer could and should be used. For the unconsolidated deposits

shown or discussed in this paper, the mechanical properties are controlled not by the behavior of the individual lamellæ, but by the strength of the interfaces between them. The presence of inter-lamella microcracks might be detrimental in tension, but is of no concern for metal shells subjected to compression.

6. Composite Structures

Given the layered and disjoint lamellæ formed in the arc–spray process, even when sprayed in oxygen free environments, we are motivated to develop processes to control the microstructure without cold or hot working the entire shell. As discussed in section 2.2.1 and Table 1, there are a number of process parameters that can be manipulated to affect the particles forming the lamella. Beyond the arc–spray process parameters, we follow two compatible directions: control the material properties by altering the materials deposited, and control the position and orientation of the lamella to improve the shell's characteristics. Our goal is to tune the material in the shell so it more successfully meets the demands of the application.

6.1 Sprayed Composite Materials One microstructure experiment has been to create a stratified shell, with each stratum being made of a distinct material.Figure 12 shows a structure made of alternating layers of 0.8% C steel and Invar. The sample has been etched with picral for 15 seconds to darken the steel. Each layer is about 0.15 mm (0.006 inch) thick.This sample was

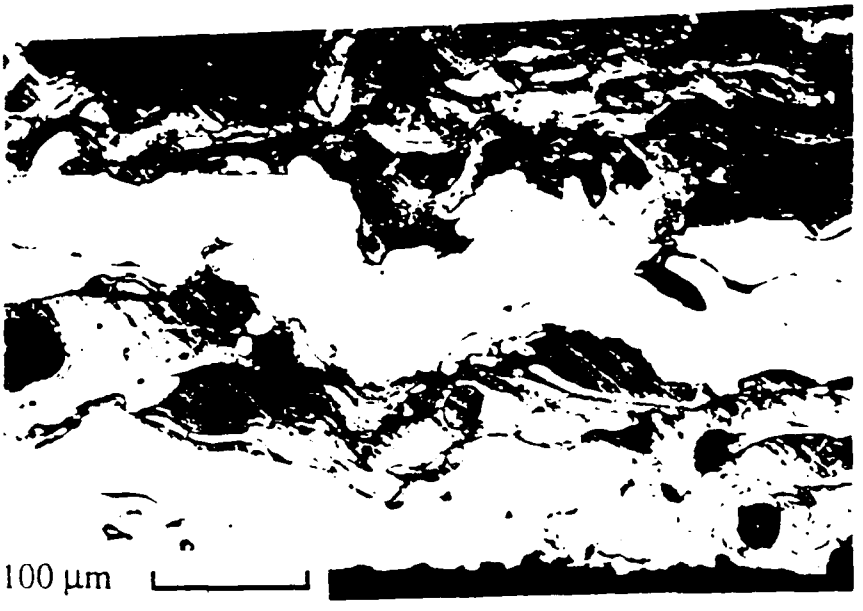

Fig. 12. Composite layered structure of 0.8% C steel and Invar.

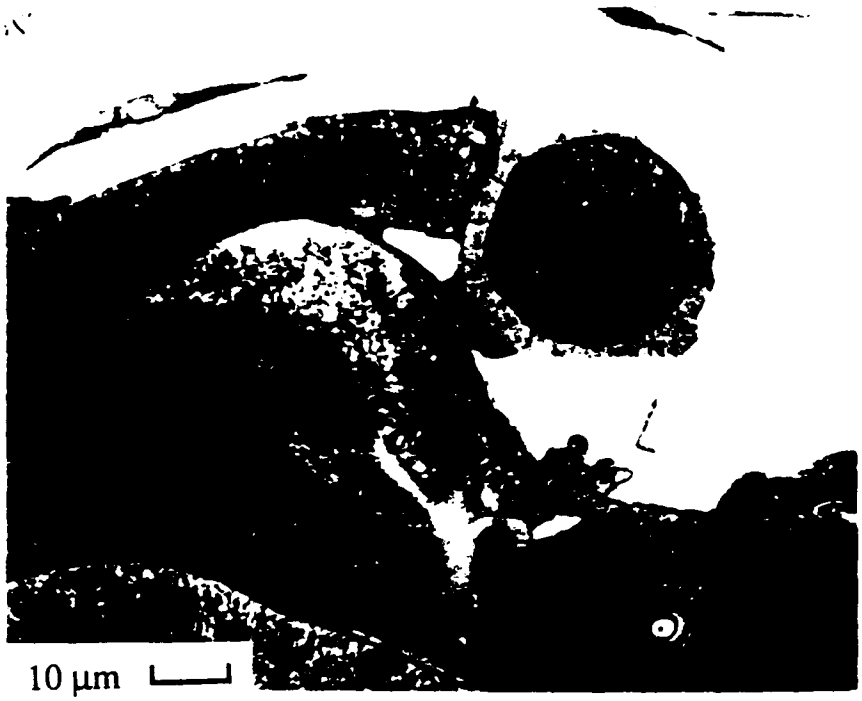

Fig. 13. Detail of interface between 0.8% C steel and Invar in layered composite.

sprayed using Argon atomization gas, a shroud, and a backfill shroud gas of Argon. Figure 13 shows a detail of the mixing region of the two materials. There are no difficulties in the inter-layer bonding of this material, even though perhaps 15 minutes passed between the deposition of the layers.

6.2 Pseudo-Alloy In another microstructure experiment we have created a shell of blended materials. The arc–spray process forms an arc between two feed wires to melt them; it is possible to have the two wires be of different material. Figure 14 shows a shell made from mixing 0.8% C steel and Invar. The sample in Figure 14 was sprayed using Argon atomization gas, a shroud, and a backfill shroud gas of Argon.

The nature of this mix is entirely different from that of the layered composite. The particles arriving molten still form flat lamellæ in the deposit, but the distinct layering of lamellæ is replaced by a random mixture of lamellæ. In Figure 14, the particles are arriving nearly simultaneously, and the bonding of the lamella is similar to that of the layered composite, as seen in Figure 15.

From the optical micrograph evident that the lamellæ are either Invar or iron. Apparently droplets detach themselves fully either the steel or the Invar wire feeding the arc, and there is little opportunity for the individual particles to mix either in flight or on the substrate; the

solidification rates are sufficient on the substrate to prevent mixing there. X-ray mapping of this deposit has verified that little mixing of the Invar and iron has occurred.

Fig. 14. Mixed pseudo-alloy of 0.8 % C steel and Invar.

Fig. 15. Detail of inter-lamella region – pseudo-alloy of 0.8 % C steel and Invar.

6.3 Oriented Laminae A shell composed entirely of laminæ oriented in one direction may show good resistance to stresses in that direction, but will also be weak to stresses applied in other directions. An appropriate control of the orientation of the lamella in a layer will improve the s[illegible]

characteristics; this is especially interesting when the orientations and positions of the lamella are designed for specific structural features.

6.3.1 Stratified Orientations The experiment shown in Figure 16 demonstrates a series of stratum, each with a new lamella orientation. The robot was used to systematically apply the material; the lamella are rotated about ±25 degrees from the horizontal. Figure 17 shows a detail of the mixing between the strata. There is mixing of lamella in this region, so there should be good vertical bonding of the strata in the composite structure.

An effort was made in spraying the shell shown in Figure 18 to remove some of the porosity in the shell by mechanically shot peening each layer after it was sprayed. Shot peening also has the effect of changing the state of stress in the shell, but this is not visible in optical metallography. In samples that are made by metal atomized by air, the shot peening also has the effect of removing a measure of the oxide on the surface.

The samples in these figures were sprayed with atmosphere atomization and no shroud. Comparison of Figures 16 and 18 shows that peening the surface between each oriented layer reduces the porosity from 13–15% porosity to 7–9% porosity and reduces the oxide from 34–36% oxide to 30–32% oxide.

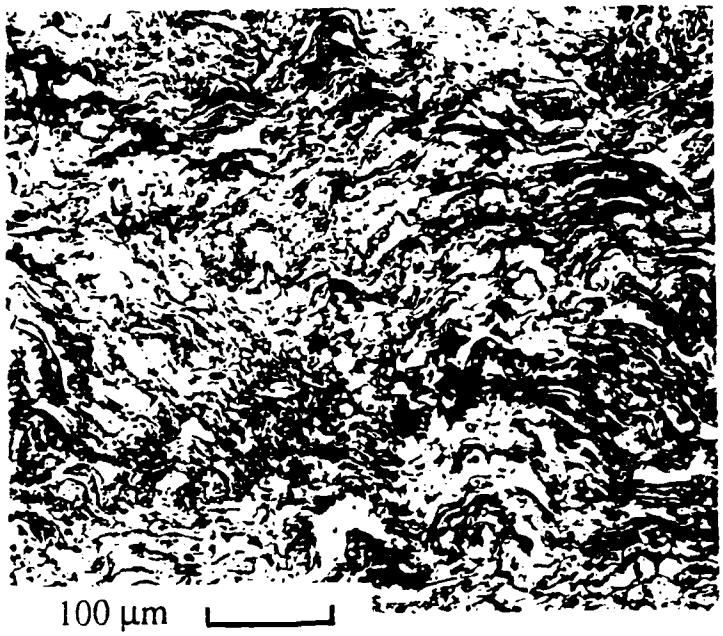

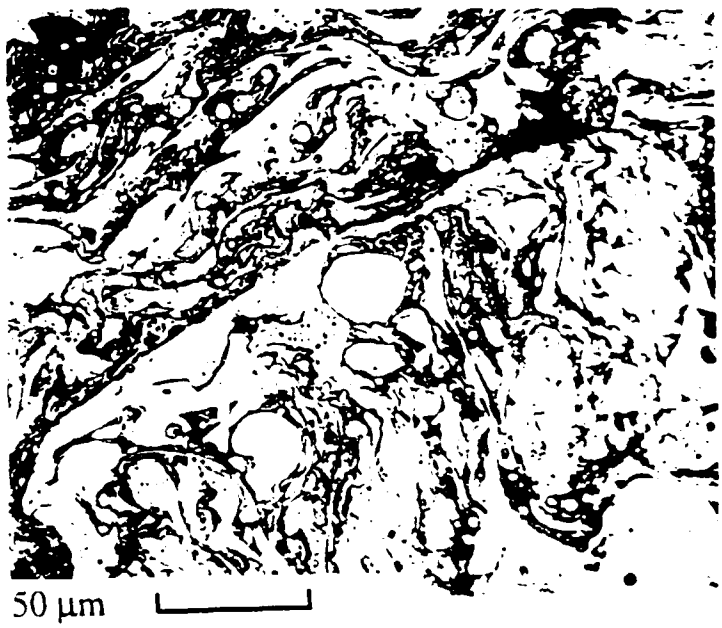

Fig. 16. Oriented lamella of 0.8% C steel. Fig. 17. Detail – oriented lamella of 0.8% C steel.

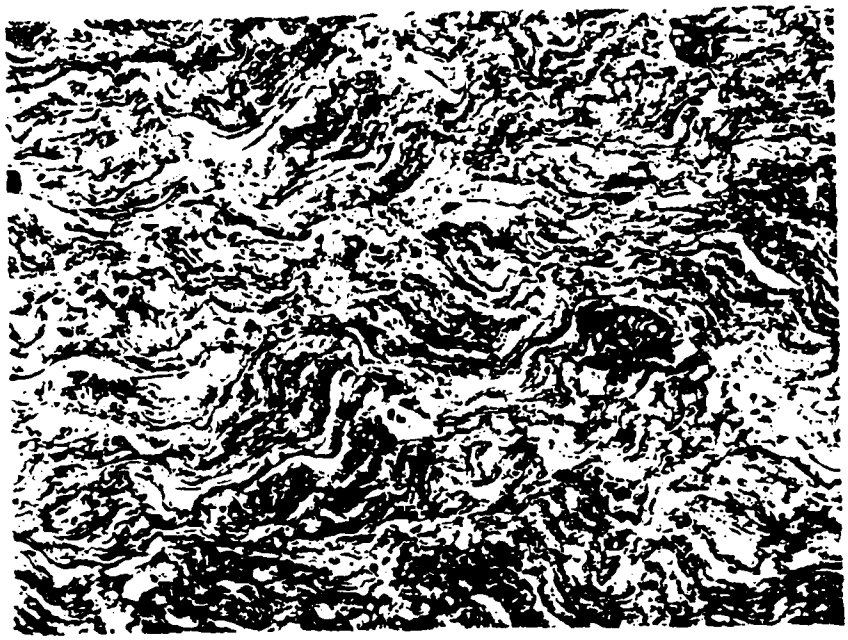

Fig. 18. Oriented lamella of 0.8% C steel with glass peening between each layer.

6.3.2 Flow of Lamella around Features The shells created by metal spraying normally include stress concentrating geometries, particular sharp corners. Arbitrary spraying onto these stress

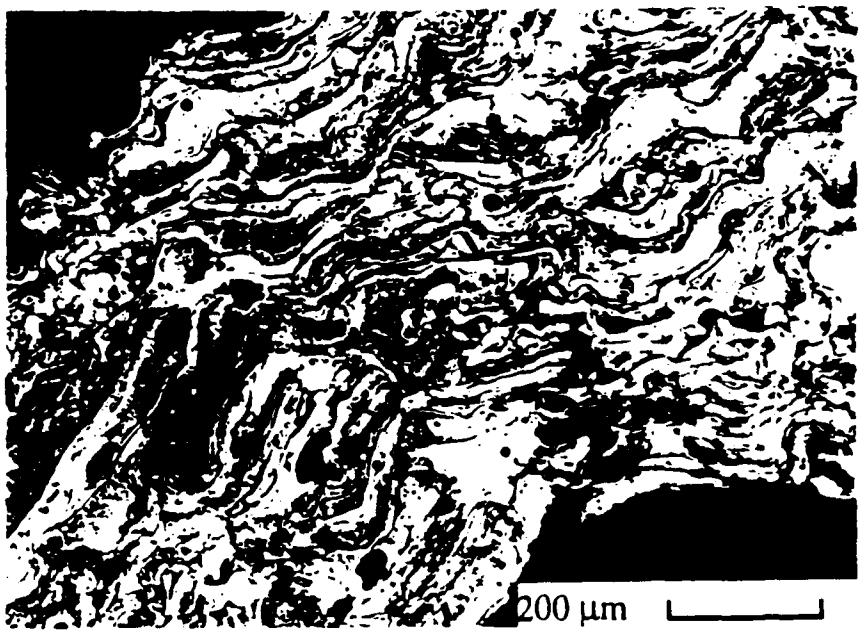

Fig. 19. Lamellæ sprayed around corner.These structures were sprayed using Argon atomization without a shroud. in part to highlight the orientation of the lamellæ.

concentrating features of the substrate can create microstructures similar to that in Figure 19. This structure will not withstand corner loading with any measure of success. As a matter of fact, the material in Figure 19 cracked during preparation. Figure 20 shows the same geometry, but a different spray strategy; the lamellæ were oriented to flow over the corner and thus present some structure to withstand the loading in the corner. Judicious control of the microstructure around asperities, wedges, corners, and similar features is essential for the assuring good mechanical behavior of the shell. The necessary intricate movements of the nozzle over the geometric features of the shell are accomplished most effectively by a robotic manipulator.

Fig. 20. Flow of oriented lamellæ around corner.

7. CONCLUSIONS

The essence of the result of the arc-spray process is a quilt of quickly solidified lamellæ laced together into a relatively weak structure, a three dimensional jig-saw puzzle. Traditionally, this type of quilt is soaked, and then hot and cold worked to dissolve the impurities; all memory of the porosity and grain boundary imperfections are erased in such processes.

We are applying the arc-spray process to quickly and repeatably create precise shapes — our particular goal is to make a tooling shapes for molds. Soaking and working are in conflict with goals of speed and precision. Fortunately the demands of tooling are centered around hoop stress, compressive loading, and wear. The sprayed metals produce shells that lend themselves to these demands.

To create successful materials in a sprayed shell, we control the levels of oxide. That is, we permit some oxide to remain — these oxides are hard, resist wear well, and are fully supported by the metal matrix surrounding them. We further tailor the microstructure to meet geometry requirements in the shell. Finally, these shells can be composed of composite structures, both in the sense of a variety of materials either mixed together or placed in stratified layers, and in the sense of differing lamella orientations. Consistent creation of this oriented structure is most effectively created by robotically manipulating the spray device.

This work is part of a more comprehensive research effort. The next steps, as guided by this microstructural understanding, must focus on the mechanical behavior of these sprayed materials, paying particular attention to the loading modes and wear conditions that are present in tooling applications. Further work will also concentrate on the failure behavior of these materials in the shells under service conditions; from this information, further design of the material will improve the robustness of the tooling. The result will be insight into the design and fabrication of microstructure and mechanical behavior to give a firm foundation upon which to rapidly build useful sprayed metal shells.

Acknowledgements—This work has been supported by the Alumimum Company of America, by Carnegie Mellon University under a DARPA contract for Shaping by Deposition, and by the Engineering Design Research Center, an NSF Engineering Research Center.

REFERENCES

1. L. E. Weiss, E. L. Gursoz, F. B. Prinz, P. S. Fussell, S. Mahalingam, and E. P. Patrick, *Manufacturing Review* **3**, 40-48 (1990).
2. MOGUL, *Metallizing Manual*. Metallizing Company of America (1963).
3. T. H. Turner and N. F. Budgen, *Metal Spraying*, p. 162, Charles Griffin & Co., London (1926).
4. P. S. Fussell and L. E. Weiss, in *Solid Freeform Fabrication Symposium*, p. 107-113, University of Texas — Austin, Austin, Texas (1990).
5. P. S. Fussell, E. P. Patrick, F. B. Prinz, L. Schultz, D. G. Thuel, L. E. Weiss, K. W. Hartmann, and H. O. K. Kirchner, in *1991 SAE Aerospace Atlantic*, SAE International, Warrendale, PA (1991).
6. E. L. Gursoz, Y. Choi, and F. B. Prinz, in *Geometric Modeling for Product Engineering*, edited by M J Wozny, J U Turner, andK Preiss, Elsevier Science Publishers (1990).
7. S. C. Gill and T. W. Clyne, *Metallurgical Transactions* **21B**, 377-385 (1990).
8. E. J. Lavernia and N. J. Grant, *Materials Science and Engineering* **98**, 381-394 (1988).
9. P. Mathur, D. Apelian, and A. Lawley, *Acta metallurgica* **37**, 429-443 (1989).
10. D. Apelian, M. Paliwal, R. W. Smith, and F. F. Schilling, *International Metals Reviews* **28**, 271-293 (1983).
11. P. Fauchais, A. Grimaud, A. Vardelle, and M. Vardelle, *Annales de Physique* **14**, 261-310 (1989).
12. H. Herman, *Scientific American*, (September) 112-117 (1988).

13. E. Pfender, *Surface Coating Technology* **34**, 1-14 (1988).

14. S. Safai and H. Herman, *Treatise on Materials Science and Technology*, p. 183-214, Academic Press, New York (1981).

15. M. L. Thorpe, in *Thermal Spray Technology: New Ideas and Processes*, ed by D. L. Houck, p. 375-383, ASM International,Metals Park, Ohio (1989).

16. L. Cifuentes and S. Harris, *Thin Solid Films* **118**, 515-526 (1984).

17. S. J. Harris and M. P. Overs, *Thin Solid Films* **118**, 495-505 (1984).

18. S. G. Harris, L. Cifuentes, C. C. Cobb, and D. H. James, in *1st International Conference on Surface Engineering*, p. 89-94, The Welding Institute, Brighton (1985).

19. S. J. Harris, L. Cifuentes, and D. H. James, *Advances in Thermal Spraying*, p. 475-484, Pergamon Press,.New York (1986).

20. J. J. Kaiser and R. A. Miller, *Advanced Materials and Processes* **136**, 37-40 (1989).

21. W. Milewski and M. Sartowski, *Advances in Thermal Spraying*, p. 467-473, Pergamon Press, New York (1986).

22. R. Kawase and K. Maehara, *Journal of High Temperature Society of Japan* **10**, 284-290 (1984).

23. Y. Arata, A. Ohmori, J. Morimoto, A. Yamaguchi, and R. Kawase, *Advances in Thermal Spraying*, p. 485-493, Pergamon Press, New York (1986).

24. C. Moreau, M. Lamoutagne, and P. Cielo, in *National Thermal Spray Conference*, ASM International, Metals Park, Ohio (1991).

25. K. H. Kuo, (editor),*Quasicrystals*, Materials Science Forum, 22–24 (1987).

26. P. J. Steinhardt and S. Ostlund (editors), *The Physics of Quasicrystals*, World Scientific Publishers, Singapore and Teaneck, NJ (1987).

27. D. B. Fowler, W. Riggs, and J. C. Russ, *Advanced Materials and Processes*, November, 41-52 (1990).

28. W. Hume-Rothery, *The Structures of Alloys of Iron*, p. 221, Pergamon Press, New York (1966).

29. M. F. Ashby and D. R. H. Jones, *Engineering Materials 2*, p. 78, Pergamon Press.Oxford (1986).

30. B. Cantor, *Rapidly Solidified Amorphous and Crystalline Alloys*, p. 317-330, B H Kear, B C Giessen, andM Cohen, (editor), Elsevier Science Publishing.Boston (1982).

31. K. Murakami, H. Asako, T. Okamoto, and Y Miyamoto, *Materials Science and Engineering A* **123**, 261-270 (1990).

AUTOMATED EJECTABILITY ANALYSIS AND PARTING SURFACE GENERATION FOR MOLD TOOL DESIGN

Rahul Bhargava, Lee E. Weiss, Friedrich B. Prinz

EDRC 24-58-91

May 1991

This work has been supported in part by the Engineering Design Research Center, an NSF Engineering Research Center.

Contents

List of Figures

Automated Ejectability Analysis and Parting Surface Generation for Mold Tool Design

Rahul Bhargava, Lee E. Weiss, Friedrich B. Prinz

The Engineering Design Research Center, and
The Robotics Institute
Carnegie Mellon University
Pittsburgh, PA 15213

Abstract

This report describes a CAD approach for automated ejectability analysis and parting surface generation for mold tool design. This design automation is incorporated into a Rapid Tool Manufacturing system which integrates stereolithography (SLA) and thermal spraying into a CAD/CAM environment for manufacturing tooling like injection molds. Design models are first evaluated for part ejectability given the desired draw direction and constrained to be manufactured in a two part mold. This information helps the designer to create manufacturable designs. The parting line and parting surface models are then created subject to geometric and process constraints. The union of part design and parting surface models forms impressions of the mold cavities. Cavity patterns are then quickly built with SLA and the molds are fabricated by spraying metal onto SLA patterns.

1 Introduction

The design of injection mold tooling has traditionally been a forte of skilled, experienced tool designers. Relatively little of this design process has been automated in the majority of industrial settings, rendering it a long and tedious task. Moreover, several *time consuming* iterations through product design, tool design and fabrication are often required to manufacture a successful tool. This is due in part to product designers creating product designs which are not "manufacturable", because they do not fully understand the constraints of downstream manufacturing processes. There are other difficulties as well, associated with predicting a tool design's actual performance, particularly for those with complex geometries or for those with new shapes for which the designer does not has any previous experience.

Two major efforts that can help reduce the tool development time include *automation and integration* of various aspects of design and analysis cycle and development of new manufacturing processes themselves. In recent years there have been several research initiatives and commercial developments to address the first one of these issues i.e. CAD packages to help reduce the tool design time and at the same time to analyze the tool from various perspectives. A large number of these analysis tools operate on a finite element mesh representation of the part. Generally, these packages which assist in analysis of designs fall in following three categories:

- **Stress Analysis:** examples include commercial systems like PATRAN, ABAQUS, ANSYS etc.
- **Mold Solidification:** Packages like C-Cool can analyze the solidification characteristics of the plastics and temperatures developed across the part during mold cooling and thus evaluate the tool from a process perspective.
- **Mold Filling Analysis:** Simulation of mold filling process is possible by specifying fixed gate positions and initial pressure or temperature. The designer can also view predicted temperature, stress, or pressure

distributions. C-Flow and MoldFlow are examples of two such analysis packages.

Finally all the above simulations can factor into a number of cost equations and thus lend themselves to an economic analysis as well.

Knowledge engineering based approaches have also been introduced in design automation. These approaches make use of heuristics and design standards used by experts in the design and manufacturing domain. PIMES, an expert system developed at Carnegie Mellon, performs a manufacturability assessment of plastic injection molded parts based on their CAD designs[1]. The heuristics employed are formally represented as rules and rely on key aspects of a part's shape features. These shape features are *extracted* from the actual part i.e. they are recognized and created from the low level CAD structures[2]. Several mold-design knowledge bases have also been developed containing rules describing complex interrelationships between temperatures and viscosities of the plastic materials, the plasticizing rate and shot capacity of injection molding equipment, pressure distribution in mold cavities and runners etc.[3]

While such automation can effectively reduce the time for tooling design and minimize the number of redesign/retooling iterations, there will always be modeling limitations and ultimately the real tool must be built and tested. For product manufacturers to be competitive they must be able to build these tools more quickly to respond to today's rapidly changing market demands.

As per the current manufacturing trends are concerned, today almost 90% of all the molds are made by machining operations, primarily turning, milling and grinding. There are several other mold making techniques particularly suited for complex part geometries e. g. investment casting, electro-deposition, cold hobbing, pressure casting, spark machining, and sprayed tooling[4]. The sprayed tool approach is one method which has long held the promise to speed up tool fabrication. This method, however, has several process limitations[1].

[1]Commercialized spray tooling is limited primarily to soft zinc alloys, Concave shapes with small aspect ratios are hard to spray, Process may be too tedious for a technician to execute, Substrate pattern fabrication is a prerequisite

and like many other manufacturing processes, has not been systematically integrated with earlier product design stages.

To address these problems, Carnegie Mellon University [CMU] is developing a Rapid Tool Manufacturing [RTM] system. The aim of the project is to reduce the time required to develop mold tooling by an *order of magnitude* by incorporating automation of design processes and their integration with the Stereolithography [2] technique [SLA] and thermal spraying into a CAD/CAM environment[5].

In this process, mold halves are fabricated by robotic arc spray deposition[3] on plastic patterns of the desired part. The sprayed metal shells are then backed with appropriate materials to form the tool. Relative to conventional machining methods, this approach has the potential to more quickly and less expensively produce tools, particularly for parts with complex geometries[4] or large dimensions.

As mentioned earlier, RTM system incorporates design automation and computer aided process planning capabilities. Some of the key features being developed in this CAD/CAM approach include:

- DFM critique of product design.
- Ejectability analysis of product designs.
- Generation of geometric models of the mold half patterns, which are to be sprayed, directly from product design models.
- Off-line robotic trajectory planning based upon design models and process information.

Each of these functions, as well as the initial product design, are implemented in a single *unifying* CAD environment based upon a non-manifold, linear, ge-

[2]Stereolithography is a relatively new free form fabrication technique which generates 3D objects by curing a polymer using laser beam. It has been commercialized by 3D Systems, Inc. (Valencia, CA)

[3]Current process research at CMU involves steel based sprayed tooling, methods for of metal onto plastic SLA, "hard-to-spray" shapes and robotic spray automation.

[4]Solid Freeform Fabrication [SFF] technologies such as SLA are easier to plan and to execute than CNC operations, but there are currently limitations with SFF precision.

ometric modeling system *nŒdles* [6],[7]. Currently the modeling system is linear which means that curves are represented by a combination of linear line segments and a model is composed of planar facets (called faces) with consistent topology and geometry. The models can be created using boolean operations on some primitives like cylinder, cone, sphere, toros etc. which are provided in the system or one may use a triangulation scheme[8] to create a model from a set of nonlinear surfaces provided in an IGES format. This modeling system provides a very powerful geometric engine for object representation and manipulation and ensures a smooth, efficient flow of information from design to manufacturing.

In this automation process, the geometrical aspects of mold design are among the first to be considered. Before analyzing the mold for a part one needs to know if such a mold is at all geometrically possible. The mold halves whose analysis is desired must be generated automatically from the part description itself. This report focuses on automated ejectability analysis and pattern generation for a part whose injection mold is desired. This sets up the input for other analysis and manufacturing processes downstream.

Automated ejectability evaluation is needed when one wants to ascertain if the part being considered can be taken out of the mold. This is very important for parts that have been designed on the computer because one may, unintentionally, design a surface which leads to an unejectable situation. Such situations can be very non-intuitive and hard to detect by visual inspection. This may lead to cracks in the final molds and molded parts during production and even failure.

Automated pattern generation involves finding the parting lines and creation of surfaces as well as the runner and gating systems[5] for ejectable parts. Some definitions are presented below which are commonly used in this paper and other literature in the field.

The **parting surfaces** of a mold are those surface areas of both mold halves, adjacent to the impressions, which are pressed against each other when

[5]Currently design of runner and gates is being developed in form of an interactive process where the designer is provided with a standard library of runners and gates. The designer selected runner and gates may then be added to the mold halves.

the mold is closed. The direction along which the mold is opened to remove the molding is known as the **draw direction**. Further, the line which forms the boundary of the cavity in the mold is termed the **parting line**. The part geometry determines the regions in which the parting line can lie and then a combination of several mechanical, metallurgical and process parameters[9] can be used to arrive at an *optimal* parting line. One important geometric consideration is that the molding should, as far as possible, be ejectable from the mold without using any sliding parts since their use is detrimental to dimensional accuracy and increases the cost of making and maintaining molds. The presented approach considers only two halves in a mold and hence parts which need slide actions are termed non ejectable.

Thus, given a part one should quickly be able to tell whether it can be ejected from a mold in a particular draw direction without any slide action. A *particular* draw direction is specified, since it is usually determined as a function of various metallurgical and geometric parameters. For example, one may wish to choose a draw direction along the width for molding a cuboidal part, whose depth is greater than its width, to minimize the pullout distance. A particular draw direction may be most suited to ensure uniform filling of the mold. Another draw direction may minimize the projection area which may be critical with respect to the capacity of molding machine at hand. Thus the decision to analyze ejectability in a particular direction seems reasonable.

Once the part is found to be ejectable, automatic generation of the parting line is the next logical step. Again, for complex parts, this step is very non-intuitive. In general, the parting line is a three dimensional, closed curve which is difficult to specify precisely by visual inspection. This is more so in case of computer designed parts where one should be able to represent the parting line accurately and in a suitable format so that it can be used in further design processes like parting surface design. However, if the part is not ejectable, the designer should be informed of the non ejectable areas. On the whole, this approach helps the designer to create manufacturable designs and reduces the expensive, time consuming iterations from design to manufacturing.

The rest of the report describes a system for such an ejectability analysis.

The following flowchart (fig. 1) highlights the major components of the system which are explained in greater detail in the following sections.

In the course of this report some simple test parts are used to describe the approach and finally some more complicated real life examples are presented to illustrate the utility of the system.

2 Ejectability Analysis

The aim of ejectability analysis is to determine whether a part is ejectable or not from a two part mold along a specified draw direction. The algorithm is primarily based on an analysis of the relationships of surface normals of the design model to the draw direction. Various regions of a given part have varying slopes with respect to the draw direction and this forces certain parts to lie in the top half or the bottom half of the mold to avoid unejectable situations. This idea is captured in mathematical terms along the following lines:

Given draw direction ($\vec{dd}$)
Let $\vec{fn_i}$ = face normal of face f_i
and Θ = angle between $\vec{fn_i}$ and $\vec{dd}$;
Then if
$abs(\Theta) < 90°$

$\Rightarrow$ Face f_i will lie in the top mold half.
$90° < abs(\Theta) \leq 180°$

$\Rightarrow$ Face f_i will lie in the bottom mold half.
$\Theta = \pm 90°$

$\Rightarrow$ Face f_i may lie in either mold half.

2.1 Theory of Patches

The above classification conforms to the intuitive idea that all the visible areas of the part, when viewed from the draw direction, should belong to the top

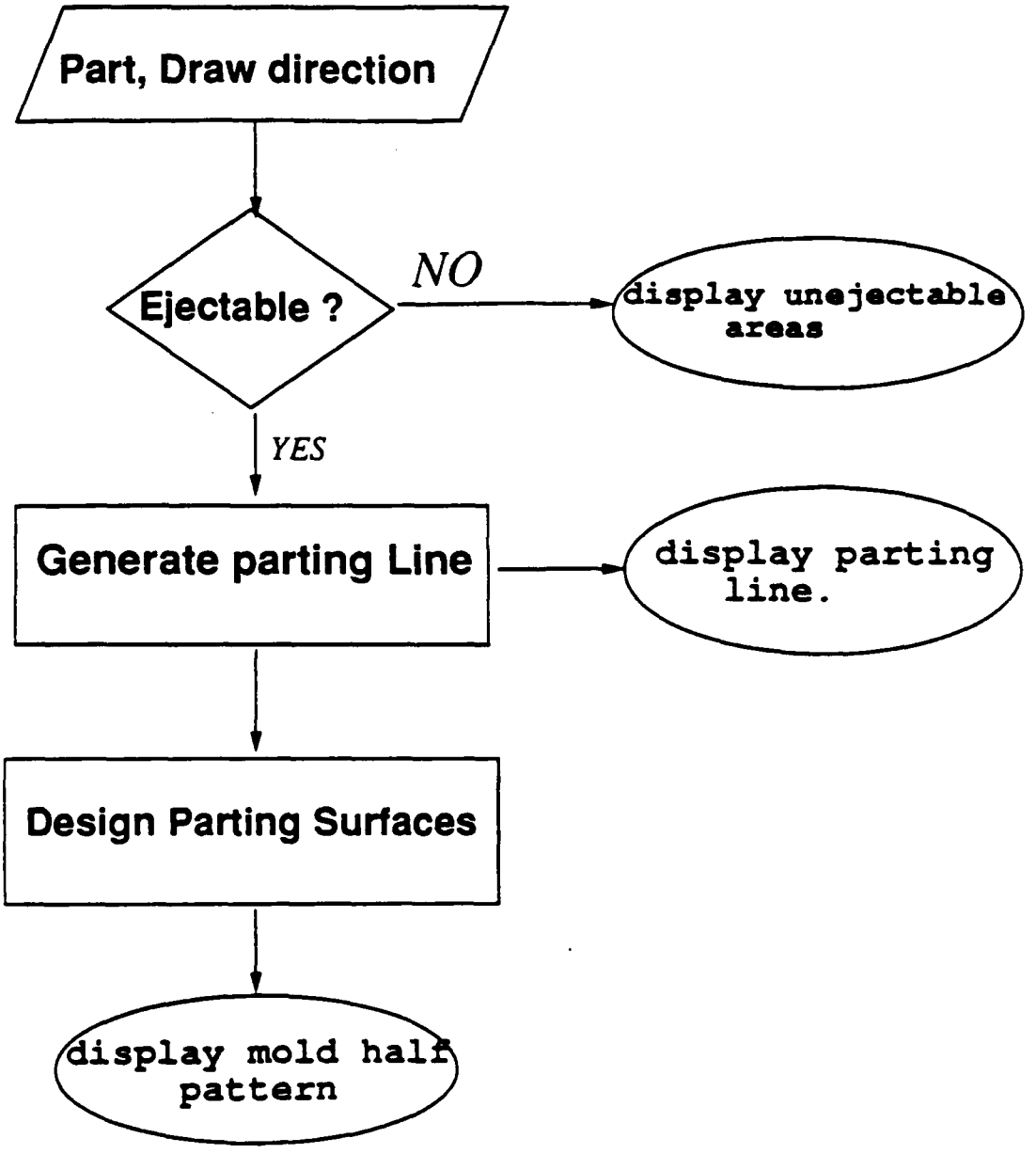

Figure 1: System Flowchart

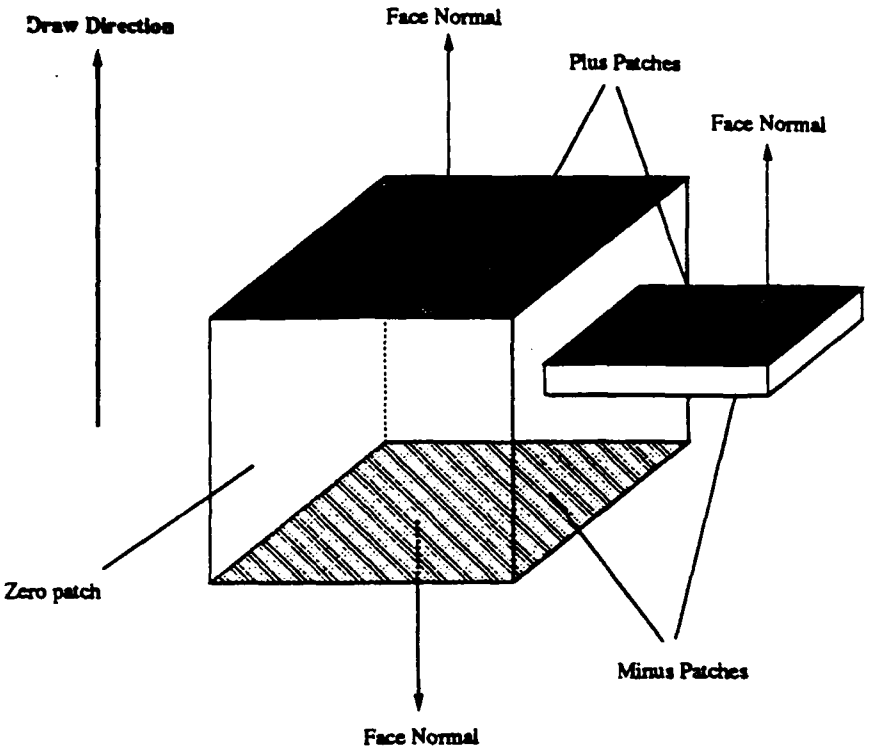

Figure 2: Classification into patches

mold half and the invisible areas to the bottom one. Thus as a first step, the part is classified into groups of faces called patches (fig 2). As is clear from the preceding material, there are three distinct type of patches which will be needed to exhaustively classify a part. These three types of patches are defined as—

Plus: Collection of adjacent faces which are to lie in the top mold half, i.e. the face normals make an acute angle with the draw direction.

Minus: faces that should go to the bottom mold half.

Zero: faces whose normals are at right angles to the draw direction and thus they may lie in either mold half. In practice, these patches are rare, since all surfaces have some draft on them.

Plus and minus patches are collectively termed as signed patches. A patch may only have unlike signed neighbor patches and a part may have multiple patches of the same type i.e. plus, minus or zero. During the development of patches, we keep track of the following three attributes which are very useful later on—

Faces A list of constituent faces which make up the patch is maintained.

Boundary The boundary, in terms of linear line segments, of the *collection* of faces in the patch. This is readily applicable to cases where the patch may include a hole. In those situations the boundary edges form multiple loops.

Neighbors This is a list of all the neighbor patches for a patch. As noted earlier, the neighbor patches are of different type as compared to the patch.

An important concept in regard to patches is the possibility of further reductions in total number of patches themselves. In case a zero patch is completely surrounded by a plus (or minus) patch or by a pair of plus (or minus) patches then it can be treated as plus (or minus) patch instead of a zero patch as depicted in fig 3.

Since all the plus (or minus) patches *have* to lie in one mold half, the zero patch which is completely enclosed by them will also lie in the same mold half. This is permissible by the definition of a zero patch according to which it can go to either top or bottom mold half. So in such cases this enclosed zero patch serves as a *link* to connect together its plus neighbor patches to form the top mold half and minus neighbor patches to form the bottom mold half. Hence, such a zero patch can be considered *reduced* to a signed patch with a simultaneous update of the attributes (outlined above) of the involved patches.

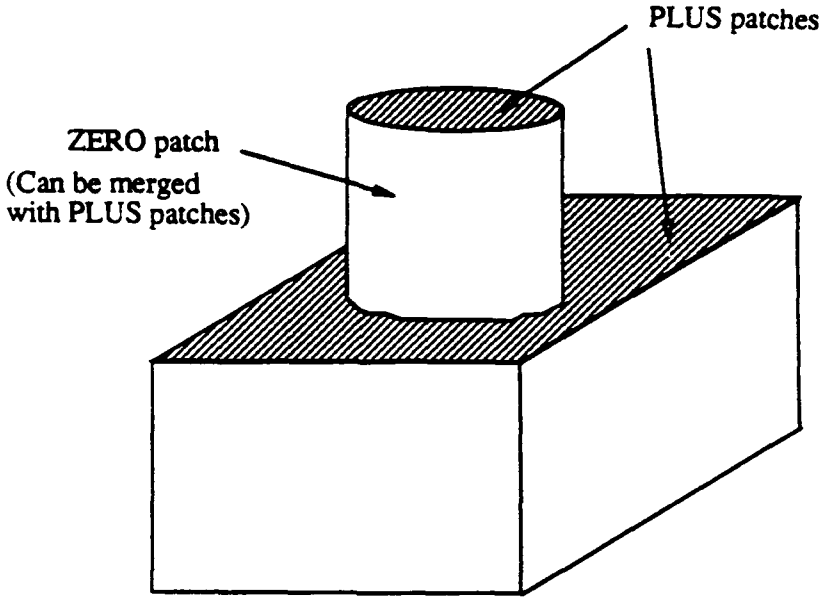

Figure 3: Reduction of patches

2.2 Ejectability Tests

The classification of a part into patches, captures the essence of faces of the part from an ejectability point of view and makes it feasible to reason with only a handful of patches instead of thousands of faces. It also helps define the ejectability conditions i.e. A part is ejectable if—

- No two *same* signed patches intersect when projected on to a common plane perpendicular to the draw direction.
- No patch boundary intersects *itself* when projected onto a plane perpendicular to draw direction.

To implement the first check, concept of projected patch areas is employed in this approach. If the sum of individual projected patch areas turns out to be greater than the merged patch area of the two patches it signifies an overlap (fig. 4) of portions of the part along the draw direction, hence forming an undercut. For projections of patches, we make use of the patch boundaries stored earlier during the patch growing stage. The second check is implemented by

looking for edge intersections among constituent edges of the patch boundary (refer to fig. 4).

However, some preliminary analysis regarding part's ejectability can also be done with the help of these patches e.g. If a part has more than one plus/minus patch and no zero patch, it is *not* ejectable. This is so because two patches of the same sign can never be adjacent and without a zero patch there is nothing which can link these same signed patches together in one of the mold halves. In Fact this indicates the presence of undercuts in the part.

In the RTM system, such unejectable geometries are brought to the attention of designer by highlighting the relevant patches on the CAD screen. The designer may now choose to redesign/reorient the part or use a sliding component to deal with the problem.

3 Parting Line Design

If the part is ejectable then the next step is to obtain a parting line and thus clearly identify the two mold halves. For ejectable parts the general idea of a parting line as put forth by Pye[10] is:

> The parting line must occur along the line round the position of maximum dimension when viewed in the draw direction.

This idea can be easily related to the boundary of the patches. Infact, the boundaries of plus and minus patches, in a plane perpendicular to the draw direction, are the same and this is also the *projection* of parting line (fig 5). However, as shown in the figure, this is not the *true* projection of parting line. The shaded area on the part represents a region, which belongs to a zero patch, where parting line cannot pass through. This area maps into a line in the projection since zero patches are always projected as lines.

Such regions are identified by looking for coincident boundaries of projected patches of any one sign (plus *or* minus). By eliminating these coincident boundaries and ordering them to form closed loops, a true projection (fig 5) of the parting line is obtained. This projection of parting line is represented as a

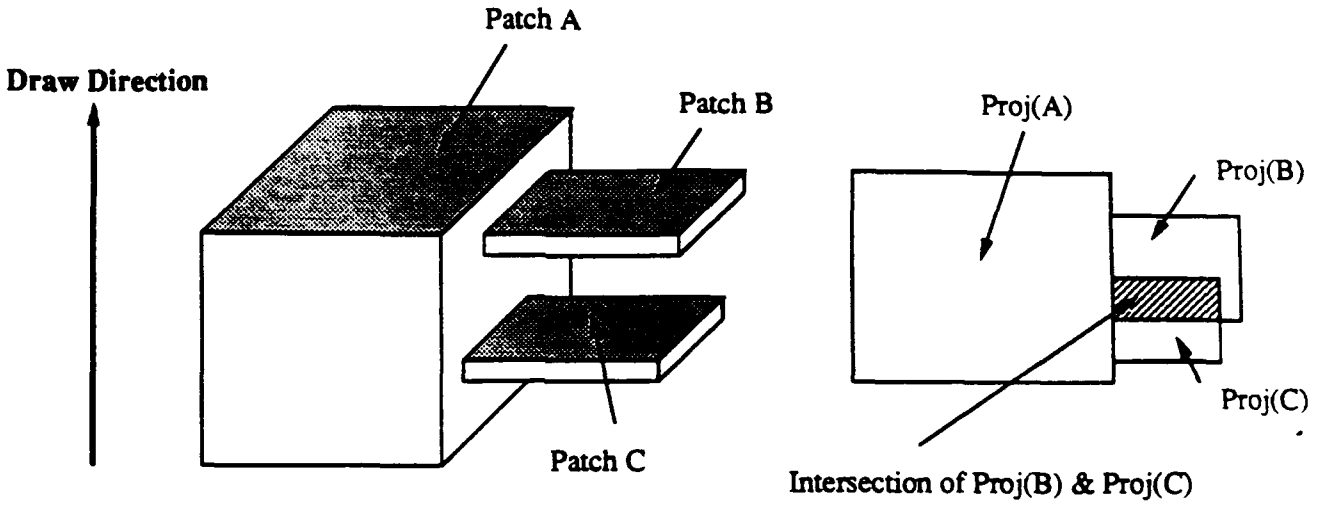

IF $area(B \cup C) < area(B) + area(C)$
$\Longrightarrow$ Intersection of B and C. "area" refers to projected area.

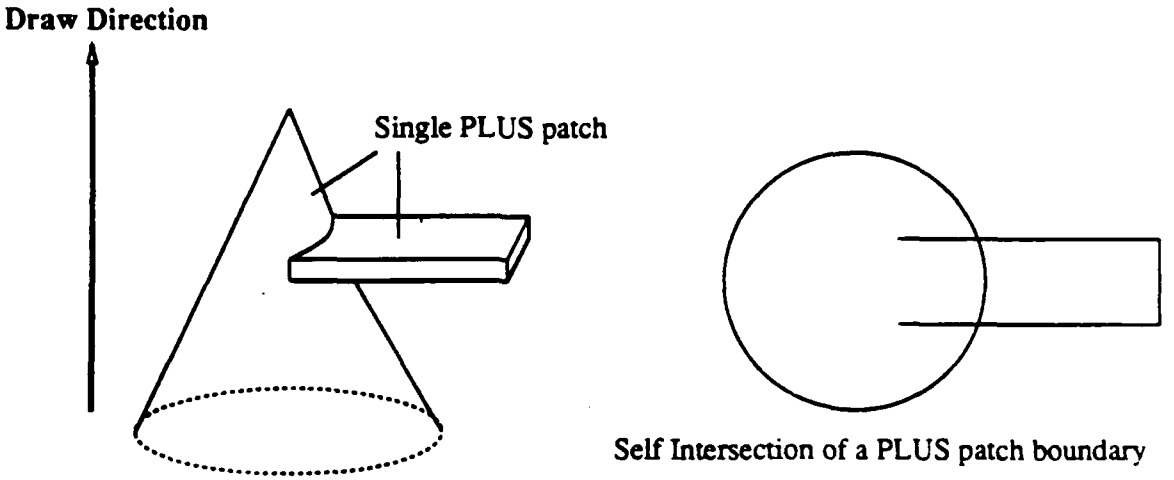

Figure 4: Checking patch intersections

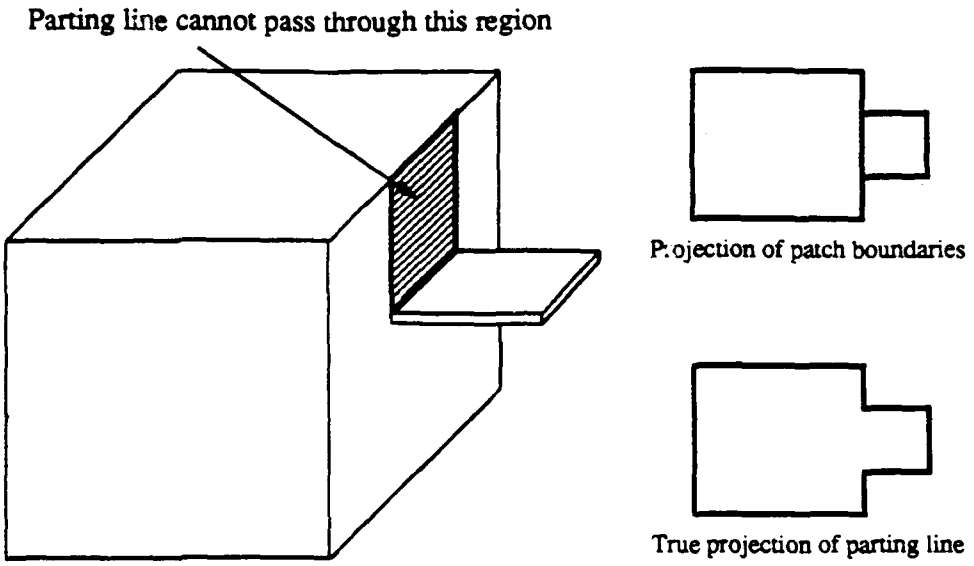

Figure 5: Projection of parting line

series of nodes[6], which are connected by straight lines. This projection is the same for *all* possible parting lines in the part. However, this is a projection in $\Re^2$ space, whereas the actual parting line is a closed, connected curve in $\Re^3$ space. To transform this projection into the three dimensional representation of the part, we need to fix a value for the z-coordinate of each node in the projection of the parting line.

This is a problem with a non-unique answer, because each of the nodes can take a *set* of values for the z-coordinate. This becomes possible due to the presence of zero patches, which map into straight lines in the projection but offer an *area* in the $\Re^3$ representation for the parting line to pass (fig 6). However, if there are no zero regions, like in the egg shaped object shown in fig 6, one does not have a choice of many parting lines. In such a case the boundary of plus and minus patches is *the* parting line.

[6]Characterized by their x; y positions; Assuming Z to be the draw direction.

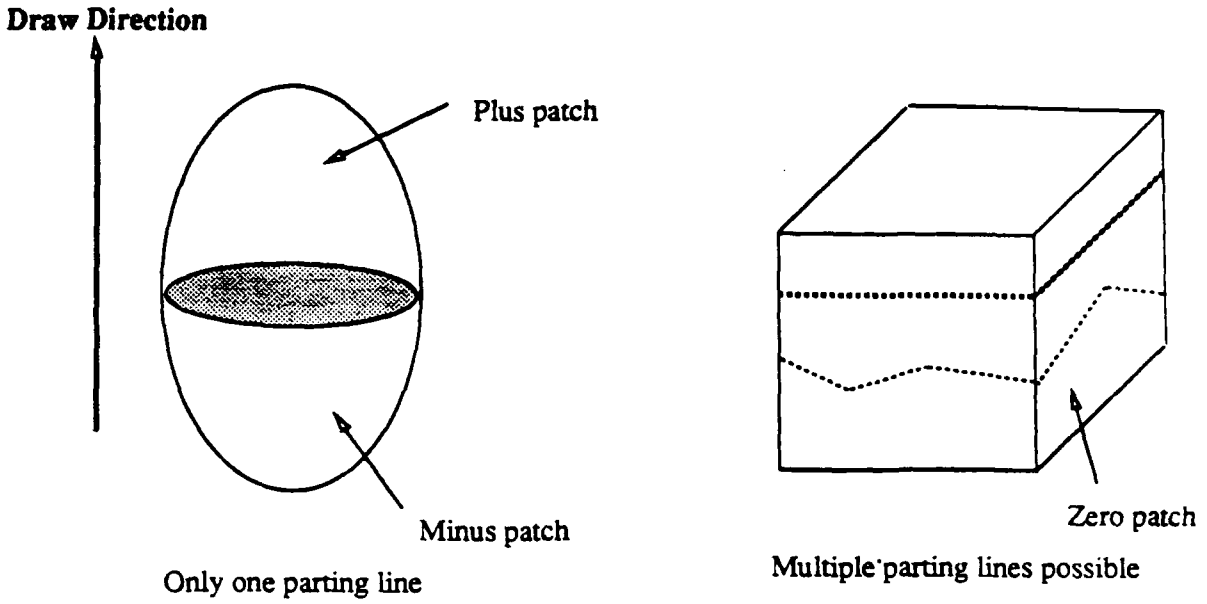

Figure 6: Non-unique parting line problem

3.1 Concept of Ranges

As illustrated in the previous section, a part containing zero patches may have a number of different parting lines in a particular draw direction but these parting lines have a common projection in a plane perpendicular to the draw direction. This brings out the fact that the variation in position of parting line nodes, along the draw direction is what forms the various parting lines. Hence the decision to keep parting line as an ordered list of nodes. Now by assigning a **range** [*high:low*] of positions (along the draw direction, say Z) to every node, the entire gamut of possible parting lines is covered. This is shown in fig 7.

The part shown in fig 7 has two small cubes cut out at the top and bottom. The true projection of all possible parting lines is shown by a dark line. The nodes of the parting line are shown with black dots. Node 1-4-5-6-7-8-9-10 are sufficient for obtaining the projection of parting line but they are *not* sufficient to cover all the parting lines by themselves. For example a line between the lowest positions of node 1 and 4 is physically not possible. For this reason

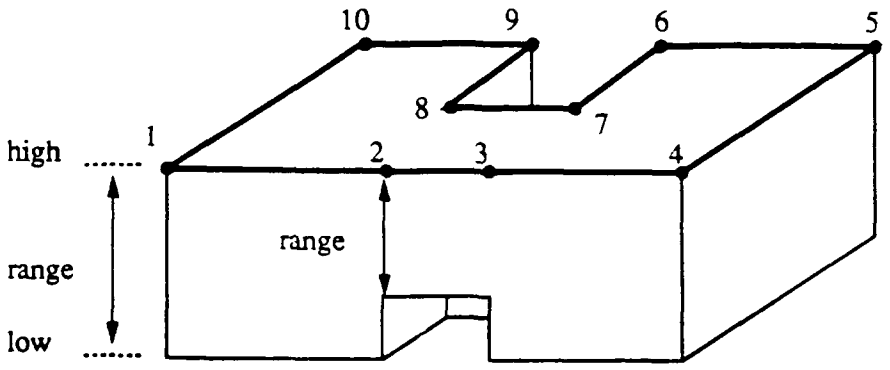

Figure 7: Assigning ranges to each node of the parting line

node 2 and 3 are included in this list of nodes. Now the range of these two nodes will prevent parting line from falling off into the cut out portion of the part.

To obtain all these nodes, projections of both plus and minus patch boundaries are needed. As mentioned earlier both these projections are *same* in terms of shape but the actual number of nodes in each projections may be different depending on the shape of the part. e.g. in fig 7 node 2 and 3 do not occur in the projection of plus patch boundaries but do appear in projection of minus patch boundaries. These two projections are combined to provide bounds on the position of the parting line by assigning range to every node of these two projections.

3.2 Development of a Parting Line

After assigning ranges the next step is to select a position for each node such that it lies within its defined range. This can be done in several ways to adapt to the kind of parting line desired. Various kinds of parting lines (fig 8) are used in mold making with each having its specific advantages.

However Flat parting lines and surfaces are preferred in most cases. The molds with flat parting line are easy to manufacture as well as maintain. Hence this kind of parting line is attempted first.

As noted earlier, the parting line design problem has a non-unique answer

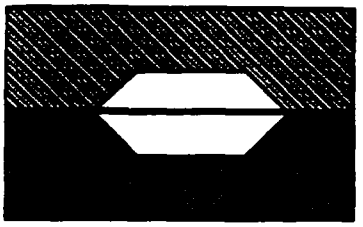

(a) Flat Parting Surface

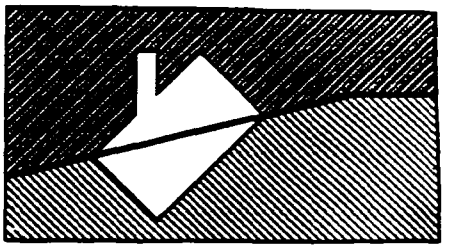

(c) Angled Parting Surface

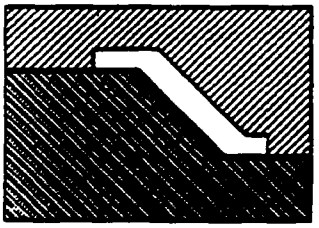

(b) Stepped Parting Surface

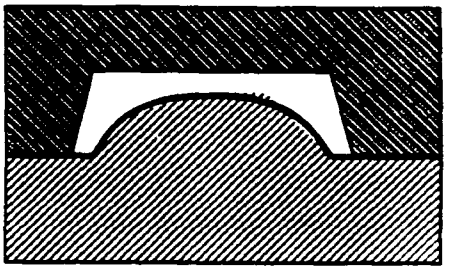

(d) Profiled Parting Surface

Figure 8: Various kinds of parting surfaces

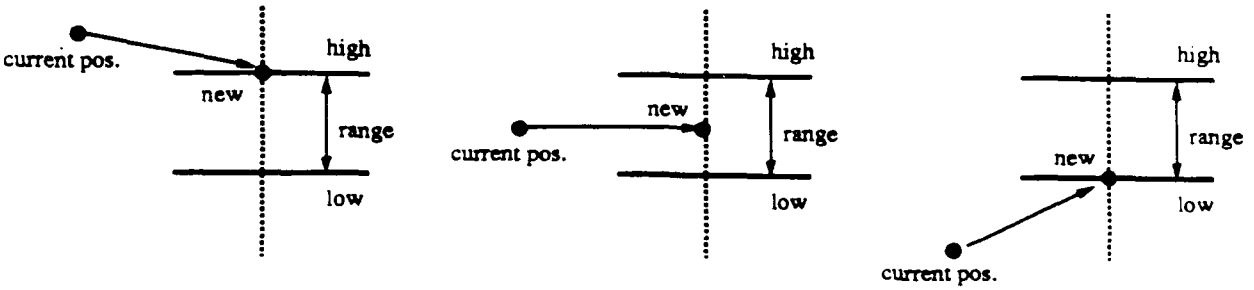

Figure 9: Development of parting line

due to the multitude of parting lines offered by presence of zero patches. However, in practice, not all nodes of the parting line are expected to have non-zero ranges because most surfaces will have drafts instead of being perfectly vertical. This means that the **parting band**[7] is composed of line segments and areas. The line segments indicate the nodes which have zero range.

To design a flat parting line, we start with the node which has minimum range, called the **primary** node. As discussed in the preceding paragraph, in most cases the range associated with the primary node will be zero. Hence this node (primary node with zero range) has to be on the parting line and if there is another node in parting line whose range does not permit the same position[8] as that of primary node, a flat parting line *cannot* be obtained. If all nodes can take positions same as primary node along the draw direction then a flat parting line is obtained. In case the range associated with primary node is not zero, it implies that primary node's position is not fixed but can be changed. In these cases the starting position for the primary node is chosen as the midpoint in its range.

In situations where a flat parting line is not possible, an attempt is made to get as close to it as possible by minimizing the deviation (along the draw direction) of a node from the previous node (fig 9).

This essentially tries to minimize the total length of the parting line by minimizing the segment length at each step. Stepped or locally stepped parting surfaces (fig 8) will result due to this approach. Options to obtain the

[7]The set of all possible parting lines

[8]along draw direction

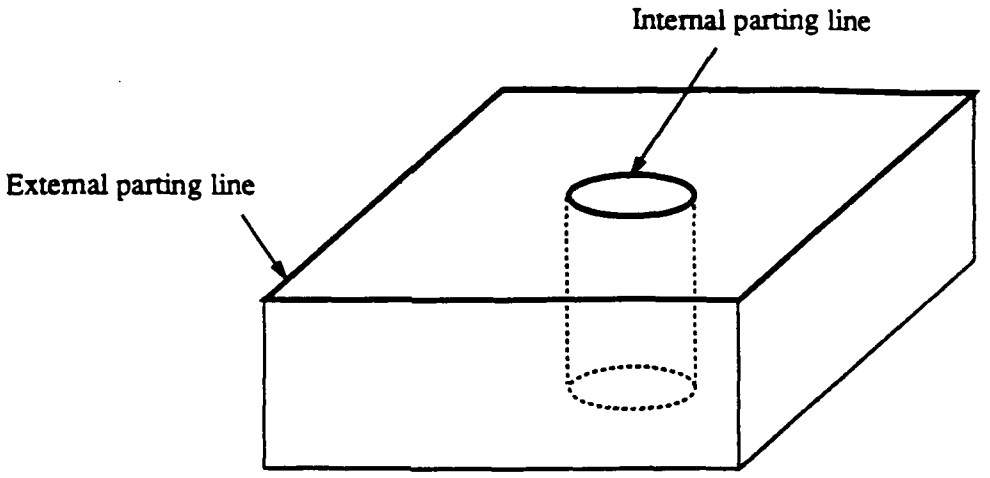

Figure 10: Internal parting lines

highest/lowest parting lines are also available. The highest parting line is obtained by fixing all node positions equal to the top of their ranges while lowest parting line fixes the positions equal to the bottom of the respective ranges.

Internal parting lines are possible in parts whose genus is greater than zero as shown in fig 10. In such parts the internal parting lines are handled in exactly the same way as the external (i.e. the outermost) parting line since they are also represented as a series of nodes joined by line segments.

Sometimes it is desirable to shift the parting line by a small amount, up or down, to intentionally create an undercut. This produces a self locking of the part inside the mold to assure that the part stays with the mold half which contains the knock-out pins when the mold is separated. This option has also been incorporated by using the information contained in the parting line. The shifting of parting line, by the desired amount, is accomplished by recalculating positions of the nodes with *zero* range (fig 11). This is so because these nodes lie at the boundary of plus and minus patches and simply shifting their position up or down will make them lie *outside* the part, which is a physically impossible situation. Hence these nodes are shifted in such a manner that they lie *on* the part even after the shift.

Other nodes are left as such since shifting them does not necessarily create

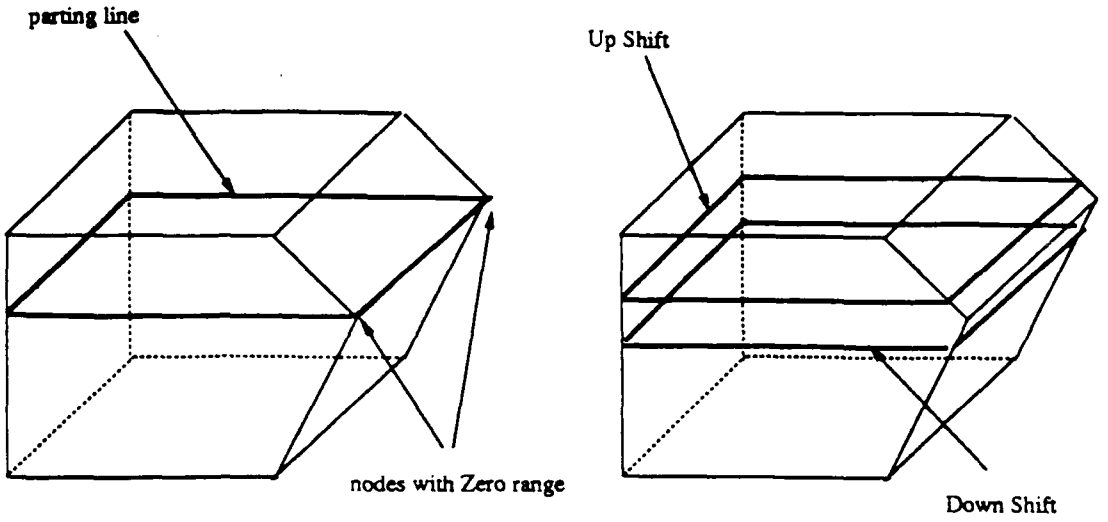

Figure 11: Shifting of parting line

an undercut. However, if a flat parting line is shifted, effort is made to restore its planarity at the new level.

4 Parting Surface Design

The next important step in this system is to design *parting surfaces*, which serve to connect the parting line to the base frame of the mold. This problem is trivial for a flat parting line since in that case the parting surface is the frame itself. However, in most of the practical situations, the parting line happens to be a three dimensional closed curve. In this situation, there are several demands that can be made on the parting surfaces. The parting surface is generally required to be at a particular angle[9] with respect to the draw direction, for ease of ejection. This is more important in the RTM system, since these surfaces also need to be sprayed with metal and the difficulty as well as quality of spray is related to the angle at which the spraying is done.

Thus we define this problem as follows:

Design a set of planar faces which connect the parting line to a flat

[9]This angle may vary from 0° to 90°

base i.e. frame, while making an angle θ with the draw direction.

This essentially is a problem of sweeping down the parting line *outward* at an angle onto a flat base frame which is it a level that is less than or at least equal to the lowest node's position, along the draw direction, in the parting line.

4.1 Theory of Cones

The approach to solve this problem is to consider a series of right circular cones centered at each node of the parting line such that—

- Apices of these cones coincide with the respective nodes of the parting line.
- Half angle of each cone is θ, as defined earlier.
- Base of each cone lies on the flat surface, called **base plane**, of the frame.

Thus, different cones along the parting line may have different heights due to non-planar nature of parting line. The idea behind using a cone at each node is motivated by the fact that all surfaces which make an angle of θ with the vertical and pass through that particular node of the parting line will be *tangential* to a right circular cone which is defined at this node in the manner described above.

Now the original problem of parting surface design reduces to finding planes which are tangential to two adjacent cones as shown in figure 12. A series of such planes then form the entire parting surface around the parting line.

As is clear, this approach requires the distinction between internal and external tangential planes i.e. the planes that would lie *inside* or *outside* the volume generated by sweeping the parting line straight down onto the base plane. The parting surface can only be composed of external planes. Also the two adjacent tangential planes at a given cone may:

1. not intersect at all.
2. intersect along a line which is tangential to the cone.

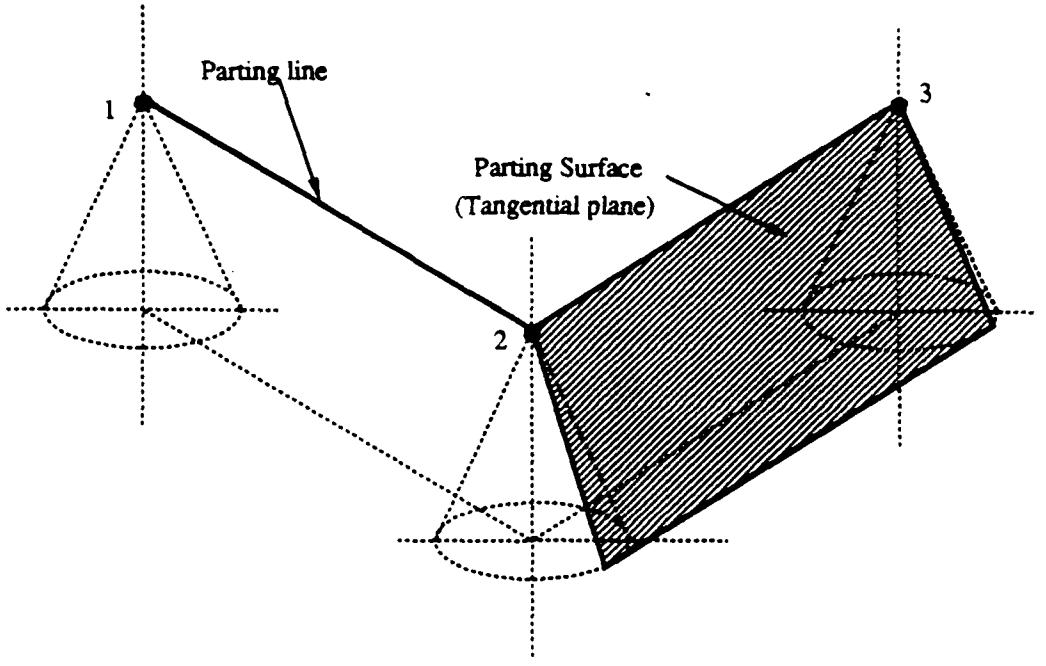

Figure 12: A Parting Surface facet

3. intersect along a line *before* making tangential contact along the cone. Thus the intersection line is *not* tangential to the cone.

4.2 Transformation to $\Re^2$ space

Fortunately, one can easily deal with all these cases in a $\Re^2$ space. If we consider each tangential plane as a *line*, along which it intersects the base plane, and the cones as *circles* on the base plane, the lines have to be tangential to the circles. Since two non-concentric, circles have at most four tangents (fig. 13), one has to choose a tangent to get the desired parting surface.

Clearly the tangents that cross the center line between the two circles are not admissible and these are eliminated from consideration. Out of the two remaining tangents, we choose the tangent which has greater length lying *outside* the bounded polygon formed by taking the projection of the parting line on the base plane (fig 14).

This ensures that the parting surface formed using this tangent will lie

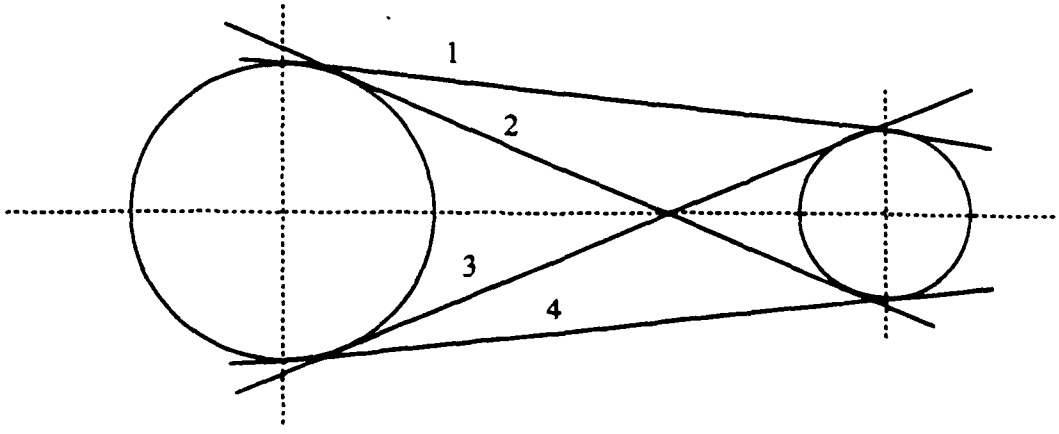

Figure 13: Common tangents for two circles

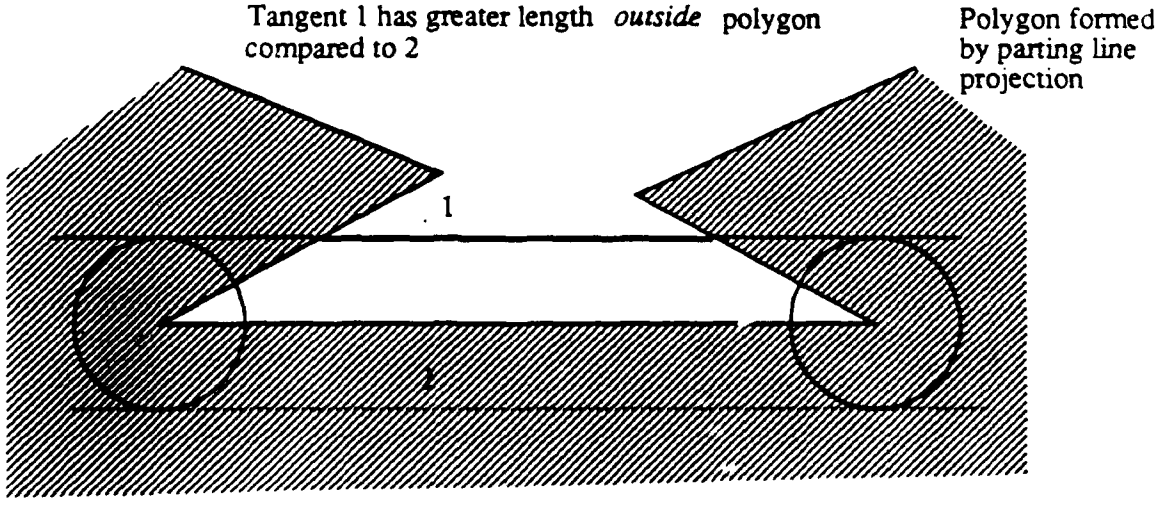

Figure 14: Choosing a tangent

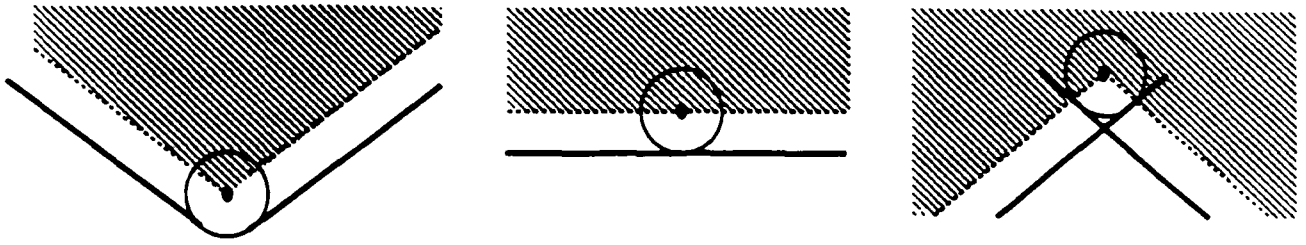

Figure 15: Transforming the cases in $\Re^2$ space

outside the swept volume of parting line.

Now, once the circle tangents are identified, we need to look at three cases which were outlined earlier. In the $\Re^2$ space, the cases are reformulated in terms of two tangents incident on a circle which may behave as follows—

1. They may not intersect at all.

2. Their intersection point lies on the circle boundary.

3. They intersect before making a tangential contact at the circle.

These cases are shown in fig 15.

First two cases are well behaved with respect to our design goals for the parting surfaces. The first case requires a portion of the circle in order to make a smooth transition to the next tangent. This is readily interpreted in $\Re^3$ space as portion of the cone's curved surface. Such a situation is infact desirable since it smoothes out the sharp corners. This is particularly helpful for metal spraying in the later stages of the RTM system. The second case is a perfect though rare case, which requires no post processing. The third case, however is a problem case.

Here creation of parting surfaces which satisfy the angle criterion is impossible. The user can be informed that the guarantee of parting surfaces being at a particular angle with respect to the draw direction will be violated here. A more practical solution to this problem is to tackle this problem during actual creation of parting surfaces. Each tangential plane is actually created in terms of two triangular faces which are adjacent to each other along the diagonal of

the plane. In case 3 situations, consider a line l joining the intersection point of the two tangents to the node i.e. apex of the cone. Now when the triangles are created around this line l, the two triangles on either side have an angle different than θ with respect to the draw direction. However, in most practical cases this deviation is negligible and thus by compromising a bit on the angle requirement, a feasible parting surface can be obtained.

Another important feature of the parting surface design includes the ability to detect if a parting surface has run into some other surface created earlier. This is due to capabilities provided by the geometric modeling system which notifies the user of such inconsistencies during the creation of the model of parting surfaces. In such situations, the designer is advised to try again with a reduced angle requirement.

4.3 Special Cases

When the angle requirement on the parting surfaces is $\theta = 0°$, the parting surfaces can be trivially generated by sweeping the segments of parting line straight down. Here the cone at each node degenerates to a straight line with base having a zero radius.

Another special case is for $\theta = 90°$. This can be supported in case of flat parting lines only. In such cases, the parting surface turns out to be a flat plane perpendicular to the draw direction. For a three dimensional parting line it becomes a degenerate case of a right circular cone whose half angle is equal to 90°, which is not possible.

4.4 SLA Pattern Creation

Once the parting surface is designed, it exists as a free standing structure. The surfaces and the frame can be merged together with the part taking advantage of *nOOdles* non-manifold capabilities and a solid pattern ready for spray can be generated. It can also be treated as a pattern for a mold cavity. However, runner and gating system needs to be integrated into the pattern. Current plans for runner and gating system include creation of a library of

standard runner and gate shapes. User would be able to pick a particular type of runner and gate at various locations and develop the entire system. In future, it is expected that a lot of process and geometry constraints would be incorporated to automatically decide the best runner and gating system for a particular mold.

Some examples are presented in the next section which illustrate the concepts presented here. The parting surfaces and patterns generated for some complex parts are shown.

5 Examples

Figure 16 shows a fan which is used in a variety of small scale cooling applications. Here a flat parting line is impossible and hence a parting line is generated which minimizes the variation (in height) from one point of parting line to the next as explained earlier in fig 9. This parting line is fairly complex as it follows the contours of fan blades. Parting surface model is generated from the parting line and is then merged with the original model to form the pattern for thermal spraying in the Rapid Tool Manufacturing System[5]. Figure 16 shows the fan, its parting line and finally the pattern.

Another example is presented in figure 17. It is a sidemarker lamp housing of a car. The original data for the part is a set of NURB[10] surfaces which is linearized for use in *nŒdles* . These complex industrial parts tend to have inconsistencies in directions of face normals, called noise, due to errors in original data generation and representation. This noise predominantly consists of a *very small* plus (or minus) patch surrounded by a big minus (or plus) patch. To eliminate this noise, these small patches[11] are merged into a surrounding bigger patch which has the longest adjacency with "noise". Care is taken to avoid treating valid patches as noise. The parting line and pattern, ready for spray, are shown in figure 17.

[10]Non-Uniform Rational B-splines

[11]whose projected areas are of the order of 1 mm^2

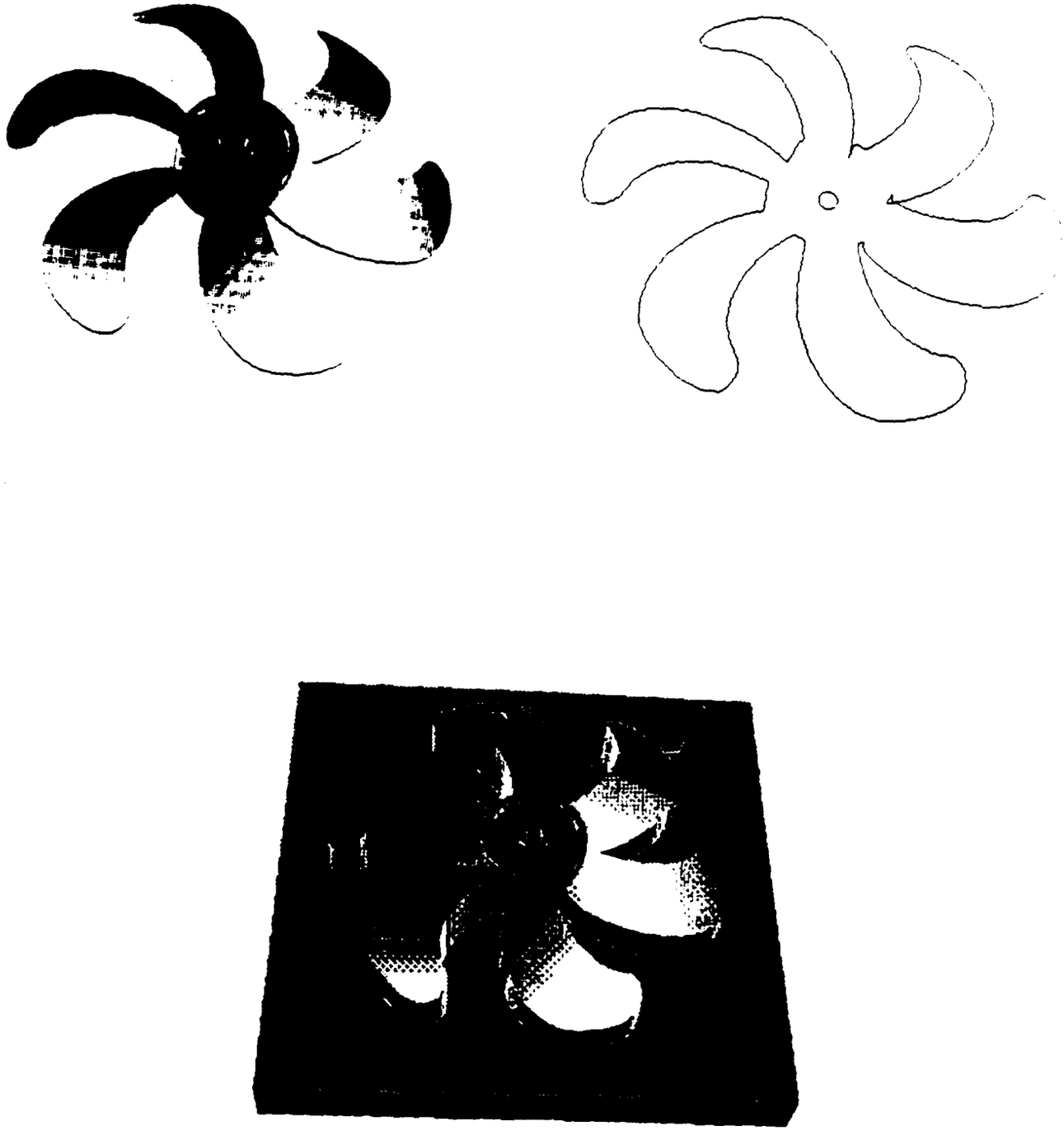

Figure 16: Parting line and surfaces for a fan

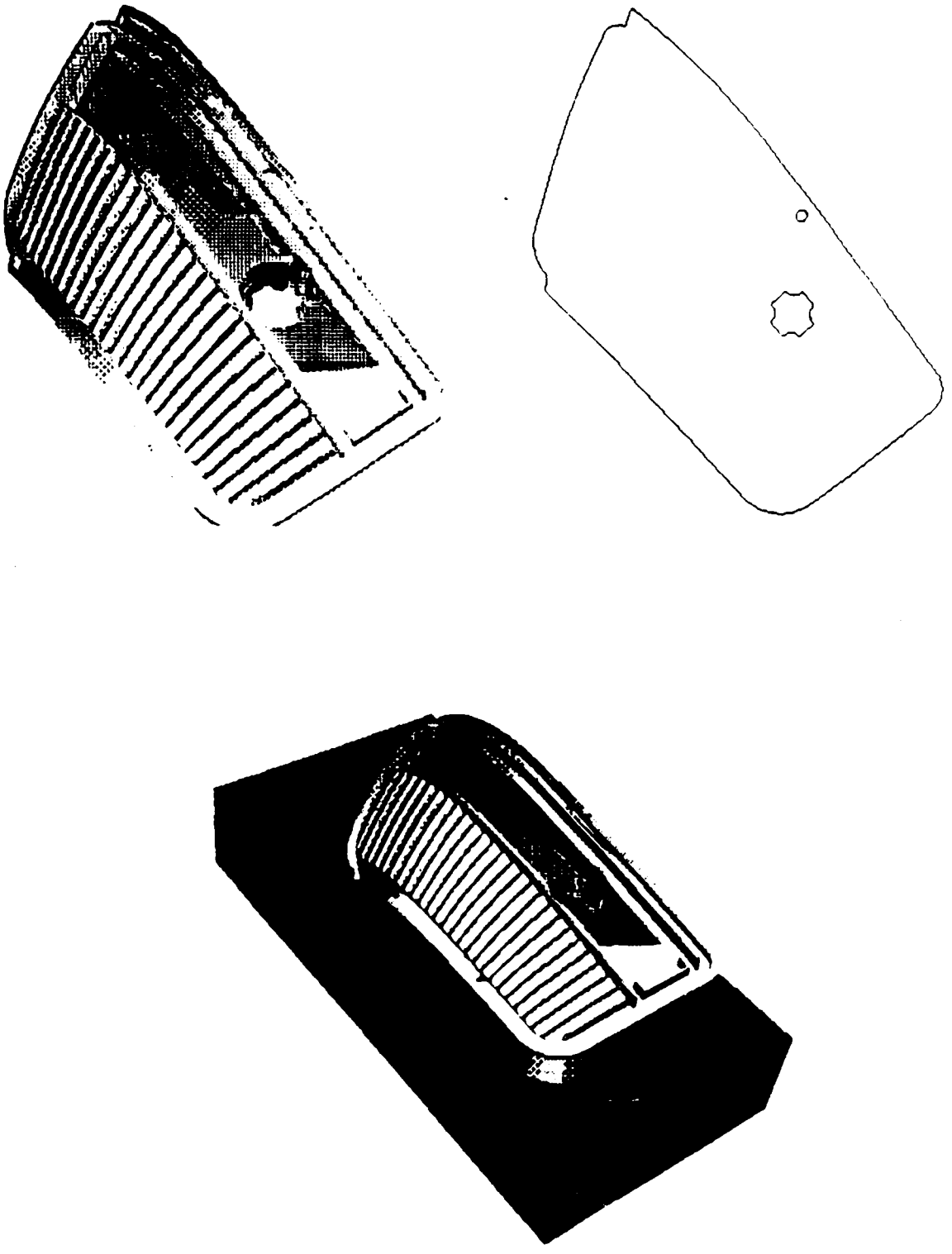

Figure 17: Parting line and surfaces for Side Marker Housing

6 Conclusions and Future Work

This report presents an approach to analyze ejectability for components manufactured in molds or dies and to automatically design parting line and surfaces. At present molds are supposed to have two mold halves with no moving parts i. e. undercuts are not allowed in ejectable parts. Application of this work to a rapid tool manufacturing system has also been illustrated. Future work will include analysis of slide actions in case of parts with undercuts. Since the problem is localized by identifying the patches which cause unejectable situations, one should be able to develop on this information. Integration of process constraints in the design of runner and gating system as well as other parts of the program is also highly desirable.

References

[1] M. Hall, "The design evaluation environment of PIMES, a plastic injection molding expert system." PhD. Proposal, Carnegie Mellon University, 1990.

[2] M. Hall, A. Sudhalkar, R. Gadh, L. Gursoz, and F. Prinz, "Feature abstraction in knowledge-based critique of designs," in *Proc. of ASME winter annual meeting 1990*, pp. 71–73, ASME Press, 1990.

[3] D. Cinquegrana, "Intelligent CAD automates mold design," *Mechanical Engineering*, vol. 112, pp. 71–73, July 1990.

[4] G. Menges and P. Mohren, *How to Make Injection Molds*. Hanser Publishers, 1986.

[5] L. Weiss, L. Gursoz, F. Prinz et.al, "A rapid tool manufacturing system based on stereolithography and thermal spraying," *Manufacturing Review*, vol. 3, pp. 40–48, March 1990.

[6] L. Gursoz, Y. Choi, and F. Prinz, "Boolean set operations on non-manifold boundary representation objects," *Computer Aided Design*, vol. 23, pp. 33–39, Jan/Feb 1991.

[7] E. L. Gursoz, Y. Choi, and F. B. Prinz, "Vertex-based representation of non-manifold boundaries," in *Geometric Modeling for Product Engineering* (M. J. Wozny, J. U. Turner, and K. Preiss, eds.), pp. 107 - 130, New York: North-Holland, 1990.

[8] J.-M. Chen, "Conversion algorithm from free form surface modeling to solid modeling," Master's thesis, Carnegie Mellon University, May 1989.

[9] B. Ravi and M. Srinivasan, "Decision criteria for computer-aided parting surface design," *Computer Aided Design*, vol. 22, pp. 11–18, Jan/Feb 1990.

[10] R. Pye, *Injection Mold Design*. Longman Scientific and Technical, 1983.